ISSN 2409–4951(Online)
ISSN 2310–1008 (Print)

Ukrainian Journal of Food Science

Volume 13, Issue 1
2025

Kyiv 2025

Ukrainian Journal of Food Science publishes original research articles, short communications, review papers, news, and literature reviews.

Topics coverage:

Food engineering	Food nanotechnologies
Food chemistry	Food processes
Biotechnology, microbiology	Economics and management
Physical property of food	Automation of food processes
Food quality and safety	Food packaging

Publication frequency – 2 issues per year (June, December).

The research must be original, have a clear revelance to food science, and appeal to the broader international scientific community.

Editors are committed to ensuring a prompt and fair peer-review process, enabling the timely publication of accepted manuscripts.

Ukrainian Journal of Food Science is abstracted and indexed in the following databases:

Directory of Open Access Journals (DOAJ) (2023)
EBSCO (2013)
Google Scholar (2013)
Index Copernicus (2014)
Directory of Open Access scholarly Resources (ROAD) (2014)
CAS Source Index (CASSI) (2016)
FSTA (Food Science and Technology Abstracts) (2018)

Reviewing a manuscript for publication. All scientific articles submitted for publication in the Ukrainian Journal of Food Science undergo double-blind peer review by at least two reviewers appointed by the Editorial Board: one member of the Editorial Board and one reviewer who is not affiliated with either the Board or the Publisher.

For a Complete Guide for Authors please visit our website:
http://ukrfoodscience.nuft.edu.ua

Editorial office address:
National University of Food Technologies
Volodymyrska str., 68
Kyiv 01601
Ukraine

E-mail:
Ukrfoodscience@meta.ua

Contents

Effects of whey and grape peels on pasta physical and sensory properties

Mădălina Ungureanu-Iuga, Claudiu Cobuz

"Ştefan cel Mare" University of Suceava, Romania

Keywords:

Grape by-product
Whey powder
Gluten-free
Pasta
Nixtamalized corn
Flour

Article history:

Received 14.04.2025
Received in revised form 12.05.2024
Accepted 30.06.2024

Corresponding author:

Mădălina Ungureanu-Iuga
E-mail: madalina.iuga @usm.ro

DOI:
10.24263/2310-1008-2025-13-1-3

Abstract

Introduction. Grape peels and whey are nutritious by-product that can be used to develop innovative foods.

Materials and methods. Pasta was made from nixtamalized white corn flour, corn starch, whey powder (5, 10, 15%), and grape peel powder (1, 3, 5%). The analyses included water absorption, cooking loss, texture (breaking force of dry pasta and firmness of cooked pasta), color, surface roughness, and sensory profile.

Results and discussion. The results indicated that quadratic models effectively described the relationships between ingredients and pasta properties, with strong statistical fits ($R^2 > 0.82$). Both ingredients and their interaction influenced cooking solid loss, water absorption, texture, roughness, and color.

Addition of whey powder in the amounts of 5, 10, and 15% reduced cooking solid loss from 15.48 to 14.24% and surface roughness from 17.75 to 14.80 μm but also decreased pasta firmness from 286.84 to 238.95 g. In contrast, grape peel increased cooking solid loss from 15.52 to 17.58% and firmness from 244.16 to 325.83 g while also raising roughness up to 3% addition, after which roughness declined. Water absorption decreased from 230.74 to 217.56% with increased levels of both additives. Texture analysis showed breaking force increased from 3239.00 to 3910.91 g with grape peel but decreased with higher whey content up to 10%, then increased.

Color (Chroma) was significantly affected: whey increased Chroma from 18.89 to 20.83 for uncooked pasta and from 16.88 to 18.18 for cooked pasta, while grape peel reduced it from 19.81 to 13.34 for uncooked pasta and from 17.65 to 10.42 for cooked pasta. Strong correlations were observed between cooking solid loss, roughness, and color parameters.

Sensory analysis showed that the sample with the highest whey concentration of 15% and the lowest grape skin content of 1% had low cooking solids loss and roughness, and received the highest scores for appearance, texture, colour, smell, taste and overall acceptability.

Conclusion. The results highlight the potential of specific combinations of whey and grape skin to enhance the quality of gluten-free pasta, providing valuable insights for product development.

Introduction

Growing global demand for healthier food options and the urgent need to address environmental concerns related to food industrial waste have spurred extensive research into fortification of staple foods, including baked goods (Stabnikova et al., 2023a, b). An example of such products is pasta, which is a widely consumed and affordable product with a long shelf life, serves as an ideal matrix for incorporating various by-products and protein concentrates to enhance its nutritional and functional attributes (Sissons, 2022; Stamatovska and Nakov, 2022; Ungureanu-Iuga et al., 2020). This approach not only provides valuable applications for industrial by-products, which are often produced in large quantities and pose disposal challenges, but also enriches the nutritional profile of common foods, offering consumers products with added health benefits (Simonato et al., 2019). The use of grape pomace, a winemaking by-product rich in various biologically active compounds, in bakery and confectionery technologies has attracted increasing attention (Grevtseva et al., 2023; Mironeasa et al., 2024; Stabnikova et al., 2021; Tolve et al., 2020).

Grape pomace peel is a valuable residue from winemaking, rich in antioxidant polyphenols, including various phenolic acids and flavonoids, and provides significant amounts of dietary fiber, helping to address common deficiencies in Western diets (Gaita et al., 2020). Increased dietary fiber intake can enhance satiety, reduce energy intake by lowering the bioavailability of fatty acids, improve glycemic control, and reduce the risk of type II diabetes and cardiovascular disease (Jane et al., 2019).

Meanwhile, whey protein and its derivatives are highly valued for their exceptional nutritional content and functional versatility, offering benefits such as immune support and improved cardiovascular health (Wani et al., 2015). Whey protein concentrate is often selected for fortifying various food products due to its favorable nutritional composition, cost-effectiveness, and wide availability (Kochubei-Lytvynenko et al., 2022; Komeroski and Oliveira, 2023; Prabhasankar et al., 2007). The incorporation of these ingredients significantly impacts several key quality parameters of pasta and other food products.

Fortification with fiber-rich by-products like grape peel often increases cooking loss, primarily due to the disruption of the gluten network (Ajila et al., 2010; Simonato et al., 2019). This effect can lead to more solids leaching into the cooking water. It has been proven that the combination of sodium caseinate and whey protein concentrate effectively reduces cooking loss in depigmented pearl millet-based gluten-free pasta (Kumar et al., 2019). The effect on pasta firmness varies depending on the specific by-product and its concentration. For example, olive pomace and mango peel fortification can increase pasta firmness due to the resistance provided by dietary fiber particles or the formation of a denser structure within the pasta matrix (Ajila et al., 2010; Simonato et al., 2019). By-product incorporation frequently alters the pasta's color, which is a significant factor in consumer perception. Overall consumer acceptability is crucial for the market success of fortified products. The high content of fiber-rich ingredients, such as fruit pomace, in the pasta led to reduced consumer acceptability (Ajila et al., 2010; Gaita et al., 2020). Notably, instant noodles fortified with ultrasound-modified whey protein achieved significantly higher sensory scores across multiple attributes, including surface appeal, hardness, stickiness, bite quality, mouthfeel, and overall acceptability.

While challenges in maintaining acceptable technological and sensory attributes exist, advancements in ingredient selection and processing techniques are proving effective in mitigating these issues, paving the way for market-ready functional foods. In this context, this paper aimed to investigate the combined effects of whey powder and grape peel on gluten free pasta based on nixtamalized corn flour. For this purpose, the cooking behavior, texture, color, roughness and sensory characteristics were considered.

Materials and methods

Materials

The ingredients used for the pasta included nixtamalized white corn flour, unhydrolyzed sweet commercial whey powder, corn starch, and grape peel powder, all purchased from a local market in Romania. The recipe for pasta samples comprised a starch-corn flour mix, whey powder, and grape peel powder, combined in varying proportions. This mixture also included 0.50% salt and 50% water (at 25 °C) to achieve optimal dough development.

Pasta dough was mixed for five minutes in a heavy-duty mixer and then extruded into rigatoni using a short pasta accessory. The pasta drying process included: air-drying for 30 min at room temperature, oven-drying with continuous ventilation for 60 min at 40 °C, followed by 120 min at 80 °C, and another 120 min at 40 °C. Finally, the pasta was cooled for 12 h at room temperature (Bergman et al., 1994).

Cooking characteristics

The water absorption capacity was determined in triplicate, adhering to the methodology delineated by Giménez et al. (2015). A 10 g sample of pasta was immersed in 200 mL of distilled water and subjected to boiling until the previously established optimal cooking time was achieved. Subsequently, the samples were drained for 3 min and their mass recorded.

The cooking loss of solids (CSL) was evaluated by collecting the cooking water obtained from the water absorption determination. This water was then placed into glass containers and dried in an oven at 105 °C to constant (Giménez-Bastida et al., 2015). The mass of the residual solids was subsequently measured, with the procedure replicated three times.

Texture determination

A Perten Instruments TVT-6700 texture analyzer, fitted with a 10 kg load cell, was used to determine the textural parameters of pasta samples.

The breaking force of dry pasta was evaluated through a three-point bend test utilizing an aluminum break probe with a 13 mm width. Each pasta piece was cut at a test speed of 3 mm/s, initiated by a 50 g trigger force. The maximum force needed to fracture the pasta was reported as its breaking force. Five measurements were conducted for each sample.

For cooked pasta firmness, a single-cycle compression method was applied. An AACC 16-50 transparent noodle probe was used, set at 0.5 mm above the scale plate, with a test speed of 0.2 mm/s. Two cooked pasta pieces were positioned on a heavy-duty stand (BB) with a polythene protection insert (HDS) and analyzed as detailed above. These measurements were performed in triplicate (Ungureanu-Iuga et al., 2020).

Color evaluation

To characterize the color of dry and cooked pasta, a Konica Minolta CR-400 colorimeter (Tokyo, Japan) was employed. The L*, a*, and b* color parameters (lightness, red-green intensity, and yellow-blue intensity, respectively) were recorded from the CIE-Lab system via reflectance measurements. Five measurements were performed for every sample to ensure consistent data collection. Chroma was calculated using equation:

$$Chroma = \sqrt{a^{*2} + b^{*2}}$$

Roughness analysis

To evaluate pasta roughness, a Mahr CWM100 microscope (Gottingen, Germany) was employed. Four distinct areas of each sample were observed, and the resulting data was subsequently analyzed using the trial version of Mountain Map software (Digital Surf, France) version 8. Roughness values were recorded in triplicate, representing the mean of computed profiles from three of the examined areas.

Sensory profile

Sensory evaluation of the pasta samples was conducted in two separate sessions by a panel of 9 semi-trained judges. The judges assessed various attributes, including color, taste, smell, texture, appearance, and overall acceptability. For evaluation, pasta samples were boiled to their predetermined optimal cooking time, then presented on white plates with a single drop of olive oil on each piece. A nine-point hedonic scale was utilized to quantify the preference for each sensory characteristic.

Statistical data processing

Data processing was done by using Design Expert (trial version). Samples were prepared as described in our previous work (Ungureanu-Iuga et al., 2020). The influence of whey (factor A) and grape peel (factor B) was evaluated by using quadratic model. To confirm the models' suitability, Analysis of Variance (ANOVA) was conducted ($p < 0.05$), taking into account the F-value, p-value, R^2, *Adjusted* R^2, and *Predicted* R^2. Whey concentration was 5, 10 or 15%, while grape peel concentration was 1, 3 of 5%. The difference between the selected samples were evaluated trough ANOVA with Tukey test ($p < 0.05$) using XL STAT 2024 version.

Results and discussion

Effects of whey and grape peels on pasta physical characteristics

Gluten free pasta quality represents a challenge for researchers and producers. The impact of whey powder and grape peel on corn pasta characteristics is described by the quadratic models (Table 1) which fitted well the experimental data ($R^2 > 0.82$, $p < 0.01$).

CSL and pasta water absorption were significantly affected by both factors (whey and grape peel), as well as their interaction (Table 1). While whey powder determined a decrease of the amount of solids released during cooking, grape peel exhibited a reversed trend. Sufficient protein can strengthen the protein network of gluten free pasta, reducing cooking loss. Adding whey powder led to starch retention within the protein matrix, improving cooked pasta shape and dough extensibility (Zhao et al., 2024). Similar to the results obtained by Zhao et al. (2024), whey powder specifically decreased gluten-free pasta's cooking loss by forming a surface film that created a tight network which inhibited starch granule expansion during gelatinization, thus minimizing cooking loss. The inclusion of by-products, particularly those rich in fiber like grape peels, disrupts the gluten and starch matrix by enhancing water penetration and competing with starch for moisture, thereby weakening the formation of a strong structural network in the pasta and leading to higher cooking loss (Dey et al., 2021).

Table 1

ANOVA results for the evaluation of whey (A) and grape peels (B) impact on pasta quality

Factor	CSL (%)	Water absorption (%)	Breaking force (g)	Firmness (g)	Chroma uncooked	Chroma cooked	Roughness (μm)
Const.	16.78	217.57	3774.78	311.96	15.17	12.52	21.56
A	-1.09**	-2.55**	236.39**	18.06*	0.72**	-0.17	-1.98**
B	1.03**	-6.59**	335.61**	40.83**	-3.23**	-3.61**	1.67**
AB	-0.48**	5.19**	-288.42**	42.00**	-0.26	-0.81*	-0.51
A^2	-0.66**	0.78	682.83**	18.72	0.05	-0.12	1.41*
B^2	-0.22	6.58**	-199.17	-26.94*	1.40**	1.52**	-5.01**
Model evaluation							
p	< 0.01	< 0.01	< 0.01	< 0.01	< 0.01	< 0.01	< 0.01
R^2	0.91	0.93	0.82	0.82	0.97	0.89	0.90
Adj. R^2	0.89	0.91	0.78	0.78	0.96	0.86	0.88
Pred. R^2	0.84	0.88	0.71	0.71	0.95	0.81	0.83

** – significant at $p < 0.01$, * significant at $p < 0.05$.

Water absorption decreased significantly ($p < 0.05$) as the addition level of both whey and grape peel increased (Figure 1). The negative effect of whey can be due to milk proteins which competitively reduce the water necessary for starch swelling during gelatinization (Kumar et al., 2019). Similar reduction of water absorption was observed for pearl millet gluten-free pasta when sodium caseinate and whey concentrate were added (Kumar et al., 2019). Padalino et al. (2018) also reported the increase of water absorption when olive pomace was incorporated in pasta. The increased water absorption observed with higher grape peel content in pasta can be attributed to several factors: higher pectin content (especially hydrophobic, highly methylated pectin's), the ability of polyphenols to form hydrogen bonds with other macromolecules, and the presence of mineral components (Gumul et al., 2023).

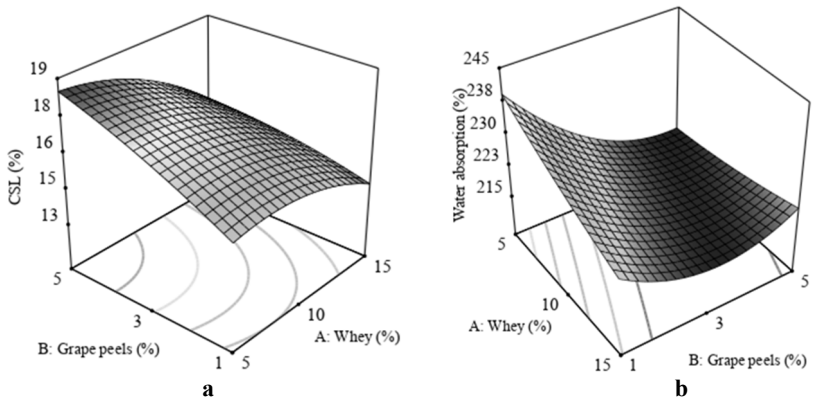

Figure 1. Combined effects of whey (A) and grape peels (B) on pasta cooking behavior: a) cooking loss of solids (CSL) and b) water absorption

Texture parameters, namely dry pasta breaking force and cooked pasta firmness were significantly influenced by both additions of whey and grape peel and their interaction (Table 1). Breaking force decreased when whey was included in corn pasta formulation up to 10%, then increased. An increase in breaking force was observed when pea protein flour was incorporated into gluten-free amaranth pasta, a finding also reported by (Gupta, 2019). Drawing from Belton's gluten model, which differentiates between linear glutenin proteins (contributing elasticity through disulfide and hydrogen bonds) and globular gliadin proteins (providing viscosity and slowing elastic recovery), it is proposed that whey proteins may either mimic gliadins by increasing viscosity and decreasing elasticity, or directly interfere with glutenin's structure by forming hydrogen and disulfide bonds, ultimately leading to a disruption of the gluten network (Prabhasankar et al., 2007).

Grape peel incorporation led to higher breaking force (Figure 2). Antioxidant compounds are hypothesized to strengthen the gluten network during both pasta dough production and the subsequent drying process (Gałkowska et al., 2022).

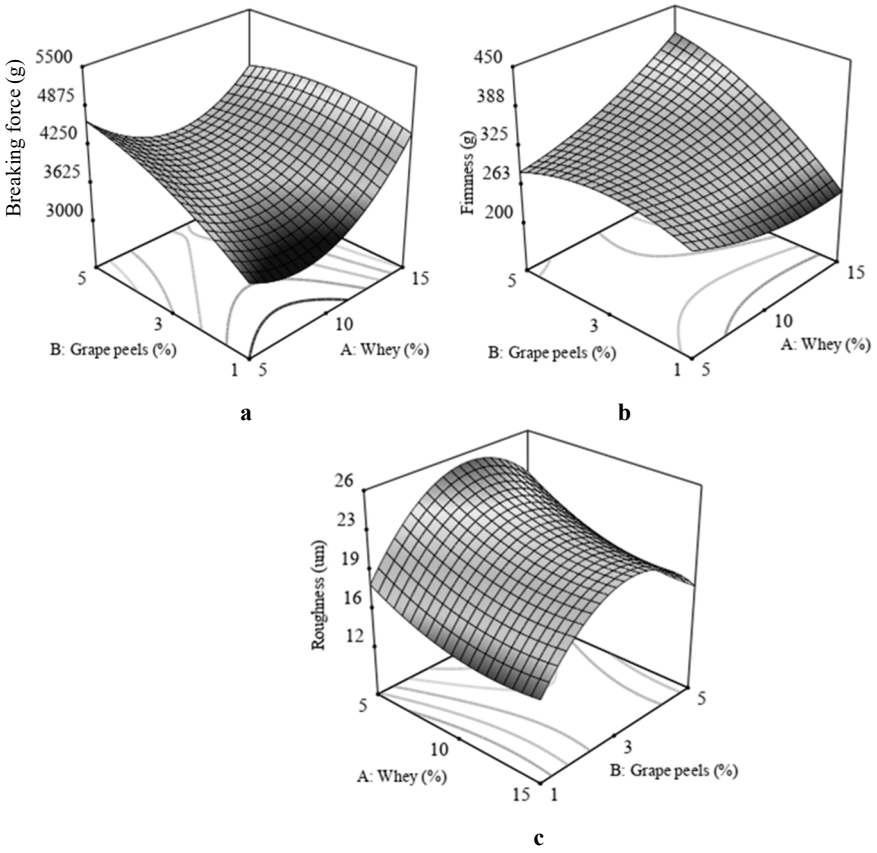

Figure 2. Combined effects of whey (A) and grape peels (B) on pasta texture: a – dry pasta breaking force, b – cooked pasta firmness, and c – roughness

Whey powder determined a decrease in cooked pasta firmness, while the opposite trend was observed for grape peel addition (Figure 2). It's possible that whey proteins contribute to reduced firmness by forming distinct entities rather than a cohesive protein gel (Kumar et al., 2019). Furthermore, sulfhydryl groups in whey proteins may oxidize gluten's disulfide bonds, which is hypothesized to reduce firmness (Kumar et al., 2019). Other studies reported that the addition of mango peel powder and olive pomace was found to increase pasta firmness, suggesting that fiber-rich by-products may enhance texture by contributing structural resistance through their dietary fiber content (Ajila et al., 2010; Simonato et al., 2019).

Roughness was affected significantly ($p < 0.05$) by both factors, but their interaction had a non-significant effect. Incorporation of whey powder in corn pasta was proved to exert a beneficial effect of pasta roughness by decreasing this parameter (Figure 2). Grape peel addition up to 3% led to an increase in surface roughness, then it decreased. Komeroski and Oliveira (2023) reported that whey can enhance water binding and stabilize dough, which in turn contributes to smoother texture and surface refinement in pasta products—suggesting a reduction in surface roughness. Aravind et al. (2012) reported that adding dietary fiber resulted in more irregular and uneven wheat spaghetti surfaces, potentially leading to a fragile structure.

Uncooked pasta color described by Chroma was significantly affected ($p < 0.05$) by whey and grape peel addition, but not by their interaction (Table 1). Cooked pasta Chroma was influenced significantly ($p < 0.05$) only by grape peel quantity and its interaction with whey powder. The combined effects of whey and grape peels addition on pasta color are displayed in Figure 3.

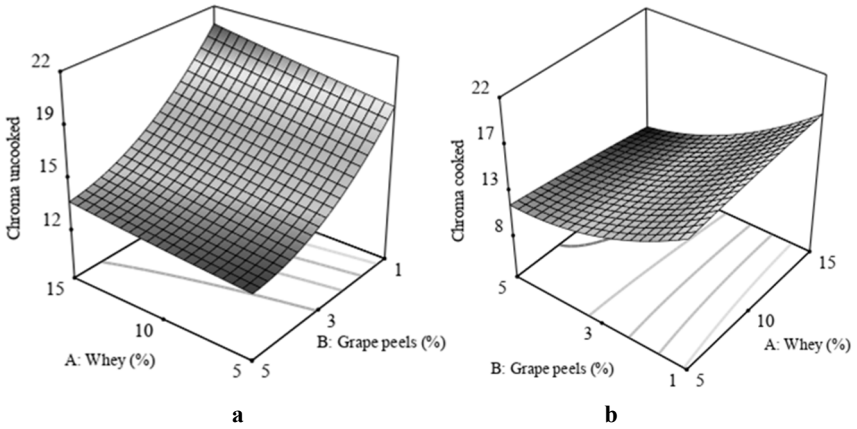

Figure 3. Combined effects of whey (A) and grape peels (B) on pasta color: a – dry pasta Chroma; b – cooked pasta Chroma

Whey powder incorporation led to higher Chroma values as the level increased for both uncooked and cooked pasta. On the other hand, grape peel level increase led to a progressive reduction in both uncooked and cooked pasta Chroma (Figure 3). It has been stated that cookies exhibited changed color when whey protein was added, likely due to sugar caramelization and whey protein darkening during baking, with general compounds degradation also contributing to color changes (Wani et al., 2015). Tolve et al. (2020)

reported changes in pasta color as the addition level on grape pomace was higher due to the presence of pigments in the ingredient added.

Correlations between variables

The relationships between dependent variables and factors are shown in Figure 4.

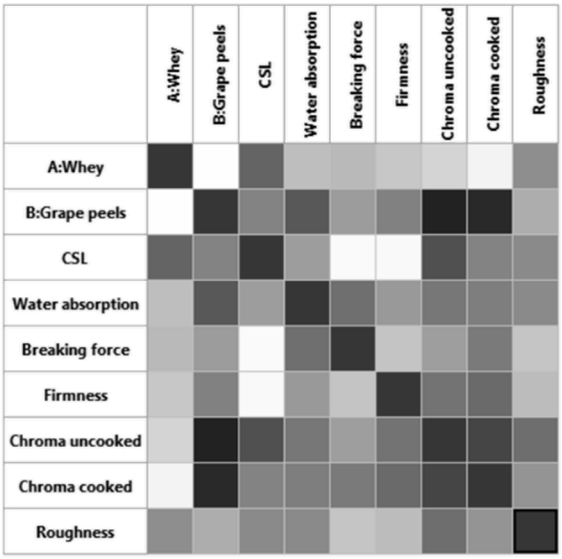

Figure 4. Correlations between variables

CSL was negatively correlated with both uncooked and cooked Chroma ($p < 0.05$, r = -0.74, r = -0.52 respectively), and positively with pasta roughness ($p < 0.05$, r = 0.58). Water absorption was negativley correlated with dry pasta breaking force ($p < 0.05$, r = -0.61), and positively with both color parameters ($p < 0.05$, r > 0.63). This is consistent with previous statements that incorporation of fiber-rich ingredients led to changes in pasta network, a weak structure absorbing more water and causing higher release of solids during cooking (Dey et al., 2021). Strong positive correlation ($p < 0.05$, r = 0.92) was obtained between uncooked and cooked pasta Chroma. Negative correlation was obtaine between roughness and uncooked pasta Chroma ($p < 0.05$, r = -0.61).

For further sensory characterization, the samples with the highest water absorption, breaking force, Chroma, and the lowest cooking loss of solids and roughness were selected (pasta firmness was considered in range). Thus, sample P1 contains 5% whey and 1% grape peels, P3 contains 15% whey and 1% grape peels, and P6 contains 15% whey and 3% grape peels (Figure 5) were evaluated.

P1 **P3** **P6**

Figure 5. Appearance of selected pasta

Physical and sensory characteristics of the selected samples

The characteristics of the selected samples are displayed in Table 2.

Table 2

Physical characteristics of the selected samples

Variable	Sample		
	P1	**P3**	**P6**
Whey (%)	5	15	15
Grape peels (%)	1	1	3
CSL (%)	15.69 ± 0.48^{a}	14.24 ± 0.48^{b}	15.09 ± 0.48^{ab}
Water absorption (%)	236.54 ± 2.31^{a}	223.78 ± 2.31^{b}	215.73 ± 2.31^{c}
Breaking force (g)	3510.22 ± 269.03^{b}	4447.64 ± 269.03^{a}	4696.74 ± 269.03^{a}
Firmness (g)	292.43 ± 25.93^{b}	238.96 ± 25.93^{b}	359.46 ± 25.93^{a}
Chroma uncooked	18.26 ± 0.57^{b}	20.84 ± 0.57^{a}	15.49 ± 0.57^{c}
Chroma cooked	16.25 ± 1.26^{a}	18.18 ± 1.26^{a}	11.66 ± 1.26^{b}
Roughness (μm)	19.06 ± 1.23^{a}	14.80 ± 1.23^{b}	21.05 ± 1.23^{a}

[a-c] – different letters in the same row indicate significant differences between samples ($p < 0.05$).

The smaller CSL was observed for the sample with the highest whey concentration (15%) and the lowest grape peel level (1%), namely P3. Whey powder could interact with starch to form a stronger matrix which led to lower CSL, similar observations being made by (Khatkar et al., 2024). Reports indicate that incorporating fiber-rich ingredients like grape peel can elevate cooking loss due to its potential to disrupt and weaken the starch-gluten network. This disruption may accelerate starch gelatinization, thereby facilitating increased leaching of gelatinized starch from the pasta during cooking (Tolve et al., 2020). The highest water absorption was observed for P1 which contained the lowest whey and grape peels amounts. Water absorption in pasta is linked to starch swelling and gelatinization, but it can be restricted by protein polymerization forming a network that entraps starch granules during drying and cooking, while gluten dilution and fiber-starch competition for water also play a role (Gałkowska et al., 2022). The sample with 15% whey and 3% grape peel (P6) exhibited the greatest breaking force and firmness, and the lowest Chroma for both uncooked and cooked state. The results were in agreement with previous study regarding the effects of blackcurrant pomace on durum wheat pasta (Gałkowska et al., 2022).

It's possible that an optimal spatial distribution of grape peel fiber particles within the pasta structure contributed to its increased firmness (Gałkowska et al., 2022). The smallest roughness was obtained for 15% whey and 1% grape peel (P3). This can be due to the

presence of fibers in dough matrix which disrupted gluten matrix. On the other hand, whey could promote the formation of stronger smoother networks (Khatkar et al., 2024).

Sensory analysis of the selected samples revealed that the sample with the highest whey concentration (15%) and the lowest grape peel amount (1%) – P3, obtained the best scores for appearance, texture, color, smell, taste and general acceptability, followed by P6 with 15% whey and 3% grape peel and P1 with 5% whey and 1% grape peel (Figure 6).

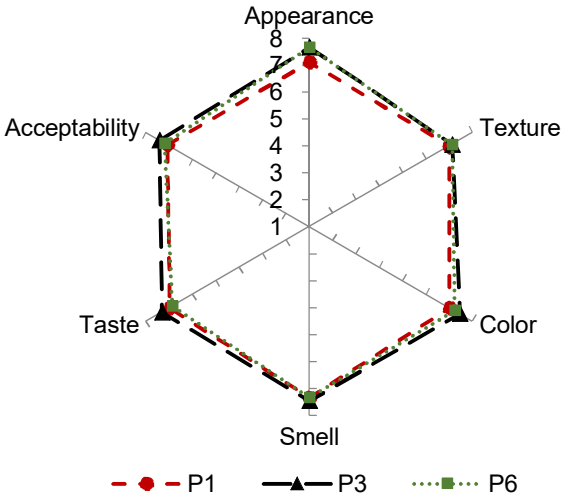

Figure 6. Sensory properties of the selected samples

It has been stated that incorporating whey into bakery and pasta products offers technological, nutritional, and sensory benefits, including enhanced sensory attributes (Komeroski and Oliveira, 2023). On the other hand, high amounts of fiber-rich ingredients like grape peel led to lower sensory characteristics, similar to the results reported by Gaita et al. (2020).

Conclusions

This research successfully demonstrated the significant impact of whey powder and grape peel powder on the quality of gluten-free corn pasta. Quadratic models accurately described these effects, showing strong fits to experimental data. Whey powder consistently improved pasta quality by decreasing cooking loss (CSL), reducing water absorption, and lowering roughness. It also increased both uncooked and cooked pasta Chroma as color intensity. Conversely, grape peel generally led to increased CSL and roughness, while reducing Chroma. However, grape peel positively influenced breaking force and cooked pasta firmness. The interplay of these ingredients is crucial. For instance, increasing whey initially decreased breaking force, while grape peel increased it. Notably, the sample with 15% whey, 1% grape peel emerged as superior, exhibiting the lowest CSL and roughness, and achieving the best sensory scores across all attributes. This highlights the potential of specific whey and grape peel combinations to enhance gluten-free pasta quality, offering valuable insights for product development.

References

Ajila C.M., Aalami M., Leelavathi K., Rao U.J.S.P. (2010), Mango peel powder: A potential source of antioxidant and dietary fiber in macaroni preparations, *Innovative Food Science and Emerging Technologies*, 11(1), pp. 219–224, https://doi.org/10.1016/j.ifset.2009.10.004

Aravind N., Sissons M., Egan N., Fellows C. (2012), Effect of insoluble dietary fibre addition on technological, sensory, and structural properties of durum wheat spaghetti, *Food Chemistry*, 130(2), pp. 299–309, https://doi.org/10.1016/j.foodchem.2011.07.042

Bergman C.J., Gualberto D.G., Weber C.W. (1994), Development of a high-temperature-dried soft wheat pasta supplemented with cowpea (*Vigna unguiculata* (L.) Walp). Cooking quality, color, and sensory evaluation, *Cereal Chemistry*, 71(6), pp. 523–527.

Dey D., Richter J. K., Ek P., Gu B.J., Ganjyal G.M. (2021), Utilization of food processing by-products in extrusion processing: A review, *Frontiers in Sustainable Food Systems*, 4, https://doi.org/10.3389/fsufs.2020.603751

Gaita C., Alexa E., Moigradean D., Conforti F., Poiana M.A. (2020), Designing of high value-added pasta formulas by incorporation of grape pomace skins, *Romanian Biotechnological Letters*, 25(3), pp. 1607–1614, https://doi.org/10.25083/rbl/25.3/1607.1614

Gałkowska D., Witczak T., Pycia K. (2022), Quality characteristics of novel pasta enriched with non-extruded and extruded blackcurrant pomace, *Molecules*, 27, pp. 1–16, https://doi.org/10.3390/molecules27238616

Giménez-Bastida J.A., Piskuła M., Zieliński H. (2015), Recent advances in development of gluten-free buckwheat products, *Trends in Food Science and Technology*, 44(1), pp. 58–65. https://doi.org/10.1016/j.tifs.2015.02.013

Grevtseva N., Gorodyska O., Brykova T., Gubsky S. (2023), The use of wine waste as a source of biologically active substances in confectionery technologies, In: O. Stabnikova, O. Shevchenko, V. Stabnikov, O. Paredes-López (Eds.), *Bioconversion of Waste to Value-added Products*, pp. 69-111, CRC Press, Boca Raton, https://doi.org/10.1201/9781003225287-3

Gumul D., Kruczek M., Ivanišová E., Słupski J., Kowalski S. (2023), Apple pomace as an ingredient enriching wheat pasta with health-promoting compounds, *Foods*, 12(4), 804, https://doi.org/10.3390/foods12040804

Gupta C. (2019), *Development of gluten-free pasta using amaranth flour and pea protein flour*, Thesis, Iowa State University Ames, Iowa.

Jane M., McKay J., Pal S. (2019), Effects of daily consumption of psyllium, oat bran and polyGlycopleX on obesity-related disease risk factors: A critical review, *Nutrition*, 57, pp. 84–91, https://doi.org/10.1016/j.nut.2018.05.036

Khatkar A.B., Kaur A., Dhull S.B., Khatkar S.K., Mehta N., Kaur J., Goksen G. (2024), Ultrasound-modified whey protein-enriched instant noodles: Enhancement in functional, rheological, cooking, and structural attributes, *Food Science and Nutrition*, 12(2), pp. 851–859, https://doi.org/10.1002/fsn3.3797

Kochubei-Lytvynenko O., Bilyk O., Bondarenko Y., Stabnikov V. (2022), Whey proteins in bakery products, In: O. Paredes-López, O. Shevchenko, V. Stabnikov, V. Ivanov (Eds.), *Bioenhancement and Fortification of Foods for a Healthy Diet*, pp. 67-88, CRC Press, Boca Raton, https://doi.org/10.1201/9781003225287-5

Komeroski M.R., Oliveira V.R.d. (2023), Influence of the amount and type of whey protein on the chemical, technological, and sensory quality of pasta and bakery products, *Foods*, 12(14), 2801, https://doi.org/10.3390/foods12142801

Kumar C.T.M., Sabikhi L., Singh A.K., Raju P.N., Kumar R., Sharma R. (2019), Effect of incorporation of sodium caseinate, whey protein concentrate and transglutaminase on the properties of depigmented pearl millet based gluten free pasta, *LWT-Food Science and Technology*, 103, pp. 19–26, https://doi.org/10.1016/j.lwt.2018.12.071

Mironeasa S., Ungureanu-Iuga M., Ursachi V.F., Mironeasa C. (2024), Seedless grape pomace to increase fiber content in extruded corn snacks, *Ukrainian Food Journal*, 13(4), pp. 657–674, https://doi.org/10.24263/2304-974X-2024-13-4-3

Padalino L., D'Antuono I., Durante M., Conte A., Cardinali A., Linsalata V., Mita G., Logrieco A.F.,

Del Nobile M.A. (2018), Use of olive oil industrial by-product for pasta enrichment, *Antioxidants*, 7(4), 59, https://doi.org/10.3390/antiox7040059

Prabhasankar P., Rajiv J., Indrani D., Rao G.V. (2007), Influence of whey protein concentrate, additives, their combinations on the quality and microstructure of vermicelli made from Indian *T. Durum* wheat variety, *Journal of Food Engineering*, 80(4), pp. 1239–1245, https://doi.org/10.1016/j.jfoodeng.2006.09.013

Simonato B., Trevisan S., Tolve R., Favati F., Pasini G. (2019), Pasta fortification with olive pomace: Effects on the technological characteristics and nutritional properties, *LWT-Food Science and Technology*, 114, 108368, https://doi.org/10.1016/j.lwt.2019.108368

Sissons M. (2022), Development of novel pasta products with evidence based impacts on health—A review, *Foods*, 11(1), 123, https://doi.org/10.3390/foods11010123

Stamatovska V., Nakov G. (2022), Management of apple and grape processing byproducts, A review, *Ukrainian Food Journal*, 11(4), 518-541, https://doi.org/10.24263/2304-974X-2022-11-4-4

Stabnikova, O., Marinin, A., Stabnikov, V. (2021), Main trends in application of novel natural additives for food production, *Ukrainian Food Journal*, 10(3), pp. 524–551, https://doi.org/10.24263/2304-974X-2021-10-3-8

Stabnikova O., Shevchenko O., Stabnikov V., Paredes-López O. (Eds.). (2023a), *Bioconversion of Waste to Value-added Products*, CRC Press, Boca Raton, https://doi.org/10.1201/9781003329671

Stabnikova O., Shevchenko A., Stabnikov V., Paredes-López O. (2023b), Utilization of plant processing wastes for enrichment of bakery and confectionery products, *Ukrainian Food Journal*, 12(2), 299-308, https://doi.org/10.24263/2304-974X-2023-12-2-11

Tolve R., Pasini G., Vignale F., Favati F., Simonato B. (2020), Effect of grape pomace addition on the technological, sensory, and nutritional properties of durum wheat pasta, *Foods*, 9(3), 354, https://doi.org/10.3390/foods9030354

Ungureanu-Iuga M., Dimian M., Mironeasa S. (2020), Development and quality evaluation of gluten-free pasta with grape peels and whey powders, *LWT-Food Science and Technology*, 130, 109714, https://doi.org/10.1016/j.lwt.2020.109714

Wani S.H., Gull A., Allaie F., Safapuri T.A. (2015), Effects of incorporation of whey protein concentrate on physicochemical, texture, and microbial evaluation of developed cookies, *Cogent Food and Agriculture*, 1(1), pp. 1-9, https://doi.org/10.1080/23311932.2015.1092406

Zhao R., Zhao R., Li Q., Li K., Liu Q., Liu W., Hu H. (2024), Improvement effect of different protein powder on cooking characteristics of gluten-free pasta and the establishment of quality evaluation based on principal component analysis, *International Journal of Food Science and Technology*, 59(2), pp. 1138–1149, https://doi.org/10.1111/ijfs.16728

Cite:

UFJ Style

Ungureanu-Iuga M., Cobuz C. (2025), Effects of whey and grape peels on pasta physical and sensory properties, *Ukrainian Journal of Food Science*, 13(1), pp. 5–16, https://doi.org/10.24263/2310-1008-2025-13-1-3

APA Style

Ungureanu-Iuga, M., & Cobuz, C. (2025). Effects of whey and grape peels on pasta physical and sensory properties. *Ukrainian Journal of Food Science, 13*(1), 5–16. https://doi.org/10.24263/2310-1008-2025-13-1-3

Assessment of whole-grain flour quality for confectionery use

Andrii Vorvykhvost, Yuliia Kambulova, Olena Kokhan, Olena Potapenko, Oleksandr Nepokrytov

National University of Food Technologies, Kyiv, Ukraine

Keywords:

Whole grain
Flour
Butter
Cookies
Enzyme
Glucoamylase
Cellulase

Article history:

Received 12.01.2025
Received in revised form 16.06.2024
Accepted 30.06.2024

Corresponding author:

Yuliia Kambulova
E-mail: kambulova.julya@ukr.net

DOI:
10.24263/2310-1008-2025-13-1-4

Abstract

Introduction. The aim of the research was to determine the quality indicators of whole grain millet flour for use in the technology of cookies from viscous-plastic dough.

Materials and methods. Millet whole grain flour (wheat, spelt, barley, amaranth, buckwheat) and enzymes – fungal glucoamylase and cellulase were used. The moisture content in the flour was determined by the thermogravimetric method, whiteness by a photoelectric device, total acidity by titration, ash content by the accelerated method, coarseness by a laboratory scatterer, gluten was evaluated by content, extensibility, elasticity, resistance to deforming load. The morphology of starch granules was examined using an electron microscope, flour color was measured with a colorimeter, and sugar accumulation was determined by the iodometric method.

Results and discussion. Whole-grain millet flour differed from high-grade wheat flour in appearance, taste, smell, and color. It was found that spelt and barley flours were the lightest in color, while wheat and amaranth flours were the darkest.

The granulometric composition of millet flour was heterogeneous, with particles of varying sizes. The main fraction of each flour type exceeded the particle size of high-grade wheat flour: amaranth and wheat – 200–150 microns; buckwheat and barley – >200 microns and 132–150 microns, respectively; spelt – >200–150 microns. It was found that the gluten complex was formed only in whole grain wheat and spelt flour. The amount of gluten in them was lower compared to high-grade wheat flour by 34.5 and 24.5%, respectively. According to the gluten deformation index, wheat flour belonged to group I, but had 10% less extensibility, spelt flour – to group II with extensibility 6.7% greater than wheat. In barley, buckwheat and amaranth flour, the gluten framework was not formed.

Each type of flour had a characteristic structure of starch grains: small ones – in amaranth and barley, large polygonal ones – in green buckwheat flour, medium ones – round or oval ones – in wheat and spelt. Dough with whole grain millet flour did not form a viscous-plastic structure sufficient for cookies.

Conclusions. When using whole-grain millet flour, the combined application of glucoamylase and cellulase was recommended, as it increased the content of water-soluble compounds and improved the viscous-plastic consistency of the cookie dough.

Introduction

One of the key requirements in cookie production is the quality of the flour, as it directly influences the structural and mechanical properties of the dough, the consistency and appearance of the cookies, and also determines the parameters for dough mixing and shaping (Boz, 2019).

The main type of flour used in cookie technology is high grade wheat flour, less often – first, second grade (Emem et al., 2024). As an alternative, for people with dietary requirements, as well as to increase the nutritional value of the finished product, pumpkin (Stabnikova et al., 2023), rice, buckwheat, amaranth, barley, corn and other types can be used (Ivanov et al., 2021). Highgrade flour has a light color, low ash content (0.5 – 0.55%) and a small amount of highly dispersed grain shell particles. Dough from this flour had delicate texture and a pleasant taste (Dziki et al., 2024). Non-traditional types of flour have specific sensory characteristics inherent in natural grain, as well as a higher content of shell particles. The absence of gluten protein fraction or the inability to form a complete gluten complex significantly affected the structure of the finished product (Xu et al., 2020). Technological tasks in such cases included the selection of structure-forming agents to form a complete coagulation structure of the dough or limiting the recipe dosage of non-traditional types of flour to an acceptable level of quality of dough and finished products (Poiana et al., 2023).

In the production of butter and sugar cookies, the technological process is aimed at forming a coagulation–crystallization structure with plastic-viscous properties. Therefore, dough mixing is carried out in a way that prevents the development of a gluten network, highlighting the inefficient use of wheat flour and supporting the search for alternative flour sources (Ferradji et al., 2024).

For the production of cookies with plastic-viscous characteristics of the dough and in line with modern trends in healthy nutrition, it is advisable to use whole grain flour from various grain crops. The natural vitamin and mineral complexes, as well as the carbohydrate–amylase and protein-proteinase systems present in such flour, offer optimal physiological availability (Khan et al., 2024).

Regulation of the dough structure based on whole grain flour in order to simplify the technological stages of kneading and shaping, ensuring high quality of the finished product is advisable to carry out by introducing enzyme preparations of a directed spectrum of action (Chowdhury et al., 2024).

The issue of studying the quality of whole grain millet flour in the technologies of flour confectionery products was not studied enough. The baking properties of whole grain wheat flour from black wheat showed that the raw gluten content in it was 23.5% of the I quality group, light brown in color with an acidity of 2.6 °H (Zhygunov et al., 2019). The flour residue when sifting on sieve with holes 670 microns was 4%, the residue on sieve with holes 380 microns was 60%. To improve the quality of flour products, it was recommended to use additives and enzymes (Gómez et al., 2020).

The need to use wheat and rye starters was proved, which caused molecular degradation of arabinoxylan with a decrease in its mass and the formation of a more heterogeneous fine dough structure (Kulathunga et al., 2024). To enhance the quality of bakery products, several biotechnological approaches have been employed. Fermentation with lactic acid bacteria has been used to improve the bioavailability of biologically active compounds in whole-grain wheat flour (Islam et al., 2024). Fermentation with yeasts of the genera *Pichia kudriavzevii*, *Saccharomyces cerevisiae*, *Pichia fermentans*, and *Kluyveromyces marxianus*, along with lactic acid bacteria such

as *Lactiplantibacillus plantarum* and *Lacticaseibacillus paracasei*, has been shown to reduce phytic acid content (Qvirist et al., 2024). Additionally, the incorporation of peroxidase into whole-wheat flour has been reported to improve the quality of the resulting products (Hemalatha and Rao, 2024). It was proven that the digestibility of bread improved when using whole grain flour of different dispersion (Jiang et al., 2024), and the glycemic load on the human body reduced when eating bread with the addition of whole grain flour (Jiang et al., 2024).

It was found that the antioxidant activity of whole wheat flour decreased during storage at different temperatures (−20 °C, 4 °C, and 20 °C), with a more pronounced decline observed at higher temperatures (60 °C) during the first 15 days (Kumar et al., 2024). Additionally, it was shown that whole-grain products such as chapatis retained more antioxidant activity than refined products such as pasta.

Processing whole-grain flour into chapatis resulted in a 30% reduction in antioxidant activity, whereas processing it into pasta led to a 70% reduction. The antioxidant properties of whole wheat flour bread enriched with *Celosia argentea* seed flour were evaluated, along with its antidiabetic potential and phytochemicals (Azeez et al., 2024). Bread crumb was characterized by total flavonoid content (0.61–0.85 mg/g), total phenolic content (1.1–1.31 gallic acid equivalents per gram (mg GAE/g), total antioxidant capacity (1.19–3.34 mg GAE/g), iron-reducing antioxidant capacity (0.13–0.54 mg/g) and DPPH (2,2-diphenyl-1-picrylhydrazyl) (42.58–49.75%). The IC50 values obtained for wheat bread substituted with *Celosia argentea* seeds ranged from 58.20 to 171.05 μg/ml.

Antioxidant properties and α-amylase inhibition showed an increase with increasing percentage of *Celosiae argentea* seed inclusion. Biologically active compounds detected in bread prepared by enriching wheat flour (whole grain and refined) with *Celosia argentea* seed flour included 9,12-octadecadienoic acid methyl ester, docosanoic acid methyl ester, E,E,Z-1,3,12-nonadecatriene-5,14-diol, linoleic acid ethyl ester and squalene. Differences in whole-grain wheat flour from various growing regions were observed in the content of phenolic compounds, carotenoids, and antioxidant activity (Kim et al., 2024).

Thus, the analysis made it possible to determine that the use of whole grain flour in flour product formulations is a relevant issue, the study of which has recently received increasing attention. However, most of the existing research is devoted to the assessment of the baking properties of flour, mainly whole grain wheat flour. Information on the possibilities of its use for cookies, as well as the analysis of the technological capabilities of whole grain flour from other cereals, is quite limited.

Therefore, the aim of the research was to determine the quality indicators of whole grain millet flour for use in the technology of cookies from viscous-plastic dough.

Materials and methods

Materials

The following materials were used in the study: whole grain millet flour from wheat, spelt, barley, amaranth, and green buckwheat (Zemledar, Ukraine). To improve the dough structure, enzyme preparations– fungal glucoamylase Omnszym 31022 and fungal cellulase Alphamalt C 21032 (Mühlenchemie, Germany) were used.

Methods

Moisture content in flour

The moisture content in flour was determined by the thermogravimetric method of accelerated drying in a drying cabinet (Hetman et al., 2021). 5 g of the test sample was weighed into two pre-dried and weighed boxes, dried in an electric drying oven at a temperature of 130 °C for 40 min, cooled, weighed and the mass fraction of moisture was calculated using formula:

$$W = \frac{m_1 - m_2}{m} \times 100\%,$$

where m is the mass of the flour sample before drying; m_1 is the mass of the box with the sample before drying; m_2 is the mass of the box with the sample after drying.

Whiteness of flour

The whiteness of the flour was assessed using a photoelectric device (Zhang et al., 2025). The essence of the method is to measure the reflectivity of the compacted-smoothed surface of the flour.

For analysis, two samples weighing 50±5 g were taken from different places of the average flour sample and filled into two cuvettes through a special sieve. The flour in the cuvette was slightly compacted, leveled over the entire surface, and the excess was removed. The photoelectric head of the device was slowly lowered onto the flour and readings were taken using a digital indicator with an accuracy of 0.1 unit of the conventional scale of the device.

Total acidity of flour

Total acidity was determined by titration of a flour suspension of 5 g of flour and 50 ml of distilled water with a 0.1 mol/l alkali solution of KOH or NaOH (Shevchenko, 2018).

Ash content in flour

The ash content in flour was determined by an accelerated method by burning a sample with an accelerator $Mg(CH_3COO)_2$ (Czaja et al., 2020).

Flour particles size

The size of the flour particles was determined using a laboratory disperser with an oscillation frequency of 180–200 min^{-1}, and a set of sieves for determining the size and mass fraction of flour particles. Sieves designed for different types of flour were used with holes 750, 670, 200, 150, and 132 microns (Shevchenko et al., 2022).

Gluten quantity and quality

The raw gluten content and its quality were determined in dough from a 25 g flour sample and 14 ml water after 20 min of exposure. To determine extensibility, elasticity, and resistance to deforming load, 4 g gluten samples were rolled into balls and immersed in water at a temperature of 18–20°C for 15 min.

The elasticity of gluten was assessed by the speed of recovery of the initial length of the gluten ball after stretching for a distance of about 2 cm. By the degree and speed

of recovery of the initial length, elasticity was assessed as: good – gluten stretched quite strongly with mandatory almost complete recovery of the shape; unsatisfactory – did not recover at all, with partial ruptures of individual layers and after removing the force quickly compresses (elastic, inelastic); satisfactory elasticity – an intermediate position between good and unsatisfactory.

The extensibility of gluten was assessed over a ruler according to the following gradation: short – up to 10 cm, medium – 10–20 cm, long – more than 20 cm. The resistance of gluten to compressive deformation load was determined on the gluten deformation index device (Shevchenko, 2023).

Shape of starch grains in flour

The determination of the shape of starch grains was assessed visually, using an electron microscope (Red'ko et al., 2021) at a magnification of 10x10. To prepare the test sample, the flour suspension was applied to a glass slide, stained with iodine solution, a coverslip was placed on top and fixed on the microscope.

Flour color

The color of the flour was determined on a Konica Minolta CR-400 colorimeter (Japan) in CIELab Cartesian coordinates, where L* denoted lightness (from 0 – black to 100 – white), a* and b* represented opposite color coordinates, varying from – 50 to +50. In this case, negative a* was green, and positive a* was red, while negative b* was blue, and positive b* was yellow. The parameters were calibrated against a standard white porcelain with a measuring area of 8 mm in diameter, an observation angle of 10° and a D65 light source with a mirror component included (Paquet-Durand et al., 2012).

Accumulation of sugars in the dough

The quality of enzymatic processes under the influence of hydrolases was assessed by the accumulation of sugars in the dough, in terms of glucose. For this purpose, dough was kneaded from a 25 g of flour, an enzyme preparation of fungal glucoamylase or fungal cellulase, or their complex, and 14 ml of water, and the dough was left for fermentation for 360 min in a thermostat at a temperature of 32±ºC.

During fermentation, dough samples were taken and the accumulated glucose was quantitatively determined by the iodometric method. Glucoamylase was introduced at the rate of 12.5 g per 100 kg of flour, cellulase – 20 g per 100 kg of flour. When glucoamylase and cellulase were simultaneously introduced, the same calculated amounts were used (Shevchenko et al., 2021).

Statistical analysis

The statistical processing of the results was performed by sequential regression analysis using the Microsoft Excel XP and Origin Pro8 software calculating correlation coefficients (Hinkle et al., 2003).

Results and discussion

The quality indicators of products are mainly influenced by the properties of the raw materials. The characteristics of millet whole grain wheat flour, spelt, barley, amaranth, and green buckwheat flour were determined and are presented in Table 1.

Table 1

Sensory characteristics of whole grain flour

Indicator	High grade wheat flour	Whole grain wheat flour	Whole grain spelt flour	Whole grain barley flour	Whole grain amaranth flour	Whole grain green buckwheat flour
Appearance	Homogeneous powdery mass, without lumps	Homogeneous powdery mass, without lumps, visible particles of grain shells were present				
Color	Light cream	Light gray with shades of light brown	Light cream with a gray tint	Light gray with a beige tint	Light yellow with a gray tint	Light gray with a beige tint
Taste and smell	Grain-specific, clean, without foreign tastes and odors					
Moisture content, %	12.20±0.24	12.00±0.21	11.9±0.25	12.00±0.22	9.60±0.20	11.70±0.21
Total acidity, degrees	1.40±0.15	5.10±0.20	5.00±0.18	7.20±0.07	10.80±0.07	6.60±0.05
Ash content, % dry matter	0.55±0.01	1.34±0.03	1.67±0.02	1.00±0.02	1.67±0.02	2.33±0.03
Whiteness, units	59.00±0.5	-43.85±0.5	29.05±0.5	33.00±0.5	-49.20±0.5	5.85±0.50

* Results given as: M±SD (mean±standard deviation) of triplicate trials

According to the evaluation of sensory indicators, all types of flour corresponded to the signs inherent in the original grain. In each type, crushed particles of grain shells were observed. The moisture content for all samples had approximately the same values, with the exception of amaranth flour, in which this indicator was lower. This was due to the low moisture content of the amaranth grain itself and was consistent with the studies (Mykolenko et al., 2020), which found a moisture content of 9.7 – 9.9% for various samples of full-fat amaranth flour. Amaranth flour was also characterized by the highest values of the total acidity indicator among the studied samples (7.7 times higher than wheat flour), which was associated with a high content of peptides and amino acids, fats and fat-like substances, enzymes, and a significant amount of minerals, as indicated in the publication (Stankevych et al., 2021).

Also, quite high values of total acidity were noted for barley flour – 5.1 times higher compared to wheat flour. At the same time, other types of tested flours exceeded the value of the control sample of high grade wheat flour in terms of total acidity (green buckwheat flour – 5.1 times, spelt and whole wheat flour – 3.6 times), which was due to the high content of shell and germ particles, fats and proteins. The ash content of all samples of whole grain flour naturally exceeded the ash content of high grade wheat flour, with the lowest values of the indicator observed for whole barley flour, and the highest values – for green buckwheat flour.

The whiteness indicator, which was determined by the amount of dietary fiber, natural carotenoids, minerals and was associated with the color of the grain, allowed to distinguish the lighter samples – spelt and barley flour, and the darkest – wheat and amaranth flour.

In more detail, the color of flour was determined using a colorimeter (Table 2).

Table 2

Flour color indicators

Samples of four	*L*	*a**	*b**
High grade wheat	94.70±1.50	0.46±0.10	7.62±0.90
Whole grain wheat	79.53±1.20	3.60±0.50	11.37±1.21
Whole grain spelt	91.00±1.15	1.51±0.46	8.98±1.12
Whole grain barley	92.03±1.75	0.94±0.10	7.36±0.84
Whole grain amaranth	80.74±1.10	3.38±0.35	17.03±1.96
Whole grain green buckwheat	87.73±1.50	1.28±0.12	7.41±0.85

* Results given as: M±SD (mean±standard deviation) of triplicate trials

The results correlate with the obtained data on the whiteness of flour (Table 1) and confirm that the lightest among the flour samples were spelt and barley, for which the whiteness index L* was higher than other types, and the darkest were whole wheat and amaranth flour. At the same time, the spectrum of color coordinates a* showed the absence of green shades in all samples, and the presence of red, weakly expressed ones – for whole grain barley, spelt and green buckwheat flour, more intense ones – for wheat and amaranth. The spectrum b* showed pronounced yellow shades of wheat and amaranth whole grain flour, and for barley, green buckwheat flour, spelt – lower values of yellowness, which were closer to high grade wheat flour. Thus, the natural pigmentation of wheat and barley flour was characterized by more saturated yellow-red shades compared to barley, spelt and green buckwheat flour.

The structural and mechanical properties of dough and finished products are significantly affected by the size of flour particles. The results of determining the size are presented in Table 3.

Table 3

Flour particles size

Sieve	Hole size, microns	High grade wheat flour	Whole grain wheat flour	Whole grain spelt flour	Whole grain barley flour	Whole grain amaranth flour	Whole grain green buckwheat flour
Residue on sieve, %							
075	750	–	2.55±0.4	0.49±0.08	4.55±0.33	0.95±0.12	0.53±0,1
067	670	–	1.96±0.7	1.75±0.1	7.36±1.18	0.15±0.1	0.58±0,09
41/43	200	–	68.5±1.06	47.51±2.1	57.77±3.99	87.29±4.77	51.07±0,14
27	150	–	0.10±0.1	36.22±1.8	0.41±0.07	0.36±0.07	0.05±0,01
49/52	132	0.4±0.05	11.73±1.37	8.45±0.78	16.54±0.58	12.14±0.11	36.67±1,17
Passage through sieve, %							
49/52	132	99.6±0.05	15.33±1.15	3.25±0.36	12.72±2.12	2.49±0.4	10.3±0,12

* Results given as: M±SD (mean±standard deviation) of triplicate trials

The data presented in the table confirm that whole-grain millet flour exhibits a higher particle size than high-grade wheat flour. At the same time, whole grain barley and wheat flour differed in a higher content of the largest fractions by 11.91% and 4.51%, respectively. Most particles of whole grain amaranth and wheat flour had sizes in the range of 200 – 150 microns. The main fractions of whole grain green buckwheat flour and barley flour were fractions with particle sizes >200 microns, and 132–150 microns. For spelt flour, the degree of grinding varied in the particle sizes range of 150–670 microns. The content of the smallest fraction, corresponding to the passage through a 49/52 sieve and the particle size of high grade wheat flour, was highest in whole grain wheat, barley and green buckwheat flour.

The main component of flour, which is responsible for the formation of the product frame, is gluten. When determining the quantity and quality of gluten (Table 4), it was found that the gluten complex formed only in wheat and spelt flour.

Table 4

Quantity and quality of flour gluten

Indicator	Type of flour					
	High grade wheat flour	**Whole grain wheat flour**	**Whole grain spelt flour**	**Whole grain barley flour**	**Whole grain amaranth flour**	**Whole grain green buckwheat flour**
Quantity of gluten, g	24.9±0.3	16.3±0.2	18.8±0.2	Did not washed		
Elasticity	Good			–	–	–
Extensibility, cm	15.0±0.5	13.5±0.5	16.0±0.5	–	–	–
Gluten deformation index, units of device	67.9±5.0	49.4±5.0	82.2±5.0	–	–	–

* Results given as: M±SD (mean±standard deviation) of triplicate trials

At the same time, the amount of washed gluten in whole grain wheat flour was lower compared to high grade wheat flour by 34.5%, and in whole grain spelt flour – by 24.5%. The elasticity of gluten of all samples was characterized as good, but the extensibility and group were different: whole grain wheat flour belonged to group I according to the gluten deformation index, but due to dietary fiber it had 10% less extensibility compared to high grade wheat flour and had a 27% stronger structure. The gluten of spelt flour belonged to group II in terms of quality, was characterized as "satisfactorily weak", its extensibility was higher compared to the gluten of high grade wheat flour by 6.7%.

In other types of millet whole grain flour – barley, buckwheat, amaranth, the gluten framework was not formed, which was consistent with the studies of the authors who used whole grain amaranth and green buckwheat flour as gluten-free types for gluten-free cakes (Kahlon and Chiu, 2014), as well as for gluten-free bread, pasta, crackers and cookies (Khairuddin and Lasekan, 2021). The fractions of proteins insoluble in water, in combination with dietary fiber, decomposed into separate fragments, without forming a continuous structure.

The experimental flour was examined under a microscope to establish the structure of starch grains as the main carbohydrate of the flour (Figure 1).

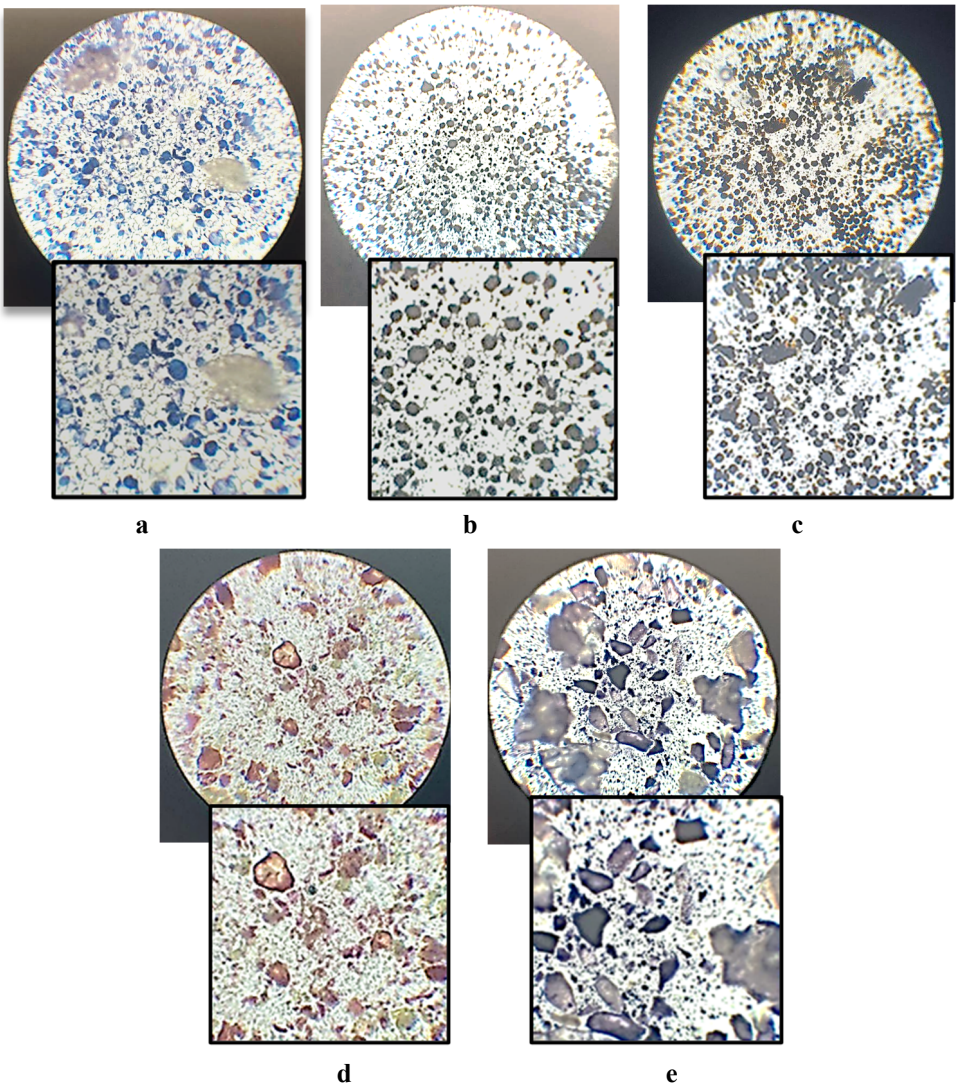

Figure 1. Samples of whole grain millet flour under a microscope:
a – wheat; b – spelt; c – barley; d – amaranth; e – green buckwheat

Microscopy showed that all types of flour had an individual structure of starch grains, determined by the nature of the grain. Amaranth flour had a significant number of small grains with a shiny surface, which alternated with a small number of large grains. Green buckwheat flour was characterized by large starch grains of polygonal shape with a somewhat granular surface. Starch grains of barley flour were generally characterized by small fractions that had a less regular shape. Wheat starch grains were round or oval in shape, medium in

size, with clear contours. In spelt flour, starch grains were similar to wheat, but somewhat elongated and thinner.

The selection of rational heat treatment modes for finished products is influenced by the boiling point of the flour suspension. The boiling point of the flour suspension was higher than the gelatinization temperature of pure starch (Figure 2), which was due to the presence of other water-soluble components, including a significant amount of fiber, protein substances, vitamins, minerals. All components of the chemical composition of flour were in close interaction and changed the thermophysical characteristics, including the gelatinization temperature of starch.

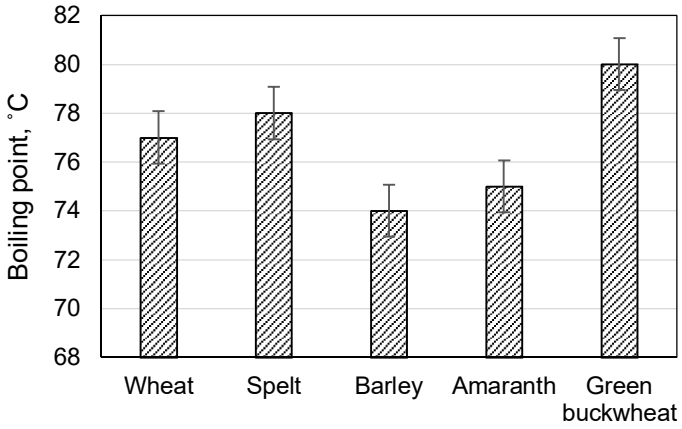

Figure 2. Boiling point of whole grain flour suspensions:
1 – wheat; 2 – spelt; 3 – barley; 4 – amaranth; 5 – green buckwheat

In the dough based on whole grain barley and amaranth flour, the process of moisture release during baking began faster, since the boiling point of their suspension was 7–7.5% lower than that of other types of flour. This predicted a reduction in the baking time of cookies.

Thus, the conducted studies determined the difference in quality indicators of millet whole grain flour from the highgrade flour, and also clarified the differences in quality indicators of different types of flour. The negative effect of millet whole grain flour on the formation of the structure of the dough for cookies and, accordingly, the consistency of the finished product was confirmed. In order to adjust the structure of the dough, and, accordingly, the consistency of the finished product, the introduction of enzyme preparations of the hydrolytic direction was proposed. Glucoamylase enzymes for the hydrolytic breakdown of flour starch, and cellulase for the hydrolytic breakdown of cellulose and its derivatives were used. Enzymes were added to the model system of flour and water separately and in combination. The results of glucose accumulation, as the main hydrolysis product, are shown in Figure 3.

It was found that the addition of enzyme preparations contributed to the accumulation of glucose, which led to an increase in the proportion of water-soluble compounds and improved the consistency of the dough. Thus, the addition of glucoamylase to whole grain wheat dough increased the amount of glucose 4.1 times during 6 hours, from spelt flour – 4.43 times, based on barley flour – 3.72 times, from amaranth flour – 9.2 times, from green buckwheat – 12.1 times.

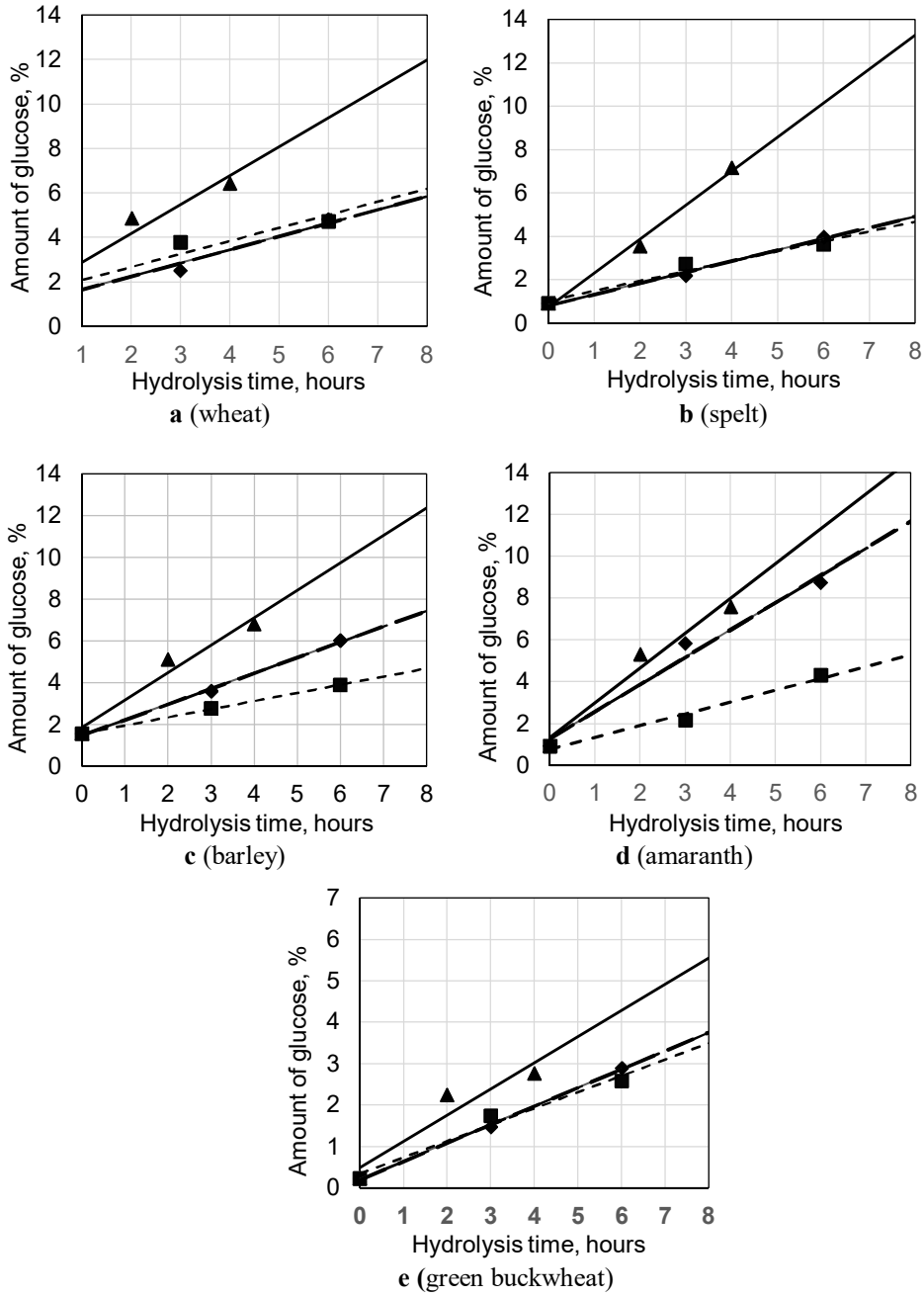

Figure 3. Enzymatic hydrolysis of whole grain flour under the influence of:
amylase;
cellulases;
amylase and cellulase complex
a) wheat; b) spelt; c) barley; d) amaranth; e) green buckwheat

The process of enzymatic hydrolysis of starch, with a smaller amount of glucoamylase used, occured faster compared to cellulose hydrolysis. That is, the flexibility of starch grains, the presence of grains damaged during the grinding process, determined better availability of the substrate and attack by the enzyme. Thus, during 6 hours of fermentation for a sample with wheat flour under the action of cellulase, 1.15% less glucose accumulated than under the action of glucoamylase, for a sample with spelt – by 9.27%, for a sample with barley – by 28.4%, with amaranth – by 50.7%, with green buckwheat flour – by 10.3%;

The combined use of enzymes sped up the process and improved the consistency of the dough, which led to a reduction in the fermentation process. Thus, for samples with wheat flour with the joint introduction of enzymes, the amount of glucose accumulated during 6 hours from the single introduction of enzymes was achieved after 2 hours. Practically the same was observed for samples with spelt flour. For samples with barley flour – in 3 hours, with green buckwheat flour – in 4 hours, with amaranth flour – in 4.5 hours. This result will have a significant impact on the technological process of producing cookies with whole grain flour and will allow adjusting the dough proofing time in the fermentation chamber.

Conclusions

1. Whole grain flour had sensory characteristics that corresponded to the specific characteristics of the grain and in terms of appearance, taste, smell and color, it was significantly different from high grade wheat flour. Spelt and barley flour were lighter in whiteness, and wheat and amaranth were the darkest.
2. The granulometric composition of millet whole grain flour was not homogeneous. The main fraction of each type of whole grain flour was larger than high grade wheat flour. The size of the main fraction of particles of whole grain amaranth and wheat flour varied in the range of 150–200 microns, green buckwheat flour and barley flour – >200 microns and 132–150 microns, spelt flour – 150–670 microns.
3. Among the studied types of flour, the gluten complex formed only in whole grain wheat and spelt flour. At the same time, the amount of washed gluten in whole grain wheat flour was 34.5% less than in high grade wheat flour, and in whole grain spelt flour – 24.5% less.
4. The studied types of flour had an individual structure of starch grains: amaranth and barley flour were characterized by small ones, green buckwheat flour was characterized by large starch grains of polygonal shape, and wheat and spelt flour starch grains were characterized by a round or oval shape of medium size.
5. The structure of the dough with whole grain flour did not correspond to the viscous-plastic characteristics of cookies, but can be improved by adding enzyme preparations of hydrolytic action. It was determined that the introduction of glucoamylase and cellulase provided an increase in the glucose level in the dough, thereby increasing the amount of water-soluble compounds and improving the consistency. The best result was obtained with the joint introduction of enzymes, when the fermentation time was reduced by 2–4 hours compared to their single introduction.

References

Azeez L.A., Babalola K.A., Osunrinade O.A. (2024), Antioxidant properties, antidiabetic activity, and GC‑MS phytochemical analysis of wheat‑based bread fortified with *Celosia argentea* seed flour, *Current Research in Agricultural Sciences*, 11(2), pp. 27–38, https://doi.org/10.18488/cras.v11i2.3866

Boz H. (2019), Effect of flour and sugar particle size on the properties of cookie dough and cookie, *Czech Journal of Food Sciences,* 37(2), pp. 120–127, https://doi:10.17221/161/2017-CJFS

Chowdhury A.H., Sarkar F., Reem C.S.A., Rahman M., Mahamud S.U., Rahman A., Ashrafudoulla M. (2024), Enzyme applications in baking: From dough development to shelf-life extension, *International Journal of Biological Macromolecules,* 282(1), 137020, https://doi:10.1016/j.ijbiomac.2024.137020

Czaja T., Sobota A., Szostak R. (2020), Quantification of ash and moisture in wheat flour by Raman spectroscopy, *Foods*, 9, 280, https://doi.org/10.3390/foods9030280

Dziki, D., Krajewska, A., Findura, P. (2024), Particle size as an indicator of wheat flour quality: A review. *Processes,* 12(11), 2480, https://doi.org/10.3390/pr12112480

Emem U.H., Emelike N.J.T., Okorie-Humphrey C., Enyi C.U. (2024), Nutritional and sensory properties of cookies produced from flour blends of African walnut (*Tetracarpidium conophorum*), *Justicia carnea* and wheat, *Journal of Food Science & Nutrition*, 10, 189, https://doi:10.24966/FSN-1076/100189

Ferradji S., Bourekoua H., Djeghim F., Ayad R., Krajewska M., Różyło R. (2024), Development of a novel gluten-free cookie premix enriched with natural flours using an extreme vertices design: physical, sensory, rheological and antioxidant characteristics, *Applied Sciences*, 14(22), 10391, https://doi:10.3390/app142210391

Gómez M., Gutkoski L.C., Bravo-Núñez Á. (2020), Understanding whole‑wheat flour and its effect in breads: A review, *Comprehensive Reviews in Food Science and Food Safety*, 19(6), pp. 3241–3265, https://doi.org/10.1111/1541-4337.12625

Hemalatha M.S., Rao U.P. (2024), Effect of peroxidase on the physico-chemical, rheological properties of whole wheat flour dough, and quality attributes of chapati and its health benefits, *Journal of Food Engineering and Technology*, 13(2), pp. 33–40, https://doi.org/10.32732/jfet.2024.13.2.33

Hetman I., Mykhonik L., Kuzmin O., Shevchenko A. (2021), Influence of spontaneous fermentation leavens from cereal flour on the indicators of the technological process of making wheat bread, *Ukrainian Food Journal*, 10(3), pp. 492–506, https://doi.org/10.24263/2304-974X-2021-10-3-6

Hinkle D.E., Wiersma W., Jurs S.G. (2003), *Applied statistics for the behavioural sciences*, 5th ed, Houghton Mifflin, London

Islam S., Miah M.A.S., Islam M.F., Bhuiyan M.N.I., Tisa K.J., Naim M.R. (2024), Exploring the effects of spontaneous and solid‑state fermentation on the physicochemical, functional and structural properties of whole wheat flour (*Triticum aestivum* L.), *Innovative Food Science & Emerging Technologies*, 97, 103798, https://doi.org/10.1016/j.ifset.2024.103798

Islam S., Miah M.A.S., Islam M.F., Tisa K.J., Bhuiyan M.H.R., Bhuiyan M.N.I., Hossain M.H. (2024), Fermentation with lactic acid bacteria enhances the bioavailability of bioactive compounds of whole wheat flour, *Applied Food Research*, 4(2), 100610, https://doi.org/10.1016/j.afres.2024.100610

Ivanov V., Shevchenko O., Marynin A., Stabnikov V., Gubenia O., Stabnikova O., Shevchenko A., Gavva O., Saliuk A. (2021), Trends and expected benefits of the breaking edge food technologies in 2021–2030, *Ukrainian Food Journal*, 10(1), pp. 7–36, https://doi.org/10.24263/2304-974X-2021-10-1-3

Jiang Y., Li J., Qi Z., Xu X., Gao J., Henry C.J., Zhou W. (2024), Role of superfine grinding in whole-purple-wheat flour. Part II: Impacts of size reduction on dough properties, bread

quality and in vitro starch digestion, *Food Chemistry*, 461, 140862, https://doi.org/10.1016/j.foodchem.2024.140862
Kahlon T.S., Chiu M.C.M. (2014), Ancient whole grain gluten-free flatbreads, *Food and Nutrition Sciences,* 5, pp. 1717–1724, https://doi.org/10.4236/fns.2014.517185
Kim J., Moon Y., Kim H., Gőksen G., Kweon M. (2024), Quality and nutritional attributes of whole einkorn flour and its suitability for fresh noodle production compared to whole wheat flour, *Cereal Chemistry*, 101(6), pp. 1316–1326, https://doi.org/10.1002/cche.10832
Khairuddin M.A.N., Lasekan O. (2021), Gluten-free cereal products and beverages: A review of their health benefits in the last five years. *Foods,* 10(11), 2523, https://doi.org/10.3390/foods10112523
Khan J., Gul P., Liu K. (2024), Grains in a modern time: A comprehensive review of compositions and understanding their role in type 2 diabetes and cancer, *Foods,* 13, 2112, https://doi.org/10.3390/foods13132112
Kumar S., Gupta O.P., Sirohi M., Verma P., Kumar A., Pandey V., Singh G. (2024), Effect of storage and processing on bioactive compounds and antioxidant activity in whole wheat flour of Indian wheat cultivars, *Journal of Cereal Research*, 16(1), pp. 60–66, https://doi.org/10.25174/2582-2675/2024/149796
Kulathunga J., Whitney K., Simsek S. (2024), Changes to structural and compositional features of water-soluble arabinoxylans in sourdough bread, *Journal of Agricultural and Food Chemistry*, 72(36), pp. 20056–20063, https://doi.org/10.1021/acs.jafc.4c05380
Mykolenko S., Hez Ya., Pivovarov O. (2020), Effect of bioactivated amaranth grain on the quality and amino acid composition of bread, *Ukrainian Food Journal*, 10(3), pp. 576–591, https://doi: 10.24263/2304- 974X-2021-10-3-11
Mykolenko S., Zhygunov D., Rudenko T. (2020), Baking properties of different amaranth flours as wheat bread ingredients, *Food Science and Technology*, 14(4), pp. 62–71, https://doi.org/10.15673/fst.v14i4.1896
Qvirist L., Scarafile D., Patrignani F., Modesto M., Lanciotti R., Andlid T., Mattarelli P. (2024), Phytate degradation in wheat, buckwheat, soy, and rice flours by lactobacilli and yeast isolated from African and Asian traditional fermented food, In: *Food Micro 2024 – Book of Abstracts*, pp. 98–99.
Paquet-Durand O., Solle D., Schirmer M., Becker T., Hitzmann B. (2012), Monitoring baking processes of bread rolls by digital image analysis, *Journal of Food Engineering*, 111(2), pp. 425–431, https://doi.org/10.1016/j.jfoodeng.2012.01.024
Poiana M.A., Alexa E., Radulov I., Raba D.N., Cocan I., Negrea M., Misca C.D., Dragomir C., Dossa S., Suster G. (2023), Strategies to formulate value-added pastry products from composite flours based on spelt flour and grape pomace powder, *Foods*, 12(17), 3239, https://doi.org/10.3390/foods12173239
Red'ko Y., Garanina O., Romanyuk E. (2021), *Development of textile materials with electromagnetic characteristics using nanotreatment and surface modification*, In: Technical research and development: collective monograph, International Science Group, Boston: Primedia eLaunchp.
Shevchenko A. (2018), Biochemical processes in the dough for diabetic bakery products, enriched with proteins and food fibers, *Scientific Works of the National University of Food Technologies*, 24(2), pp. 187—194, https://doi.org/10.24263/2225-2924-2018-24-2-22
Shevchenko A., Galenko O. (2021), Citrates of mineral substances in the technological process of manufacturing bakery products, *Scientific Works of National University of Food Technologies*, 27(1), pp. 182–187, https://doi.org/10.24263/2225-2924-2021-27-1-19
Shevchenko A., Drobot V., Galenko O. (2022), Use of pumpkin seed flour in preparation of bakery products, *Ukrainian Food Journal*, 11(1), pp. 90–101, https://doi.org/10.24263/2304-974X-2022-11-1-10
Shevchenko A. (2023), Protein substances of rice flour and its use in wheat bread technology, *Scientific Works of National University of Food Technologies*, 29(1), pp. 141–150, https://doi.org/10.24263/2225-2924-2023-29-1-13

Stabnikova O., Shevchenko A., Stabnikov V., Paredes-López O. (2023), Utilization of plant processing wastes for enrichment of bakery and confectionery products, *Ukrainian Food Journal*, 12(2), pp. 299–308, https://doi.org/10.24263/2304-974X-2023-12-2-11

Stankevych G., Valentiuk N., Ovsiannykova L., Zhygunov D. (2021), Changes in quality of amaranth grain in the course of postharvest handling and storage, *Food Science and Technology*, 15(1), pp. 80–90, https://doi.org/10.15673/fst.v15i1.1959

Xu J., Zhang Y., Wang W., Li Y. (2020). Advanced properties of gluten-free cookies, cakes, and crackers: A review, *Trends in Food Science & Technology*, 103, pp. 200-213, https://doi:10.1016/j.tifs.2020.07.017

Zhang H., Zhang B., He H., Zhang L., Hu X., Wu C. (2025), Evaluation of wheat grain and processing quality under fusarium head blight control using strong oxidizing radicals, *Foods*, 14, 1236, https://doi.org/10.3390/foods14071236

Zhygunov D, Khorenghy N, Voloshenko O, Zhyhunova H. (2019), Investigation of the bakery properties of wholemeal flour obtained from black wheat. *Food Science and Technology,* 13(3), pp. 26–35, http://dx.doi.org/ 10.15673/fst.v13i3.1474

Cite:

UFJ Style

Vorvykhvost A., Kambulova Yu., Kokhan O., Potapenko O., Nepokrytov O. (2025), Assessment of whole-grain flour quality for confectionery use, *Ukrainian Journal of Food Science*, 13(1), pp. 17–30, https://doi.org/10.24263/2310-1008-2025-13-1-4

APA Style

Vorvykhvost, A., Kambulova, Yu., Kokhan, O., Potapenko, O., & Nepokrytov, O. (2025). Assessment of whole-grain flour quality for confectionery use. *Ukrainian Journal of Food Science, 13*(1), 17–30. https://doi.org/10.24263/2310-1008-2025-13-1-4

Characterization of biodegradable seaweed-based film from *Kappaphycus alvarezii* incorporating aloe vera gel as a plasticizer

Veronica Kyla R. Encinas[1], Sophia C. Oco[1], Jeffrey D. Perigrino[2], Marvy Claire N. Mortega[1], Benyl John A. Arevalo[1], Ian Cris R. Buban[1]

1 – Bicol University Tabaco, Tabaco City, Albay, Philippines
2 – Bicol University Regional Center for Food Safety and Quality Assurance, Legazpi City, Philippines

Keywords:

Film
Kappaphycus alvarezii
Aloe vera
Gel
Plasticizer
Biodegradability

Article history:

Received 17.03.2025
Received in revised form 21.06.2024
Accepted 30.06.2024

Corresponding author:

Veronica Kyla R. Encinas
E-mail: veronicakylaramos.encinas@bicol-u.edu.ph

DOI: 10.24263/2310-1008-2025-13-1-5

Abstract

Introduction. Plastic packaging materials have been the perennial cause of global plastic pollution, highlighting the urgent need for alternative biodegradable substitutes. This study explored the potential of using aloe vera gel (AVG) as a sustainable plasticizer for *Kappaphycus alvarezii*-based films, comparing it to a traditional glycerol plasticizer.

Materials and methods. Different concentrations of AVG (10, 20 and 30%) were tested to prepare biodegradable films, and the properties of these films including water solubility, mechanical properties (tensile strength and elongation at break), biodegradability, and microbial load were evaluated.

Results and discussion. The results show that AVG concentration significantly affects film characteristics. Water solubility was significantly reduced with 20% and 30% AVG, showing values of 18.87% and 26.57%, respectively, compared to 84.87% for the control and 84.02% for 10% AVG. Notably, a lower concentration of AVG (10%) resulted in the highest tensile strength (61.64 N/mm²), while higher plasticizer concentrations exhibited lower values corresponding to 35.60 N/mm² and 29.90 N/mm² for 20% and 30% AVG, respectively. In addition, the elongation at break was significantly reduced in treatments with AVG (1.37% – 3.07%) when compared to the control (17.81%), indicating increased brittleness of the film with AVG. However, AVG enhanced the biodegradability at all concentrations, with more than 50% of the films decomposed within 12 days, exceeding the 37.63% biodegradability of the control. Furthermore, 10% AVG significantly reduced microbial load to 1 colony forming units per g, demonstrating antimicrobial properties compared to the control.

Conclusions. "The study concluded that *Kappaphycus alvarezii* and aloe vera gel are promising components for the development of biodegradable films. *K. alvarezii* provides a strong and adaptable film matrix, while aloe vera gel serves as an effective alternative plasticizer. Further research is recommended to explore the potential application of these films as edible food packaging materials.

Introduction

Traditional plastic films pose significant environmental challenges due to their non-biodegradability, leading to their accumulation as persistent waste in the environment. Since the 1950s, over 8.3 billion metric tons of plastic have been produced, of which only about 9% has been recycled, 12% incinerated, and the remaining 79% either deposited in landfills or released into natural ecosystems (Geyer, 2020; Stabnikova et al., 2021). This environmental crisis underscores the urgent need for sustainable plastic alternatives.

Developing biodegradable films from biopolymers offers a viable solution to waste plastic concerns. These biodegradable films break down naturally and are suitable for medical, packaging, and agricultural uses (Mapossa, 2023; Chandra at al., 1998). *Kappaphycus alvarezii*, a widely cultivated red seaweed with established economic value (Bindu at al., 2010; Rupert et al., 2022; Stabnikova et al., 2025), shows promise as a source for these materials due to the film-forming properties of its carrageenan content (Tye et al., 2018). Its status as a top aquaculture commodity (Irawati et al., 2024) ensures cost-effectiveness and availability. Carrageenan provides a strong and flexible film foundation (Rhein-Knudsen et al., 2015) and has antimicrobial properties with versatile applications (Rupert et al., 2022), making *K. alvarezii* a sustainable alternative.

In biofilm production, plasticizers are essential to ensure the film's flexibility; however, common phthalate-based options are toxic (Hauser et al., 2005), driving demand for healthier substitutes. Aloe vera gel (AVG), known for its medicinal properties, is a suitable material in biopolymer research. Its polysaccharides, vitamins, enzymes, and amino acids suggest plasticizing effects (Hamman, 2008). Furthermore, research indicates it can enhance moisture content, mechanical strength, and gas barrier properties (Hadi et al., 2022a; Tambe, 2024). Its film-forming, antimicrobial, and biodegradable properties make it a good natural preservative coating (Berihu et al., 2022; Misir et al., 2014). Therefore, exploring the combination of *K. alvarezii* and aloe vera gel in film production could create enhanced, sustainable packaging materials, particularly for food applications.

Existing research has investigated other plasticizers, including aloe vera gel as an additive for different biopolymers (Hadi et al., 2021, 2022a). Research using *K. alvarezii* to create biodegradable films, as well as studies using aloe vera gel as a film additive, remains mostly independent from one another. Therefore, the optimal combination and interaction between these two specific materials for improved film performance remains largely unexplored.

This study aims to characterize the formulated films' physical (water solubility), mechanical (tensile strength and elongation at break), biodegradability properties, and antimicrobial potential. The findings of this research provide valuable insights and baseline data on biopolymer combinations for developing sustainable film that may used for various applications, particularly as a food packaging material.

Materials and methods

Materials

The Alkali-Treated Cotonii Chips (ATCC), a form of semi-refined carrageenan (SRC) and also known as the Philippine Natural Grade (PNG), was sourced from the Bureau of Fisheries and Aquatic Resources – National Seaweeds Technology Development Center (BFAR-NSTDC) in Cabid-an, Sorsogon. The ATCC is made from the species *K. alvarezii* using the alkali extraction method described in Bixler (1996). Fresh aloe vera leaves were purchased from Tabaco City, Albay.

a

b

c

d

Figure 1. Alga *Kappaphycus alvarezii (a)*, fresh aloe vera leaves (b), aloe vera gel platicizer (c), a *Kappaphycus alvarezii*-based film incorporating aloe vera gel as a plasticizer (d)

Preparation of aloe vera gel

The extraction of AVG followed the method of Maan et al. (2021), where mature aloe vera leaves were washed, trimmed, and soaked for 1 hour to remove aloin. After removing tips and spines, one side of the rind was peeled, and the inner gel was scraped out. The extracted gel was then homogenized in a blender for 3 minutes, filtered through cheesecloth to remove impurities, and the resulting pure gel was refrigerated for later use.

Preparation of films

The solution was prepared following a slightly modified method based on Farhan and Hani (2017). The ATCC (2% w/w) was dissolved in 90°C distilled water with continuous stirring for 30 minutes. After adjusting the volume and filtering, AVG was added at varying concentrations (10%, 20%, and 30% w/w) and stirred for 2 minutes. A total of 150 mL of the solution was poured into plates, dried in a hot-air oven at 60 °C for 4 hours, and then carefully peeled off. Composition of prepared seaweed-based films is shown n Table 1.

Table 1

Composition of seaweed-based film using Alkali-Treated Cotonii Chips (ATCC) with varying plasticizers

Seaweed-based films	Compositions
Film (Control)	4g ATCC + 20% glycerol
Film 1	4g ATCC + 10% AVG
Film 2	4g ATCC + 20% AVG
Film 3	4g ATCC + 30% AVG

Determination of solubility in water

Water solubility was assessed using a slightly modified version of the Romero-Bastida et al. (2005) method. Film samples (2x2 cm) were dried at 60°C for 1 hour to obtain the initial dry weight (Si) and then immersed in 50 ml of distilled water at room temperature for 4 hours with periodic agitation. After immersion and filtering, the film pieces were dried again at 60°C for 3 hours to determine the final dry weight (Sf). Water solubility was calculated as the percentage weight loss using the formula:

$$\text{Solubility (\%)} = [(Si - Sf) / Si] \times 100.$$

Determination of tensile strength and elongation at break

Tensile strength and elongation at break were determined using a Universal Testing Machine (UTM) extensometer operated in accordance with the standard method ASTM D882 (ASTM, 2018). The prepared film samples were sent to the Materials R&D Consulting Facility at the University of the Philippines Diliman for testing. The samples were cut and measured, with an average thickness of 0.04628±0.00459 mm, a width of 15.00 mm, and a gauge length of 100.00 mm, before being tested.

Determination of biodegradability

Biodegradability was assessed through soil and burial tests following the method from Sari et al. (2024) with slight modification. Film strips (2 x 3 cm) were buried in plastic pots containing 300 g of damp soil and sand. Samples were retrieved every 4 days, cleaned, dried at 60°C for 1 hour, and weighed. The test lasted for 12 days when one treatment already achieved the 50% degradation. The percentage weight loss (WL) of the film was calculated using the following equation:

$$WL\% = (Wi - Wf / Wi) \times 100$$

where Wi is the film's initial weight, Wf is its weight after degradation.

Determination of microbial load

The microbial load of the film with the best mechanical properties was analyzed using the Compact Dry TC (total count) – AOAC 010404 method at the Bicol University Regional Center for Food Safety and Quality Assurance (BURCFSQA). Following the standard method, film samples were cut into thin strips, diluted 1:10 with distilled water, and standardized using the 0.5 McFarland turbidity test. One ml of the diluent was plated on Compact Dry TC and incubated for 24 hours at 35 ± 1°C, after which the number of colonies was counted to quantify bacterial growth.

Data analysis

Statistical analysis using Analysis of Variance (ANOVA) was performed to evaluate significant differences in the tested film properties among experimental groups, with normality and homogeneity of variances checked using the Shapiro-Wilk and Levene's tests, respectively. In cases of significant ANOVA results, Tukey's multiple-range test was used to identify significantly different groups. All statistical analyses were conducted at a 5% alpha level.

Results and discussion

Film solubility in water

Significant variations in water solubility were observed among seaweed-based films with different plasticizers (Figure 2). Specifically, seaweed-based films 2 and 3 have significantly low water solubility as compared to the control and seaweed-based film 1 ($p<0.05$). Thus, incorporation of higher amounts of AVG (>20%) into seaweed-based films will result in their lower solubility in water.

The high water solubility of film 1 (84.02%), comparable to the control film (84.87%), indicates that the addition of 10% AVG enhances water absorption and breakdown, likely due to AVG's inherent hydrophilic nature (Hadi et al., 2021) and plasticizing effect, which increases space between polymer chains (Hadi et al., 2022b). This comparable solubility suggests that AVG behaves similarly to glycerol in terms of water solubility at low concentrations. However, increasing AVG concentrations to 20% (film 2, 18.87%) and 30% (film 3, 26.57%) significantly decreased solubility. This finding contradicts the results of Hadi et al. (2022b) and may be due to differences in the base film composition or aloe vera gel properties.

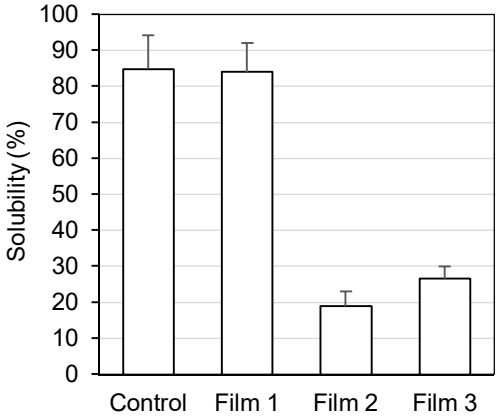

Figure 2. Comparison of the solubility properties of films with different contnent of aloe vera gel (AVG) relative to the control: film 1, 10% of AVG; film2, 20% of AVG; film 3, 30% of AVG

The film developed with 20% aloe vera gel exhibited properties comparable to the starch-based film reported by Chavan et al. (2022), which demonstrated a solubility range of 5.5% to 19.1% through the incorporation of nanostarch particles to enhance film's mechanical and barrier properties. Similarly, studies such as that of Bajer et al. (2020) have shown that water solubility in starch/chitosan/aloe vera composites decreases following UV irradiation, suggesting that external treatments can significantly influence solubility behavior. Meanwhile, based on Abd Karim et al. (2024), thermoplastic starch films formulated with 30% aloe vera experienced a significant reduction in water solubility from 48.46% to 32.39% with the incorporation of 10% polyethylene, a reduction that remained consistent even with higher polyethylene concentrations (20%-40%). These findings collectively underscore that while AVG concentration significantly influences solubility, with higher levels generally leading to reduced water interaction, additional factors such as film composition, polymer modifications, and external treatments like UV exposure are equally crucial in tailoring the film's water resistance properties.

The varying solubility of the developed films indicates their potential for diverse applications. Films with high solubility, such as film 1, are suitable for applications requiring rapid dissolution, including those in the food and detergent industries, similar to PVOH-based films for detergent capsules (Byrne et al., 2021) or edible films for instant food. Conversely, films with lower solubility, such as films 2 and 3, are more suitable for applications requiring water resistance, such as biodegradable food packaging for perishable goods. Thus, the balance between solubility and water resistance in these seaweed-aloe vera gel-based films allows for a range of practical uses in food packaging and agriculture.

Mechanical properties

All films incorporating aloe vera gel showed no significant differences in tensile strength compared to the control, with an average value of 42.64 ± 6.32 N/mm² ($p > 0.05$). On the contrary, film 1 has significantly higher tensile strength (61.63 ± 10.54 N/mm²) compared to film 3 (29.90 ± 1.42 N/mm²). In addition, film 1 with the lowest AVG concentration also shows the highest tensile strength among the films and control, indicating that 10% aloe vera gel is the most effective for enhancing the film's tensile strength. Further increasing the concentrations of aloe vera gel leads to reduced tensile strength (Figure 3).

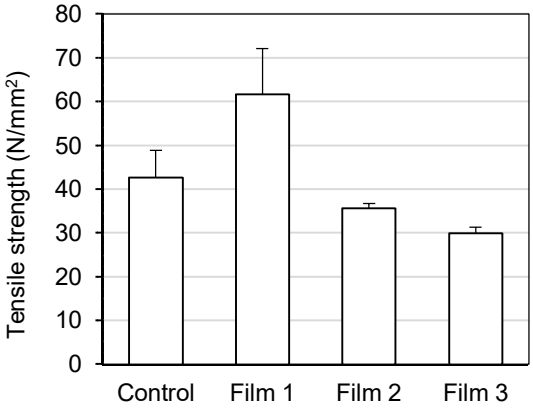

Figure 3. Comparison of the tensile strengths of films with different contnent of aloe vera gel (AVG) relative to the control: film 1, 10% of AVG; film2, 20% of AVG; film 3, 30% of AVG

Additionally, the incorporation of AVG into the *K. alvarezii*-based films significantly affected elongation at break (Figure 4). Analysis showed statistically significant reductions in elongation across all aloe vera gel films compared to the glycerol control (17.81 ± 3.34%, mean ± SE) ($p<0.05$). Subsequently, mean values (± SE) decreased from 3.07 ± 0.73% (film 1) to 1.49 ± 0.06% (film 2) and 1.37 ± 0.06% (film 3), indicating a clear inverse relationship between AVG concentration and film flexibility.

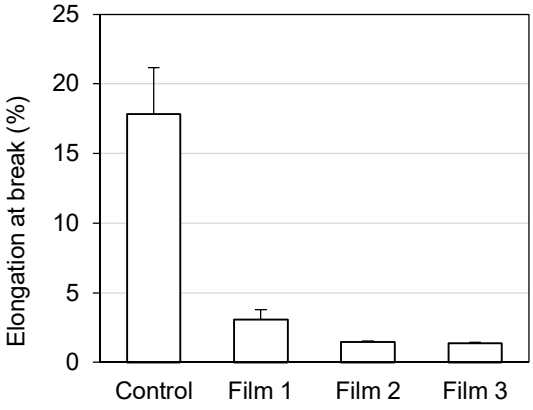

Figure 4. Comparison of the elongation at break (%) of films with different contnent of aloe vera gel (AVG) relative to the control: film 1, 10% of AVG; film2, 20% of AVG; film 3, 30% of AVG

The preceding results highlight a complex relationship between tensile strength and elongation at break in the *K. alvarezii*-based biodegradable films (Figure 5). The control films based on *K. alvarezii* exhibited a balance of moderate tensile strength and high elongation at break. On the contrary, presence of AVG in films indicates inverse relationship between film strength and elongation. This observation is a common trade-off in composite materials, likely because the aloe vera gel creates stronger connections within the film (Rahmiatiningrum et al., 2019; Tambe et al., 2024), which can make the material more brittle (Chen et al., 2019).

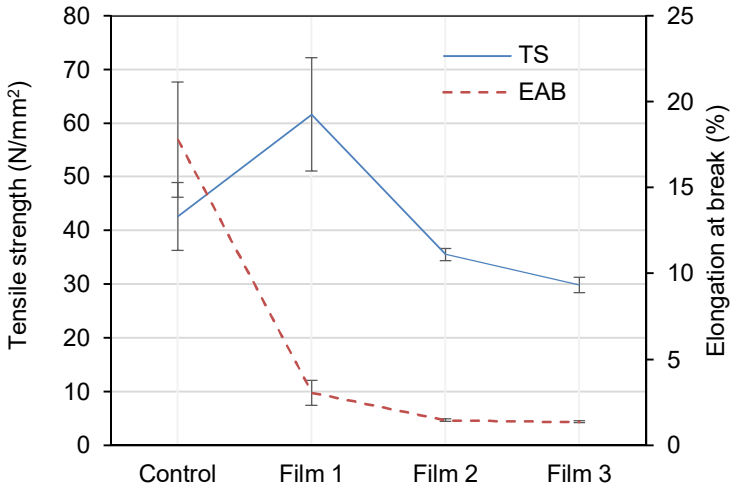

Figure 5. Relationship of tensile strength (TS) and elongation at break (EAB) of films with different contnent of aloe vera gel (AVG) relative to the control: film 1, 10% of AVG; film2, 20% of AVG; film 3, 30% of AVG

Specifically, when AVG content exceeded 10%, tensile strength decreased while elongation at break remained low. This might be because the higher amount of AVG disrupts the film's structure (Lagos et al., 2015; Ramos et al., 2013), making it difficult to create flexible films with high AVG content. Therefore, plasticizer addition requires an optimal point beyond which strength decreases.

Compared to traditional plastics, the *K. alvarezii*-based films exhibit similar if not superior strength, but limited flexibility. For instance, Pradhan et al. (2020) have shown that high-density polyethylene has a tensile strength of 20–40 N/mm² with high elongation at break (100-1000%), while low-density polyethylene shows 7–17 N/mm² tensile strength with elongation at break of 200-900%. In addition, the same study suggests that polypropylene has 28-40 N/mm² tensile strength with moderate elongation at break of 20–75%. In contrast, the film with 10% of AVG has a higher tensile strength (61.63 N/mm²), but significantly reduced elongation (3.07%), while other films with AVG displayed comparable or slightly lower tensile strength alongside similarly limited flexibility. Thus, the impressive tensile strength exhibited by the developed film shows its potential for applications requiring mechanical durability such as food packaging.

Biodegradability

The results demonstrate that addition of AVG significantly enhances the biodegradability of the films compared to the glycerol-plasticized control (Figure 6). Notably, all films incorporating AVG resulted in over 50% film degradation after 12 days. Specifically, the biodegradability of film 2 (53.55%) is significantly higher than the control (37.63%) ($p<0.05$). These findings confirm the positive impact of aloe vera addition on film degradation and prompt further examination of the optimal concentration range for maximum biodegradability.

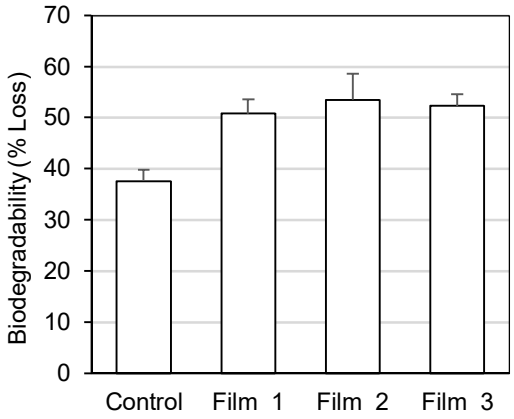

Figure 6. Comparison of biodegradability of the different films with AVG relative to the control

The rapid degradation of the AVG-plasticized films, with over 50% degradation within 12 days, indicates that AVG might accelerate biodegradation compared to some glycerol-plasticized carrageenan films. For example, findings from Sari et al. (2024) show biodegradable film with glycerol took about 40 days to reach similar levels, emphasizing the effect of plasticizer type on the film's natural degradation. This enhanced biodegradability with AVG is likely due to its complex composition, which provides readily available microbial carbon sources like polysaccharides, organic acids, and enzymes (Babu et al., 2020). Therefore, the overall faster degradation of the aloe vera gel-plasticized films highlights AVG's potential to enhance the biodegradability of polymer matrices. This suggests that incorporating AVG into seaweed-based films could be a significant step in developing sustainable plastic alternatives suitable for applications prioritizing environmental compatibility.

Effects on microbial load

Adding 10% AVG to the film decreased aerobic bacterial counts, indicating its antimicrobial contribution. The minimal bacterial count (1.0 colony forming units per g) in film 1 indicates the effective control of bacterial accumulation. The control film demonstrated bacterial contamination with a high level too numerous to count (TNTC), indicating the lack of antimicrobial properties. These differences show AVG's antimicrobial ability as an essential additive for creating biodegradable plastics.

The observed antimicrobial effects are consistent with previously published research. For instance, Ghafoor et al. (2016) found that biodegradable polymer films containing aloe vera showed substantial bacterial growth reduction, confirming the current study results. Similarly, Yoshida et al. (2021) found that biofilms made from chitosan had enhanced antimicrobial activity when they included aloe vera extract. Research evidence demonstrates that particular compounds in aloe vera, including anthraquinones, saponins, tannins, flavonoids, ascorbic acid, and pyrocatechols, provide broad-spectrum antibacterial effects. The antimicrobial properties of anthraquinones in aloe vera are due to their ability to inhibit protein synthesis in bacteria (Fani at al., 2012; Zahra et al., 2022). The compounds penetrate microbial membranes to cause bacterial cell lysis, resulting in decreased bacterial viability, especially against Gram-positive *Staphylococcus aureus* strains (Chelu et al., 2023; Parnomo et al., 2021). The current research, along with previous studies, demonstrates how aloe vera gel enhances biodegradable film antimicrobial properties, which drives the creation of safer, sustainable alternatives.

Conclusions

In conclusion, this study demonstrates the promising potential of aloe vera gel as a sustainable plasticizer in seaweed-based biodegradable films. Varying the concentration of aloe vera gel produced films with properties suitable for a wide array of applications, particularly as food packaging materials. Notably, aloe vera gel enhanced biodegradability and provided significant antimicrobial activity, surpassing the performance of traditional glycerol-plasticized films. While lower concentrations improved tensile strength, higher concentrations led to reduced solubility and increased brittleness, highlighting the importance of precise formulation. Overall, the findings suggest that aloe vera gel offers a promising alternative to conventional plasticizers, contributing to the development of enhanced, environmentally friendly packaging materials. Future research into the optimization of aloe vera gel concentration and its applications within specific packaging applications would be useful in exploring the full extent of its potential.

Acknowledgements. The researchers express their sincere gratitude to BFAR-NSTDC for generously providing the essential raw materials for this study.

References

Abd Karim S.F., Jai J., Abdol Aziz R.A., Maqsood-Ul-Haque S.N.S., Ku Hamid K.H., Mulana F. (2024), Production of thermoplastic starch-aloe vera gel film embedded with polyethylene for improved tensile strength and water absorption, *Journal of Mechanical Engineering*, 21(3), pp. 93-107.

Alahmed A., Simsek S. (2024), Improving biodegradable films from corn bran arabinoxylan for hydrophobic material and green food packaging, *Foods*, 13(12), 1914, https://doi.org/10.3390/foods13121914

ASTM (2018), *Standard test method for tensile properties of thin plastic sheeting (ASTM D882)*, ASTM International.

Babu S.N., Noor A. (2020), Bioactive constituents of the genus *Aloe* and their potential therapeutic and pharmacological applications: A review, *Journal of Applied Pharmaceutical Science*, 10(11), pp. 133–145, https://doi.org/10.7324/japs.2020.101118

Bajer D., Janczak K., Bajer K. (2020), Novel starch/chitosan/aloe vera composites as promising biopackaging materials, *Journal of Polymers and the Environmen,* 28, pp. 1021–1039, https://doi.org/10.1007/s10924-020-01661-7

Bixler H.J. (1996), Recent developments in manufacturing and marketing carrageenan, *Hydrobiologia*, 326(1), pp. 35-57, https://doi.org/10.1007/BF00047785

Berihu H., Zegeye A. (2022), Enhancement of quality and storability of avocado (*Persea americana*) fruit using a blend of aloe vera gel and corn starch as surface coating, *International Journal of Food Engineering and Technology*, 6(1), pp. 21–27, https://doi.org/10.11648/j.ijfet.20220601.14

Bindu M.S., Levine I.A. (2010), The commercial red seaweed *Kappaphycus alvarezii* – an overview on farming and environment, *Journal of Applied Phycology*, 23, pp. 789–796, https://doi.org/10.1007/s10811-010-9570-2

Byrne D., Boeije G., Croft I., Hüttmann G., Luijkx G., Meier F., Parulekar Y., Stijntjes G. (2021), Biodegradability of polyvinyl alcohol-based film used for liquid detergent capsules, *Tenside Surfactants Detergents*, 58(2), pp. 88–96, https://doi.org/10.1515/tsd-2020-2326

Campo V.L., Kawano D.F., da Silva D.B., Carvalho I. (2009), Carrageenans: Biological properties, chemical modifications and structural analysis – A review, *Carbohydrate Polymers*, 77(2), pp. 167–180, https://doi.org/10.1016/j.carbpol.2009.01.020

Chandra R., Rustgi R. (1998), Biodegradable polymers, *Progress in Polymer Science*, 23(7), pp. 1273–1335, https://doi.org/10.1016/s0079-6700(97)00039-7

Chavan P., Sinhmar A., Sharma S.D., Dufresne A., Thory R., Kaur M., Sandhu K.S., Nehra M., Nain V. (2022), Nanocomposite starch films: A new approach for biodegradable packaging materials, *Starch – Stärke*, 74(5–6), 2100302, https://doi.org/10.1002/star.202100302

Chelu M., Musuc A.M., Aricov L., Ozon E.A., Iosageanu A., Stefan L.M., Prelipcean A.M., Popa M., Moreno J.C. (2023), Antibacterial aloe vera based biocompatible hydrogel for use in dermatological applications, *International Journal of Molecular Sciences*, 24(4), 3893, https://doi.org/10.3390/ijms24043893

Chen J., Li H., Fang C., Cheng Y., Tan T., Han H. (2019), *In situ* synthesis and properties of Ag NPs/carboxymethyl cellulose/starch composite films for antibacterial application, *Polymer Composites*, 41(3), pp. 838–847, https://doi.org/10.1002/pc.25414

Fani M., Kohanteb J. (2012), Inhibitory activity of aloe vera gel on some clinically isolated cariogenic and periodontopathic bacteria, *Journal of Oral Science*, 54(1), pp. 15–21, https://doi.org/10.2334/josnusd.54.15

Farhan A., Hani N.M. (2017), Characterization of edible packaging films based on semi-refined kappa-carrageenan plasticized with glycerol and sorbitol, *Food Hydrocolloids*, 64, pp. 48–58, https://doi.org/10.1016/j.foodhyd.2016.10.034

Freile-Pelegrín Y., Madera-Santana T.J. (2017), Biodegradable polymer blends and composites from seaweeds, *Handbook of Composites from Renewable Materials*, pp. 419–438, https://doi.org/10.1002/9781119441632.ch98

Geyer R. (2020), Production, use, and fate of synthetic polymers, In: T.M. Letcher (Ed.), *Plastic Waste and Recycling*, pp. 13–32, Academic Press, London, https://doi.org/10.1016/B978-0-12-817880-5.00002-5

Ghafoor B., Ali M.N., Ansari U., Bhatti M.F., Mir M., Akhtar H., Darakhshan F. (2016), New biofunctional loading of natural antimicrobial agent in biodegradable polymeric films for biomedical applications, *International Journal of Biomaterials*, pp. 1–9, https://doi.org/10.1155/2016/6964938

Hadi A., Nawab A., Alam F., Zehra K. (2021), Physical, mechanical, optical, barrier, and antioxidant properties of sodium alginate – aloe vera biocomposite film, *Journal of Food Processing and Preservation*, 45(5), https://doi.org/10.1111/jfpp.15444

Hadi A., Nawab A., Alam F., Zehra K. (2022a), Sustainable alginate/aloe vera composite biodegradable films reinforced with carboxymethyl cellulose and hydroxypropyl methylcellulose, *Polymer Composites*, 43(6), pp. 3471–3480, https://doi.org/10.1002/pc.26629

Hadi A., Nawab, A., Alam, F., Zehra, K. (2022b), Sustainable food packaging films based on alginate and aloe vera, *Polymer Engineering and Science*, 62(7), pp. 2111–2118, https://doi.org/10.1002/pen.25992

Hamman J.H. (2008), Composition and applications of aloe vera leaf gel, *Molecules*, 13(8), pp. 1599–1616, https://doi.org/10.3390/molecules13081599

Hauser R., Calafat A.M. (2005), Phthalates and human health, *Occupational and Environmental Medicine*, 62(11), pp. 806–818, https://doi.org/10.1136/oem.2004.017590

Irawati B.A., Affandi R.I. (2024), Tissue culture of *Kappaphycus alvarezii* seaweed by somatic embryogenesis method, *Ganec Swara*, 18(1), 358, https://doi.org/10.35327/gara.v18i1.768

Lagos J.B., Vicentini N.M., Dos Santos R.M.C., Bittante A.M.Q.B., Sobral P.J.A. (2015), Mechanical properties of cassava starch films as affected by different plasticizers and

different relative humidity conditions, *International Journal of Food Studies*, 4(1), pp. 116–125, https://doi.org/10.7455/ijfs/4.1.2015.a10

Lim H., Hoag S.W. (2013), Plasticizer effects on physical–mechanical properties of solvent cast Soluplus® Films, *American Association of Pharmaceutical Scientists PharmSciTech*, 14, pp. 903–910, https://doi.org/10.1208/s12249-013-9971-z

Maan A.A., Reiad Ahmed Z.F., Khan M.K.I., Riaz A., Nazir A. (2021), Aloe vera gel, an excellent base material for edible films and coatings, *Trends in Food Science & Technology*, 116, pp. 329–341, https://doi.org/10.1016/j.tifs.2021.07.035

Mapossa A.B., da Silva Júnior A.H., de Oliveira C.R., Mhike W. (2023), Thermal, morphological and mechanical properties of multifunctional composites based on biodegradable polymers/bentonite clay: A review, *Polymers*, 15(16), 3443, https://doi.org/10.3390/polym15163443

Misir J., Brishti F.H., Hoque M.M. (2014), Aloe vera gel as a novel edible coating for fresh fruits: A review, *American Journal of Food Science and Technology*, 2(3), pp. 93–97, https://doi.org/10.12691/ajfst-2-3-3

Parnomo T., Pohan D.J. (2021), Test the effectiveness of aloe vera extract on the growth of *Escherichia coli* in vitro, *International Journal of Health Sciences and Research*, 11(8), pp. 211–224, https://doi.org/10.52403/ijhsr.20210831

Pradhan S., Dikshit P.K., Moholkar V.S. (2020), Production, characterization, and applications of biodegradable polymer: Polyhydroxyalkanoates. In: V. Katiyar, A. Kumar, N. Mulchandani (Eds.), *Advances in Sustainable Polymers. Materials Horizons: From Nature to Nanomaterials*, pp. 51-94, Springer, Singapore, https://doi.org/10.1007/978-981-15-1251-3_4

Rahmiatiningrum N., Sukardi S., Warkoyo W. (2019), Study of physical characteristic, water vapor transmission rate and inhibition zones of edible films from aloe vera (*Aloe barbadensis*) incorporated with yellow sweet potato starch and glycerol, *Food Technology and Halal Science Journal*, 2(2), 195, https://doi.org/10.22219/fths.v2i2.12985

Ramos Ó.L., Reinas I., Silva S.I., Fernandes J.C., Cerqueira M.A., Pereira R.N., Vicente A.A., Poças M.F., Pintado M.E., Malcata F.X. (2013), Effect of whey protein purity and glycerol content upon physical properties of edible films manufactured therefrom, *Food Hydrocolloids*, 30(1), pp. 110–122, https://doi.org/10.1016/j.foodhyd.2012.05.001

Rhein-Knudsen N., Ale M., Meyer A. (2015), Seaweed hydrocolloid production: An update on enzyme assisted extraction and modification technologies, *Marine Drugs*, 13(6), pp. 3340–3359, https://doi.org/10.3390/md13063340

Romero-Bastida C.A., Bello-Pérez L.A., García M.A., Martino M.N., Solorza-Feria J., Zaritzky N.E. (2005), Physicochemical and microstructural characterization of films prepared by thermal and cold gelatinization from non-conventional sources of starches, *Carbohydrate Polymers*, 60(2), pp. 235–244, https://doi.org/10.1016/j.carbpol.2005.01.004

Rupert R., Rodrigues K.F., Thien V.Y., Yong W.T. (2022), Carrageenan from *Kappaphycus alvarezii* (*Rhodophyta*, *Solieriaceae*): Metabolism, structure, production, and application, *Frontiers in Plant Science*, 13, https://doi.org/10.3389/fpls.2022.859635

Sari W.M., Supartono W., Suharno. (2024), Characterization of biodegradable films from raw seaweed (*Kappaphycus alvarezii*) and glycerol, *IOP Conference Series: Earth and Environmental Science*, 1364, 012081, https://doi.org/10.1088/1755-1315/1364/1/012081

Siracusa V., Rocculi P., Romani S., Rosa M.D. (2008), Biodegradable polymers for food packaging: A review, *Trends in Food Science & Technology*, 19(12), pp. 634–643, https://doi.org/10.1016/j.tifs.2008.07.003

Stabnikova O., Stabnikov V., Marinin A., Klavins M., Klavins L., Vaseashta A. (2021), Microbial life on the surface of microplastics in natural waters, *Applied Sciences*, 11, 11692, https://doi.org/10.3390/app112411692

Stabnikova O., Stabnikov V., Paredes-López O. (2025), Wild edible plants, berries, mushrooms and seaweeds in food production, In: S. Gubsky, O. Stabnikova, V. Stabnikov, O. Paredes-López (Eds.), *Wild Edible Plants: Improving Foods Nutritional Value and Human Health through Biotechnology*, pp. 1-47, CRC Press, Boca Raton, https://doi.org/10.1201/9781003486794-1

Tambe S.S., Zinjarde S., Athawale A.A. (2024), Aloe vera gel–reinforced biodegradable starch–PVA blends for sustainable packaging of green chillies, *Packaging Technology and Science*, 37(7), pp. 605–617, https://doi.org/10.1002/pts.2812

Tye Y.Y., Abdul Khalil H.P., Kok C.Y., Saurabh C.K. (2018), Preparation and characterization of modified and unmodified carrageenan based films, *IOP Conference Series: Materials Science and Engineering*, 368, https://doi.org/10.1088/1757-899x/368/1/012020

Yoshida C.M.P., Pacheco M.S., de Moraes M.A., Lopes P.S., Severino P., Souto E.B., da Silva C.F. (2021), Effect of chitosan and aloe vera extract concentrations on the physicochemical properties of chitosan biofilms, *Polymers*, 13(8), 1187, https://doi.org/10.3390/polym13081187

Zahra N., Saeed M., Nawaz S., Gulzar E. (2022), Aloe vera cookies preparation, nutritional aspects, DPPH assay and physicochemical assay, *Bangladesh Journal of Scientific and Industrial Research*, 57(2), pp. 117–122, https://doi.org/10.3329/bjsir.v57i2.60408

Cite:

UFJ Style

Encinas V.K.R., Oco S.C., Perigrino J.D., Mortega I.C.R, Arevalo I.C.R, Buban I.C.R. (2025), Characterization of biodegradable seaweed-based film from *Kappaphycus alvarezii* incorporating aloe vera gel as a plasticizer, *Ukrainian Journal of Food Science*, 13(1), pp. 31–44, https://doi.org/10.24263/2310-1008-2025-13-1-5

APA Style

Encinas, V.K.R., Oco, S.C., Perigrino, J.D., Mortega, I.C.R, Arevalo, I.C.R, & Buban, I.C.R. (2025). Characterization of biodegradable seaweed-based film from *Kappaphycus alvarezii* incorporating aloe vera gel as a plasticizer. *Ukrainian Journal of Food Science, 13*(1), 31–44. https://doi.org/10.24263/2310-1008-2025-13-1-5

Application of protein-berry concentrates in sauce compositions

Olena Grek, Tetiana Pshenychna, Volodymyr Lisniuk

National University of Food Technologies, Kyiv, Ukraine

Keywords:

Protein-berry concentrate
Sauce
Rheology
Sensory

Article history:

Received 12.01.2025
Received in revised form 16.06.2024
Accepted 30.06.2024

Corresponding author:

Tetiana Pshenychna
E-mail: tanya5031@ukr.net

DOI:
10.24263/2310-1008-2025-13-1-6

Abstract

Introduction. This study aimed to evaluate the effect of incorporating protein–berry concentrates, obtained by thermo-acid coagulation of milk proteins with the use of blueberry paste as a coagulant, into sauces on their structural, sensory, and physicochemical properties.

Materials and methods. In the sauce formulations, a part of the milk protein products was replaced with protein–berry concentrates, which were added at levels of 30–50%, with a variation step of 10 %. Structural and mechanical characteristics were assessed using deformation kinetics curves. Active acidity was measured potentiometrically; moisture content was determined using the thermogravimetric method.

Results and discussion. A sharp decrease in the effective viscosity of the sauces by 1.45–1.73 kPa·s was observed in the shear rate range of 1–3 s^{-1}. In the range of 3–5 s^{-1}, structural breakdown of the sauce matrix based on protein–berry concentrate (PBC) occurred, with partial structural recovery noted. At higher shear rates (5–9 s^{-1}), changes in effective viscosity were minimal (0.15–0.4 kPa·s), and the viscosity curves became linear.

The active acidity of the studied sauce samples decreased from 4.75 to 4.5 pH with the increase of protein-berry concentrate (PBC) content from 30 % to 50 %, showing values that were 0.05 to 0.25 pH units higher than those of the control sample.

The moisture content in sauces containing protein-berry concentrates was by 4.8–12.3% lower than in the control, decreasing from 57.2% to 49.7% as the content of PBC increased from 30% to 50%.

The highest effective viscosity (5.63 kPa·s) was observed in the sauce containing 50% protein–berry concentrate. This sample was characterized by a homogeneous, plastic, creamy consistency, a pronounced berry flavor, and a natural purple color.

Conclusions. The effectiveness of using protein–berry concentrates as a formulation component for developing sauces with improved sensory and rheological properties, as well as enhanced nutritional value, has been confirmed.

Introduction

The production of natural sauces enriched with beneficial compounds and featuring reduced caloric content aligns with modern consumer demands for healthier food products. Sauces are commonly used in cooking or served with dishes to enhance flavor, aroma, appearance, and nutritional value (Maoloni et al., 2022). They are characterized by specific structural and mechanical properties, which can be achieved through targeted technological processing of vegetable or dairy raw materials, in combination with the use of structure-forming agents and acidulants (Benderska et al., 2019). However, many commercially available sauces contain preservatives, artificial stabilizers, and emulsifiers (Lebedenko et al., 2021). Despite this, insufficient attention has been given to the development of new formulations and technologies for the industrial production of milk-based sauces.

When developing sauce formulations, particularly those based on protein-berry concentrates, attention must be paid to the consumer-relevant characteristics of the final product (Grek et al., 2020). To achieve the desired rheological properties, structure-forming agents are commonly employed (Lystopad et al., 2020). In berry sauce technologies, these structure formers typically include thickeners such as starches, gums, and similar ingredients, which influence the structural and mechanical characteristics of the product (Kim et al., 2014). However, these conventional structuring agents are often high in calories, poorly digestible, and do not contribute significantly to the nutritional value of the final product (Yalcinoz et al., 2016).

Most existing research focuses on the use of structuring agents and flavor enhancers, which complicate the technological process and increase production costs (Hernández-Carrión et al., 2015; Honchar and Gnitsevych, 2024; Shalaby et al., 2017; Zaouadi et al., 2015). Meanwhile, there is a lack of studies dedicated to the development of sauces based on milk concentrates, including protein-berry concentrates, with adjustable structural and mechanical properties, moisture content, active acidity, and natural color.

Dairy-plant products are widely developed and introduced into the human diet (Nascimento et al., 2023; Onopriichuk and Skuibida 2024; Skuibida et al., 2022). It is known that berry raw materials contain a significant amount of pectin substances, which have a structure-forming effect (Bélafi-Bakó et al., 2012). Blueberries are rich in vitamins, including vitamin C (14.1–26.4 mg%), pectic substances (0.32–0.45%), phenolic compounds (339–364 mg%), as well as macro- and microelements, and other biologically active substances essential for normal body function. These components also contribute to improved consumer properties of food products (Białoszycka et al., 2025). In addition, berries contain flavones, flavonols, catechins, oxycinnamic acids, which cause the natural purple colour of the product. It is known that the complex of phenolic compounds of blueberries is represented by chlorogenic acid; glycosides of kaempferol and quercetin; free, condensed catechins and proanthocyanidins (Guiné et al., 2018). Coloring substances of berry raw materials are low molecular weight phenolic compounds related to bioflavonoids, in particular anthocyanins, which are found in plants in the form of glycosides. It is the presence of anthocyanins in berries that enables their use as natural food colorants (Stabnikova et al., 2024).

The incorporation of protein–berry concentrates into sauce formulations could potentially eliminate the need for traditional thickeners and artificial colorants. The final product would be characterized by a natural composition, improved digestibility, enhanced biological value, and favorable rheological properties. The aim of the present research was to evaluate the effect of incorporating protein–berry concentrates, obtained by thermo-acid coagulation of milk proteins using blueberry paste as a coagulant, into sauces on their structural, sensory, and physicochemical properties.

Materials and methods

Materials

Protein–berry concentrates (PBC) were incorporated into the sauce formulations. The production of PBC involved thermo-acid coagulation of milk proteins using berry raw material as a coagulant, under classical conditions: a temperature of 93–95 °C with a 5-minute holding time. Homogenized blueberry paste with a pH of 2.6 ± 0.2 was used as the coagulant at a concentration of 8%, which adjusted the active acidity of the mixture to achieve an equilibrated isoelectric state of the milk proteins (pH 4.1–4.5), thereby promoting their effective coagulation (Grek et al., 2017).

Blueberry paste was obtained using the processes of hydrodynamic cavitation treatment of berry raw material on the units of TEK-SM type (Bessarab et al., 2014). The products of this process step are protein-blueberry concentrates and the coloured whey with the tint of blueberry coagulant introduced (Grek et al., 2020).

In the sauces composition containing traditional components (cream, hard rennet and processed cheeses, milk powder or whey, stabilising and flavouring additives) a part of milk-protein products was replaced by protein-berry concentrates, which were added in the amount of 30-50 %, with a variation step of 10 % of the component composition.

Methods for determining the quality indicators of sauces based on protein-berry concentrates

Structural and mechanical characteristics (effective viscosity, boundary shear stress) of sauces based on PBC were determined on a rotational viscometer by taking curves of deformation (flow) kinetics. The measurements were carried out in the 'a' mode set experimentally taking into account the structural and mechanical properties of the studied samples. The measuring cylinder was selected so that the gradient layer spreads over the entire thickness of the product layer in the annular gap of the viscometer measuring device. Shear stress τ (Pa) was measured at twelve values of shear rate gradient γ. For this purpose, readings were taken at the maximum angle of deflection of the arrow on the instrument scale. Dependences of effective viscosity (η, Pa·s) on the displacement rate (γ, s^{-1}) of sauces based on PBC were plotted on the basis of the obtained data.

The effective viscosity was determined at increasing values of cylinder speed. Tested samples of sauces based on PBC were placed in the gap between the working cylinders of the viscometer. The measurement was made at temperature (20±2) °C (Pshenychna et al., 2018).

Sensory parameters including product appearance, colour of sauces based on PBC were controlled visually; taste and smell, consistency – organoleptically at sauce temperature from 18°C to 20°C.

Active acidity of sauces based on PBC was determined potentiometrically on a universal pH-meter Sartorius PB-20. To determine the pH, 40 g of sauces was taken into the beaker, the electrodes are immersed in the beaker and after 10-15 seconds the readings of the device are recorded. The electrodes are rinsed with distilled water and wiped off with filter paper after each measurement.

The moisture content of sauces based on PBC was determined by the accelerated method (using a «Quartz» device). To determine the moisture content of the sauces, 150x150 mm newsprint bags (single or double layers) were rolled diagonally, the corners and edges were bent. The package was placed in a sheet of parchment slightly larger than the package,

without wrapping the edges. The finished bags were dried on a «Quartz» apparatus for 3 min at a temperature of 150–152 °C.

The prepared bag was weighed with 5 g of the test product to the nearest 0.01 g. The product was distributed evenly over the entire surface of the bag. The bag with the sample was closed and placed in the device between the plates heated to 150–152 °C for 5 min. The bags with dried samples were cooled in a desiccator for 3–5 min and weighed. The moisture content of the product was determined by the formula:

$$W = \frac{M - M_1}{5} \cdot 100,$$

where, W is the mass fraction of moisture, %; M is the mass of the bag with the sample before drying, g; M_1 is the mass of the bag with the sample after drying, g; 5 is the mass of the product, g. The difference between the parallel determinations did not exceed 0.5 %. The final result was the arithmetic mean of three parallel determinations (Onopriichuk et al., 2024).

Results and discussion

Structural and mechanical characteristics of sauces based on protein-berry concentrates

At the first stage, the primary raw materials directly influencing the structural–mechanical and organoleptic quality indicators of the final product were investigated. Depending on the formulation and technological purpose, pasty products must exhibit specific structural and mechanical characteristics. Structural and mechanical characteristics of sauces based on PBC were determined by the nature of bonds arising between protein particles during the structure formation. They can be classified as thixotropic structures in which the effective viscosity decreases with increasing shear rate, reversible bonds are restored after the mixture structure is disturbed. The rheological curves presented in Figure 1 describe the effect of shear rate on the effective viscosity of sauces based on PBC.

The character of curve changes indicates that the studied sauce samples are pseudoplastic in structure and flow as abnormal viscous liquids in the whole range of shear rates from 1 s^{-1} to 5 s^{-1}. The analysis of flow curves indicates that the effective viscosity of sauces under the same conditions decreases with decreasing mass fraction of protein-berry concentrate. Probably, it is connected with the change of their spatial structure, which is formed as a result of direct phase contacts of particles adhesion of the newly formed phase – caseinate calcium phosphate complex and constituents of berry coagulant. The latter are characterised by high strength. Pectin substances as surfactant compounds form a strong framework due to the convergence of hydrophobic methoxyl groups in aqueous medium, and free carboxyl groups dissociate into ions, which interact with NH_3^+ groups on the protein surface. The growth of contact strength between particles is accompanied by the appearance of crystallisation bridges. The sauce structure is elastic, dense, after mechanical breakage the bonds are slowly restored, as a consequence, the thixotropic properties are reduced in such systems.

The highest viscosity of 5.63 KPa·s was found in the sauce sample with a mass fraction of 50 % PBC. This may be due to the optimally selected amount of formulation components, which favours the formation of a compound of stable three-dimensional spatial structures and enhances the viscous characteristics of the product. When assessing organoleptic parameters of the samples under study, homogeneous, plastic, creamy consistency of sauces was noted.

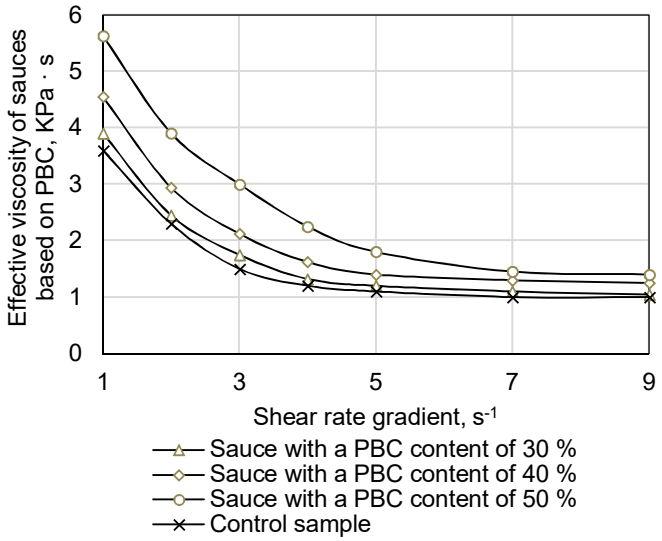

Figure 1. Effect of shear rate gradient on the effective viscosity of sauces depending on the amount of protein–berry concentrate (PBC)

Previous studies (Benderska et al., 2019) on the structural and mechanical characteristics of sauces confirm an increase in the effective viscosity values of sauces when the concentration of tomato seed paste is increased in the system. By increasing the amount of tomato paste added from 5 % to 11 %, the structural and mechanical properties of the finished product change significantly: its viscosity increases 2.46 times – from 147 Pa·s to 363 Pa·s. This can be attributed to the presence of significant content of proteins, pectin and hemicellulose in tomato seed paste with moisture-binding capacity.

There are 3 sections on the rheological curves (Figure 1). A sharp drop in effective viscosity by 1.5-2 times is observed in the range of displacement velocity (1-3) s^{-1}. This effect is due to the fact that protein-berry concentrates form a continuous three-dimensional coagulation structure under the action of Van-der-waals cohesive forces. The process occurs through the interaction between the protein globules of casein and whey proteins with the pectin substances of blueberry paste. The flow resistance in this case is insignificant, which causes a decrease in the effective viscosity of sauces by 1.45-1.73 KPa·s at shear rates up to 2 s^{-1}.

At the second section, in the range of shear rate (3-5) s^{-1}, the non-Newtonian fluidity of the viscous system of sauces based on concentrates and destruction of the partially recovering structure are observed. At the third section at high values of shear rate (5-9) s^{-1} the effective viscosity of sauces changes by 0.15-0.4 KPa·s, and the curves of effective viscosity have a linear character. The recovery process of the sample with a mass fraction of PBC 30 % is slower (deformation is greater and recovery is less pronounced), suggesting a less stable structure compared to samples with mass fraction of PBC 40 % and 50 %.

Other experimental data (Lebedenko et al., 2021) also confirm that the sauce with complete replacement of flour by a structuriser of polysaccharide nature had the highest viscosity, while the control sample had the lowest. Thus, at a shear rate of 0.3333 s^{-1}, the

viscosity of the control sample is 14.32 Pa·s, the samples with replacement of 50 % flour, 10 g fat and 100 % flour, 10 g fat are 16.49 and 19.6 Pa·s, respectively. Scientists have stated that the sauce with complete replacement of flour by plant polysaccharides has a thicker, more viscous consistency, affecting organoleptic properties.

The determining quality indicator for sauces is their consistency, so the obtained data of rheological parameters of experimental samples correlated with organoleptic perception. The type of product structure determines its qualitative and technological characteristics. Based on the obtained results, organoleptic evaluation of the developed samples of sauces based on PBC was carried out, which is presented in Table 1.

Table 1

Sensory characteristics of sauces based on protein-berry concentrates

Amount of protein-berry concentrate, %	Sensory characteristics		
	Consistency and appearance	Taste and smell	Colour
30	Homogeneous, mastic, slightly viscous	Clear, milky, with a slight blueberry flavour	Barely noticeable pale purple, uniform throughout the whole mass
40	Pasty, homogeneous, moderately thick	Moderately noticeable blueberry flavour and aroma	Light purple, uniform throughout the mass
50	Thick, homogeneous creamy consistency	Pronounced flavour and aroma of berry raw material	Pronounced purple, uniform throughout the mass

The visualization of the obtained sauce samples based on protein-berry concentrates is shown in Figure 2. The samples had a purple, uniform color, a noticeable berry taste and aroma, and a delicate, moderately mastic consistency with single inclusions of berry shells.

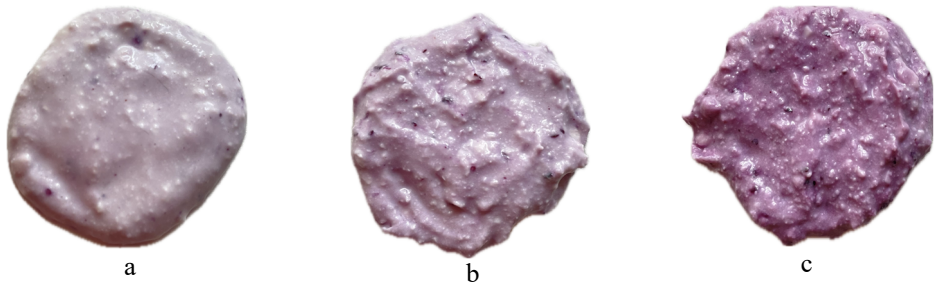

Figure 2. Sauces based on protein-berry concentrate (PBC): a, 30 % PBC; b, 40 % PBC; c, 50 % PBC

Physicochemical parameters of sauces based on protein-berry concentrate

Since PBC have a higher acidity compared to classical types of milk-protein concentrates, it is reasonable to determine the effect of different amounts of PBC on the acidity in the finished product and the mass moisture fraction (Figure 3).

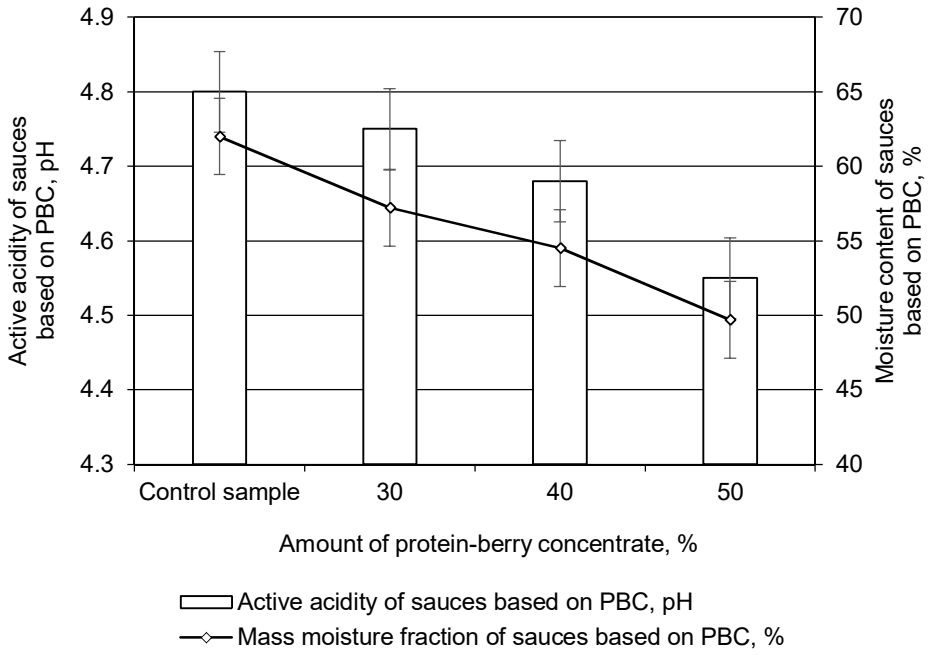

Figure 3. Change in active acidity and moisture content of sauces depending on the amount of protein-berry concentrate (PBC)

The active acidity of the sauce samples increased from 4.75 to 4.5 pH with increasing the amount of PBC used from 30 % to 50 % and was 0.05-0.25 pH units higher than in the control sample. For comparison, the active acidity values for functional sauces using whey and vegetable powders ranged from 3.50 to 4.45 pH (Khatko et al., 2021).

The obtained results confirm that protein-berry concentrates are characterized by an increased content of organic acids contained in the berry coagulant. When developing formulations, this will allow artificial citric acid to be replaced by natural organic acids, which are contained in significant amounts (2.0-4.3 %) in blueberry paste (Yavorska et al., 2020).

The mass fraction of moisture in sauces based on PBC was 4.8-12.3 % lower compared to the control sample and continued to decrease from 57.2 to 49.7 % with increasing concentrate use from 30 to 50 %. Probably, it is connected with transformation of the spatial structure, which is formed as a result of direct contacts of the adhesion of particles in the formed phase – caseinate calcium phosphate complex and carbohydrate components of blueberry paste.

The sauce is characterised by a high content of high-grade animal proteins due to the introduction of milk-protein concentrates with essential amino acids, which are of great importance in dietary, medical and preventive nutrition, and determines its high biological value.

The technology of sauces based on PBC can be realised on the equipment for production of pasty cheeses. Due to the use of a wide range of berry raw materials in the production of protein-berry concentrates, sauces can acquire a variety of taste, aroma and natural colouring, which significantly increases the possibility of their use in cooking.

Conclusions

1. By varying the amount of protein-berry concentrate (PBC) from 30% to 50% in the sauce formulation, it is possible to predict one of the key quality indicators—effective viscosity. The sauce containing 50% PBC demonstrated the highest effective viscosity (5.63 kPa·s) and was characterized by a homogeneous, plastic, creamy consistency, a pronounced berry flavor, and a natural purple color.

2. The active acidity of the studied sauce samples increased from 4.75 to 4.5 pH with the increase in the use of protein-berry concentrates from 30 % to 50 %, and the mass moisture fraction on the contrary decreased from 57.2 % to 49.7 % under the same manufacturing conditions.

3. The presence of natural berry flavor and color in sauces made with protein-berry concentrates eliminates the need for artificial flavors and colorants.

4. Based on the specific characteristics of sauces containing protein–berry concentrates, a sensory evaluation scale was developed according to the concentrate content, allowing for the production of sauces with predictable sensory properties. The obtained data also make it possible to forecast the influence of mechanical processing of the formulation components on the rheological characteristics of the final product.

References

Bélafi-Bakó K., Cserjési P., Beszédes S., Csanádi Z., Hodúr C. (2012), berry pectins: microwave-assisted extraction and rheological properties, *Food and Bioprocess Technology,* 5(3), pp. 1100–1105.

Benderska O., Bessarab A., Shutiuk V. (2019), Research of structural-mechanical properties of tomato sauce, *Food Industry,* 26, pp. 64-70.

Bessarab O.C., Osypenko S.B., Stoianova L.O., Pakhomova K.Yu. (2014), Innovative development of homogenized fruit products of increased biological value based on hydrodynamic processing of raw materials, *Equipment and Technologies for Food Production,* 32, pp. 7-19.

Białoszycka Ż., Białoszycka M., Pachevska A., Istoshyn V., Biloshytska A. (2025), Application of medicinal properties of blueberries (*Vaccinium myrtillus*), *Journal of Education, Health and Sport,* 80, pp. 58369, https://doi.org/10.12775/JEHS.2025.80.58369

Grek O., Onopriichuk O., Pshenychna T. (2017), The rationalization of the parameters of milk proteins' thermo acid coagulation by berry coagulants, *Food and Environment Safety,* 16(1), pp. 47-53.

Grek O., Pshenychna T., Tymchuk A., Savchenko O., Ochkolyas O. (2020), Research of quality indicators in protein-blueberry concentrates, *Slovak Journal of Food Sciences*, 14, pp. 156-163, https://doi.org/ 10.5219/1255

Guiné R.P.F., Matos S., Gonçalves F.J., Costa D., Mendes M. (2018), Evaluation of phenolic compounds and antioxidant activity of blueberries and modelization by artificial neural networks, *International Journal of Fruit Science,* 18(2), pp. 199-214, https://doi.org/10.1080/15538362.2018.1425653

Hernández-Carrión M., Sanz T., Hernando I., Llorca E., Fiszman S. M., Quiles A. (2015), New formulations of functional white sauces enriched with red sweet pepper: a rheological, microstructural and sensory study, *European Food Research and Technology,* 240, pp. 1187-1202, https://doi.org/10.1007/s00217-015-2422-1

Honchar Yu., Gnitsevych V. (2024), Improving the quality of dairy sauces by using condensed low-lactose milk whey, In: O. Priss (Ed.), *Food Technology Progressive Solutions*, pp. 152-168, Scientific Route, Tallinn, Estonia, https://doi.org/10.21303/978-9916-9850-4-5.ch6

Jeske S., Zannini E., Arendt E. K. (2018), Past, present and future: The strength of plant-based dairy substitutes based on gluten-free raw materials, *Food Research international,* 110, pp. 42-51, https://doi.org/10.1016/j.foodres.2017.03.045

Khatko Z.N., Tamakhina M.A. (2021), Development of white and red low-calorie functional purpose sauces using vegetable powders, *New Technologies*, 17(2), pp. 67–76, https://doi.org/10.47370/2072-0920-2021-17-2-67-76

Kim S.G., Yoo W., Yoo B. (2014), Relationship between apparent viscosity and linespread test measurement of thickened fruit juices prepared with a xanthan gum-based thickener, *Preventive Nutrition and Food Science*, 19(3), pp. 242–245, https://doi.org/10.3746/pnf.2014.19.3.242

Lebedenko T., Krusir G., Shunko H., Korkach H. (2021), Development of technology of sauces with functional ingredients for restaurants, *Scientific Messenger LNUVMB. Series: Food Technologies,* 23(95), pp. 57-64, https://doi.org/10.32718/nvlvet-f9510

Lystopad T., Deinychenko G., Pasichnyi V., Shevchenko A., Zhukov Y. (2020), Rheological studies of berry sauces with iodine-containing additives, *Ukrainian Food Journal,* 9(3), pp. 651-663, https://doi.org/10.24263/2304-974X-2020-9-3-13

Maoloni A., Cardinali F., Milanović V., Garofalo C., Osimani A., Mozzon M., Aquilanti L. (2022), Microbiological safety and stability of novel green sauces made with sea fennel (*Crithmum maritimum* L.), *Food Research International*, 157, 111463, https://doi.org/10.1016/j.foodres.2022.111463

Nascimento L.G.L., Odelli D., de Carvalho A. F., Martins E., Delaplace G., de Sá Peixoto Júnior P.P, Silva N.F.N., Casanova F. (2023), Combination of milk and plant proteins to develop novel food systems: What are the limits? Foods, 12(12), 2385, https://doi.org/10.3390/foods12122385

Onopriichuk O., Skuibida V. (2024), Improvement of fermented dairy-plant concentrate technology, *Ukrainian Journal of Food Science,* 12(2), pp. 117–130, https://doi.org/10.24263/2310-1008-2024-12-2-4

Pshenychna T.V., Grek O.V., Onopriichuk O.O., Pasichnyj V.M., Chubenko L.M. (2018), Quality indicators of multicomponent clots obtained by thermo acid coagulation of milk proteins, *Food Industry AIC,* 1, pp. 24-29.

Shalaby S.M., Mohamed A.G., Bayoumi H.M. (2017), Preparation of a novel processed cheese sauce flavored with essential oils, *International Journal of Dairy Science,* 12, pp. 161-169, https://doi.org/10.3923/ijds.2017.161.169.

Skuibida V., Onopriichuk O., Tymchuk A., Soloviov N., Grek O. (2022), Quality indicators of multicomponent dairy-vegetable concentrates, *Ukrainian Food Journal*, 11(2), pp. 247-258, DOI: 10.24263/2304-974X-2022-11-2-5

Stabnikova O., Stabnikov V., Paredes-López O. (2024), Fruits of wild-grown shrubs for health nutrition, *Plant Foods for Human Nutrition*, 79(1), pp. 20-37, https://doi.org/10.1007/s11130-024-01144-3

Yalcinoz S.K., Ercelebi E. (2016), Rheological and sensory properties of red colored fruit sauces prepared with different hydrocolloids, *Journal of International Scientific Publications: Agriculture and Food,* 4, 1000020, pp. 496–509, https://www.scientific-publications.net/en/article/1001065/

Yavorska N.Y., Vorobets N.M. (2020), Seasonal variation in the ascorbic and organic acids content in shoots of highbush blueberry cultivars during vegetation stages, *Medicinal and Clinical Chemistry,* 2, pp. 31-38, https://doi.org/10.11603/mcch.2410-681X.2020.v.i2.11355

Zaouadi N., Cheknane B., Hadj-Sadok A., Canselier J.P., Ziane A.H. (2015), Formulation and optimization by experimental design of low-fat mayonnaise based on soy lecithin and whey, *Journal of Dispersion Science and Technology,* 36(1), pp. 94-102, https://doi.org/10.1080/01932691.2014.883572

Cite:

UFJ Style

Grek O., Pshenychna T., Lisniuk V. (2025), Application of protein-berry concentrates in sauce compositions, *Ukrainian Journal of Food Science*, 13(1), pp. 45–54, https://doi.org/10.24263/2310-1008-2025-13-1-6

APA Style

Grek, O., Pshenychna, T., & Lisniuk, V. (2025). Application of protein-berry concentrates in sauce compositions. *Ukrainian Journal of Food Science, 13*(1), 45–54. https://doi.org/10.24263/2310-1008-2025-13-1-6

Effect of pregelatinized corn starch on the technological and quality properties of pea dough and snacks

Kateryna Rubanka, Olha Pysarets, Tetyana Levkivska, Oleksandr Samoilik, Vladyslav Shpak

National University of Food Technologies, Kyiv, Ukraine

Keywords:

Pea flour
Corn
Starch
Dough
Snack
Strength
Viscosity

Article history:

Received 29.01.2025
Received in revised form 01.06.2024
Accepted 30.06.2024

Corresponding author:

Kateryna Rubanka
E-mail: rubanka_ekaterina@ukr.net

DOI:
10.24263/2310-1008-2025-13-1-7

Abstract

Introduction. The aim of the work was to study the effect of pregelatinized corn starch on the technological and quality properties of pea dough and snacks.

Materials and methods. Pea flour was used as the main raw material, and corn starch was used as the structure-forming agent. Structural and mechanical properties of the dough and snacks were determined by the elasticity, adhesion strength, dough viscosity, and snack strength. Sensory quality indicators were determined with the involvement of tasters using a 5-point scale, taking into account the importance of each indicator.

Results and discussion. It was shown that the addition of up to 20% pregelatinized corn starch to the formulation of pea-based snacks positively influenced dough structure formation. Specifically, elasticity increased to 37 g, which was by 25.6% higher compared to the control sample containing 5% native corn starch, while viscosity increased to 171 cP.

A further increase in the dosage of pregelatinized corn starch, however, resulted in a decline in these quality indicators. A similar trend was observed in the final product: as the starch dosage increased, snack firmness decreased, making them easier to chew. However, when the starch content exceeded 15%, the finished product became excessively thin, negatively affecting its structural integrity. This will negatively affect the quality of the snacks during transportation due to the possibility of a large number of scraps.

The analysis of the effect of pregelatinized corn starch dosage on sensory characteristics showed a positive impact on product appearance, as it contributed to the formation of thinner snacks. No noticeable changes in taste were observed. Nutritional value calculations indicated a slight decrease: with a 15% starch addition, protein content was reduced by 5.2%, and fat content by 5.3%, compared to the control sample containing 5% native corn starch. Meanwhile, the carbohydrate content increased by only 10.9%.

Conclusion. The use of pregelatinized corn starch allowed to ensure high structural and mechanical properties of both dough and snacks based on pea flour. It is recommended to incorporate pregelatinized corn starch into the formulation of pea snacks at a level not exceeding 15%.

Introduction

Snack products are one of the most popular in the global market (Chehtman, 2022). Since such products are thermally processed, which facilitates digestion by the human body, dehydrated, therefore they have a low mass, ready for consumption, which is important in the conditions of urbanization of life (Rubanka et al., 2022). However, most of these products are made on the basis of cereals (wheat, rice, barley) a lot of sugar is added as a structure-forming agent, or deep-frying is used during thermal processing, which are undesirable in the case of a healthy diet. Pea flour is naturally gluten-free and considered safe for individuals with celiac disease or other gluten-related disorders.

To combine the demand for ready-to-eat products with the need to consume highly nutritious products, it is necessary to use ingredients with high biological value for their production (Ivanov et al., 2021; Tsykhanovska et al., 2023). Legumes are sources of proteins and essential amino acids. The total essential amino acid content of legume proteins is 38–45 g/100 g (Shevkani, 2023). Peas are a low-cost source of protein and energy that combines technological functionality and nutritional value (Farshi et al., 2024).

It was proven that with an increase in the extrusion temperature of 135°C, the swelling coefficient of the extruded snacks in which corn or rice flour was partially or completely replaced increased to 40% (Maskus et al., 2015). It was also proven that the presence of peas in the snack composition at an extrusion temperature (159–164°C) and a screw rotation speed (165–214 rpm) made it possible to produce high-quality snacks (Félix-Medina et al., 2020).

The use of pea and oat flours and pea isolate in cracker technology allowed the development of snacks with a high protein content (24.66 g/100 g) and a low lipid content (9.07 g/100 g). In terms of its structural properties, the snack had lower hardness (19.04 N) and stickiness (4.07 N), but higher cohesion (0.35), elasticity (0.45 mm) and chewiness (0.35) compared to commercial crackers (Morales-Polanco et al., 2017), which also confirms the feasibility of using pea flour in snack production. The snacks exhibited a higher polyphenolic content—ranging from 0.33 to 0.62 mg gallic acid equivalents (GAE) per gram of sample—along with increased antioxidant activity (up to 8.7%) and a softer texture (Wani et al., 2018).

However, the production of snacks, based on peas can be complicated. Pea proteins are characterized by high water and fat binding capacity, which led to the formation of a gel, and subsequently a hard texture of products after their thermal treatment. This property has positive potential in the case of the production of meat substitutes (Serdaroglu et al., 2005), but is undesirable in the production of snacks from pea flour, as it will give a dense structure to the finished product (Venkatachalam et al., 2025).

Therefore, to adjust the structural and mechanical properties of snacks and their sensory indicators, it is necessary to use ingredients that will provide the structure of the dough and the finished product. One of such ingredients is starch. It has a high water-binding capacity, and the nature of starch, which is determined by the structure of starch grains, affects the characteristics of the dough and the finished product (Yifei et al., 2020).

Starch is widely utilized in the food industry for a variety of purposes, including the production of bakery products (Fonseca et al., 2021), stabilization of emulsions in soft drinks (Lyu et al., 2024), encapsulation of flavorings, formulation of dairy products (Naseer et al., 2021), preparation of fruit semi-finished products (Agudelo et al., 2023), as well as in instant soups and sauces (Fonseca et al., 2021), and in the mayonnaises and salad dressings (Block et al., 2023). It is also used in meat products (Marynin et al., 2023), including the use of electrochemically activated water for the preparation of starch suspensions (Marynin et al., 2022), giving them the desired physicochemical, functional, and digestible characteristics (Agama-Acevedo et al., 2019; Magallanes-Cruz et al., 2017).

The aim of the present work was to investigate the effect of pregelatinized corn starch on the technological and quality properties of dough and snacks made from pea flour.

Materials and methods

Materials and dough preparation

Pea flour (LLC "Prodenergo" Ukraine), native corn starch (PJSC "Dniprovsky Starch Molasses Combine", Ukraine), salt, (LLC "Foreign trade resource" Ukraine), mixture of spices (ground black pepper, dried granulated garlic, ground coriander) (PJSC "Ukroptbakaliya" Ukraine), pregelatinized corn starch Interstarch CWS30.50 (PJSC "Dniprovsky Starch Molasses Combine", Ukraine) were used for snack preparation.

The recipe of the control dough sample included pea flour in the amount of 92.5%, native corn starch, 5%, salt, 2%, mixture of spices, 0.5%, and water. The dough was prepared by kneading with a moisture content of 48.0%. Dough samples under study were prepared, replacing native corn starch and the corresponding part of the flour with pregelatinized corn starch in the amount of 5, 10, 15, 20 and 25%. The finished dough was deposited in an amount of 25 g and baked using a MAGIO MG-397 waffle iron (China) at a temperature of 160 ° C for 2.5 min.

Determination of structural and mechanical properties of dough and snacks

To analyze the structural and mechanical properties of the dough and finished products, a Brookfield CT3 texture analyzer was used. The elasticity of the dough and its adhesion strength were determined using a TA4/1000 nozzle (38.1 mm Diameter cylinder probe) Clear Acrylic 26 g, 20 mm Long Rad 35-43 mm. The study was carried out with the following parameters: nozzle movement speed 1 mm/s, depth of its immersion in the dough sample 10 mm. The research error was ±0.05. The viscosity of the dough was determined on a Brookfield Viscometr DV2T viscometer at a temperature of 21.8°C with a nozzle rotation speed (cylinder) of 100 rpm, torque – 30.3–69.8%.

When analyzing the strength of ready-made snacks on the Brookfield CT3 texture analyzer, a TA7 (knife edge) Clear Acrylic 8 g, 60 mm Wide nozzle was used. Research conditions: nozzle movement speed 2 mm/s, depth of its immersion in the sample 10 mm (Sobczyk et al., 2017).

Determination of sensory quality indicators of pea snacks

Sensory assessment of the quality of ready-made snacks was carried out using a complex indicator (Galenko et al., 2022). The analysis was carried out using a 5-point scale. The tasting commission consisted of 10 experts of different age categories, who established the weighting indicators for each indicator (appearance, consistency, taste, aroma) and evaluated this indicators. Based on the results of the research, quality profilograpms were constructed and a complex indicator (K_0) was calculated using the formula:

$$K_0 = M_1 \frac{P_1}{P_1^b} + M_2 \frac{P_2}{P_2^b} + M_3 \frac{P_3}{P_3^b} + M_4 \frac{P_4}{P_4^b},$$

where P_1, P_2, P_3, P_4 are arithmetic mean score for appearance, consistency, aroma, and taste, respectively;

P_1^b, P_2^b, P_3^b, P_4^b are basic score (standard) for appearance, consistency, aroma and taste, respectively (for all indicators a score of 5 was accepted);

M_1, M_2, M_3, M_4 are weighting indicators for appearance, consistency, taste and aroma, respectively.

Calculation of nutritional and energy values of pea snacks

To study the beneficial properties, including the degree of ensuring the physiological needs for basic nutrients and energy, the nutritional and energy value, the content of water-soluble vitamins and minerals of the developed products were calculated. When making calculations, the "Norms of physiological needs of the population of Ukraine for basic nutrients and energy" approved by the Ministry of Health of Ukraine for women aged 18-29 years of the 1st labor intensity group were used.

Statistical analysis

All measurements were carried out as independent experiments and triplicated accordingly.

Results and discussion

Effect of pregelatinized corn starch on the structural and mechanical properties of pea-based dough

Pregelatinized corn starch was made from waxy corn, for the modification of which physical methods were used. Such starches are rich with amylopectin, where the amylose content does not exceed 5% (according to the product specification declared by the manufacturer), which in turn will affect the structural and mechanical properties of the dough and as a consequence the process of kneading the dough and settling the dough pieces. Therefore, it was considered appropriate to investigate the influence of pregelatinized corn starch on the structural and mechanical properties of the dough. The results of studies of dough elasticity and its adhesive properties are presented in Figure 1.

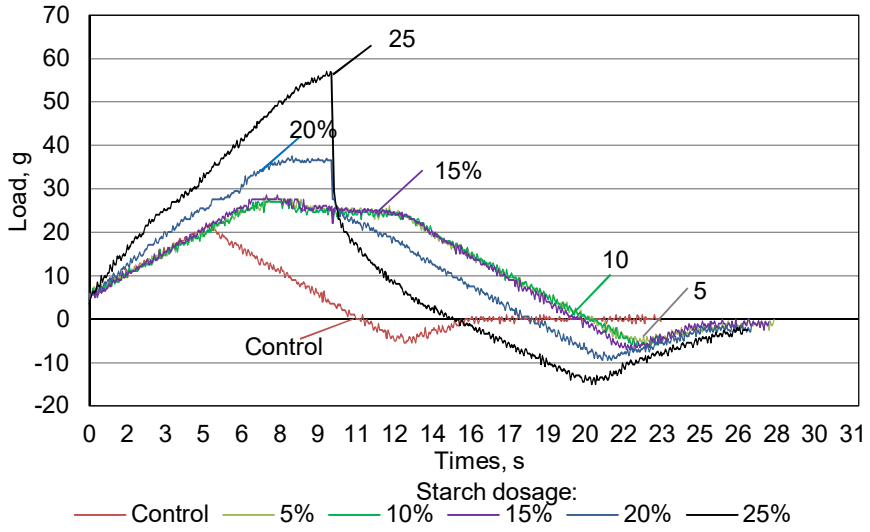

Figure 1. Changes in dough elasticity and adhesion strength depending on the dosage of pregelatinized corn starch

It was found that the introduction of pregelatinized corn starch in an amount of 5 to 15% caused a softer consistency compared to the control, due to the fact that it is cold-swelling – pregelatinized (Sugiura et al., 2017), which positively affected the elastic properties of the dough. Increasing the dosage of pregelatinized corn starch above 15% led to an increase in the amount of moisture that binded to the starch. Therefore, the dough acquired the characteristics of a soft paste, not a hard gel. Thus, its viscosity increased, which reduced the immersion time of the texture analyzer nozzle in the sample and increased the strength of the dough, which is visible in the graph. Thus, amylopectin starch from waxy corn, which contains no more than 5% amylose, forms a gel and if the starch dosage is increased, the gel turns into a paste (Varghese et al., 2022). The addition of 5, 10 and 15% of pregelatinized corn starch to the pea snack recipe moderately increased the dough elasticity to 27 g for all three samples, which was 25.6% more compared to the control sample. At the same time, the immersion time of the nozzle in the test sample was gradually increased to 10 mm. The addition of 20 and 25% of pregelatinized corn starch significantly increased the dough elasticity, namely to 37 and 57 g, respectively, which was 72.1 and 165% more compared to the control sample. During similar studies by a group of scientists from South Korea and India, they proved that in pregelatinized starches there was a hydrophilic tendency of starch and explained this by the hydrothermal treatment of starches (Singh et al., 2009). Similar results were reported by Morales-Polanco et al. (2017), in which gluten-free cracker dough had higher dough elasticity compared to commercial crackers. These results were consistent with those reported by Crocket et al. (2011), who added pea protein to gluten-free products to increase dough elasticity and improve the palatability of the finished product.

During the removal of the load from the studied samples, a decrease in stress occured, which is called relaxation, which was accompanied by the restoration of the dough shape. At the same time adhesive separation occured along the product layer (cohesive type). Thus, samples with the addition of 5, 10 and 15% of pregelatinized corn starch were characterized by gradual adhesion after 7.05, 6.7 and 6.5 s, respectively, and continued up to 12.5 s. While in samples with the addition of 20 and 25% of pregelatinized corn starch, a sharp decrease in adhesion was observed and the higher the dosage, the stronger the separation, which is possibly explained by the increase in dough viscosity and the transition from the gel to the paste state.

The results obtained are confirmed by the studies of Yousif at al. (2012), who analyzed in detail the pregelatinized corn starch pastes and found that this property was desirable and widely used for the production of many food products, while native starch paste had a non-cohesive texture, which limited its application. Morales-Polanco et al. (2017) proved that the cohesiveness of pea dough was 0.35 mm, which was higher than for commercial crackers. These results are consistent with the results reported by Crocket et al. (2011), who added pea protein to gluten-free products to increase the elastic modulus of the dough and improve the palatability of the finished product. To confirm the obtained results, the viscosity of the dough was investigated, the results are shown in Figure 2.

The addition of 5–25% of pregelatinized corn starch increased the viscosity of the dough 1.2, 1.8, 8, 11 and 17 times. The obtained research results confirm the previous ones. It was known that pregelatinized starch contained broken intermolecular bonds of starch molecules, therefore the granular structure was split (Fonseca et al., 2021), the dough absorbed more amount if water, therefore the viscosity of the dough increased, which was characteristic of the studied dough.

In addition, Oliver et al. (1995) argued that the use of pregelatinized starch was intended for thickening gluten-free dough mixtures to prevent the settling of starch granules during the dough mixing phase. This in turn allowed to thicken gluten-free dough. However, increasing the dosage of pregelatinized corn starch by more than 20% is not advisable, since the external characteristics of such dough had a structure that was characterized as pasty. Such a dough structure complicated the process of forming dough pieces, namely the settling of the dough. Therefore, to find the optimal dosage of pregelatinized corn starch to the recipe of pea snacks, additional studies of the effect of this additive on the quality of the finished product are necessary.

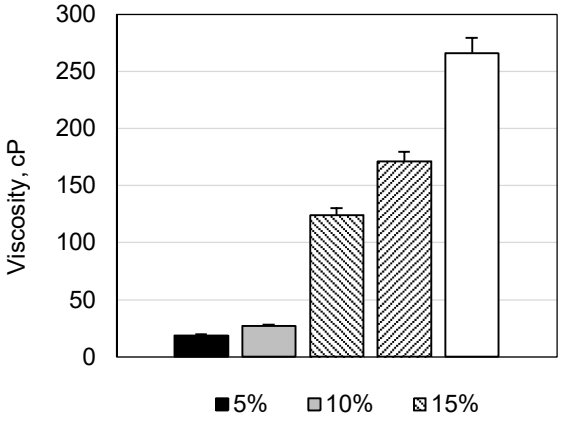

Figure 2. Effect of pregelatinized corn starch dosage on the viscosity of pea dough

Effect of pregelatinized corn starch on the strength of pea snacks

It has been demonstrated that pregelatinized starches can be used in snack technology to give them a "crispy" texture (Christaki et al., 2017; Fustier et al., 1998; Wang et al., 2019). (Christaki et al., 2017; Fustier et al., 1998; Wang et al., 2019). However, both manufacturers and researchers have reported that the incorporation of pregelatinized starch into dough formulations results in a finer but drier texture of the final product, as well as starch retrogradation during storage (Wang et al., 2019). This reduced the time of maintaining the required softness of the finished products. Therefore, the effect of the dosage of pregelatinized corn starch on the strength of pea snacks was investigated. The results of the studies are presented in Figure 3.

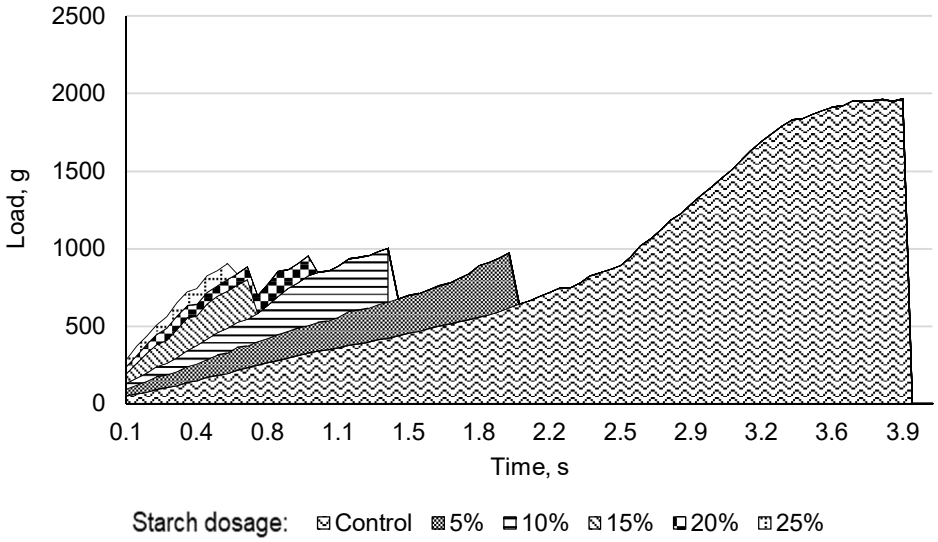

Figure 3. Effect of dosage of pregelatinized corn starch addition on pea snack strength

When 5% pregelatinized starch was added to pea snacks, the strength of the finished products decreased 5.5 times compared to the control sample. Further addition of starch in the amount of 10-25% reduced the strength of the snacks 5.7 times, 7.7 times, 15.1 times and 18.5 times compared to the control sample. Numerous studies have shown that increasing the amount of pregelatinized starch added contributes to greater water absorption in the dough, which in turn leads to an increase in its volume (Chillo et al., 2007; Christaki et al., 2017; Wang et al., 2019). Yousif et al. (2012) found that the water binding and fat binding capacity of pregelatinized corn starch increased to 1.49 and 2.35 g/g, respectively, compared to native starch, for which the water-binding capacity was 1.2 g/g, the fat-binding capacity was 1.6 g/g. The use of such starch in the production of noodles contributed to an increase in the volume of the finished product by up to 10%. The replacement of wheat flour with 5%, 10% and 15% pregelatinized corn starch did not cause any negative effects on the sensory properties of noodles.

During the heat treatment of dough pieces, moisture was removed and the finished product was loosened. Thus, the strength of pea snacks was reduced, which affected the sensory characteristics of the finished product. It was found that the addition of 20% and 25% pregelatinized corn starch resulted in obtaining snacks with a very soft structure, with a strength of only 130 g and 106 g, respectively. Such snacks broke with minimal force, and therefore, their packaging and transportation may be complicated, during which a lot of waste such as scrap and crumbs may be formed. This, in turn, may lead to additional costs for product production and a decrease in their sensory quality in terms of appearance.

Influence of pregelatinized corn starch on the sensory characteristics of pea snacks

As it is known (Meiselman, 2013; Torrico et al., 2023) sensory indicators such as appearance, color, consistency, taste and aroma primarily affect consumer choice. Therefore, the sensory characteristics of snacks made with the addition of different concentrations of starch were evaluated. The quality profile of the finished snacks is presented in Figure 4.

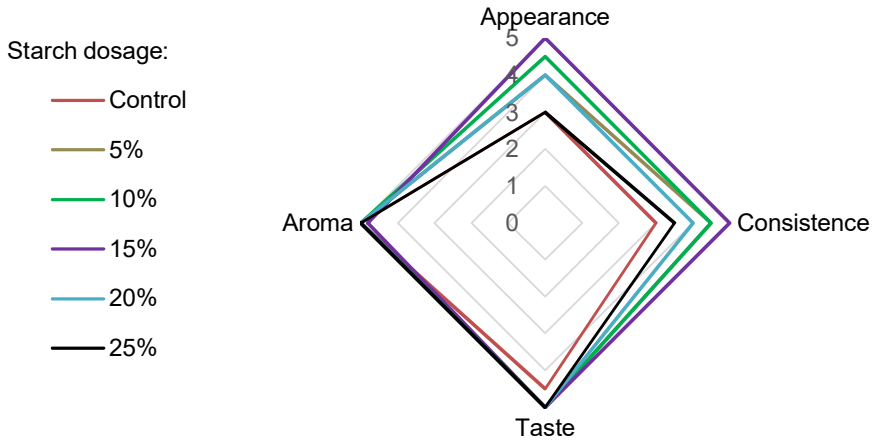

Figure 4. Profilogram of sensory quality assessment of pea snacks made with the addition of pregelatinized corn starch

The introduction of pregelatinized corn starch into the recipe of pea snacks improved the appearance and consistency of the finished products. The more starch was added, the thinner the snacks were obtained, which became more crispy and tender in consistency. However, the introduction of 20 and 25% of pregelatinized corn starch led to a too thin structure. Thus, the snacks became tenderer but dry, easily broke and a lot of crumbs were formed. Pregelatinized corn starch did not affect the taste and aroma. All samples had a pleasant aroma and a clear pea flavor, the color was from light yellow to cream. When comparing snacks made with pregelatinized corn starch and the control sample, even a dosage of 5% pregelatinized corn starch promoted obtaining snacks more crispy in consistency, which confirmed the results of the analysis of the strength of the finished snacks shown on Figure 4.

The results were also confirmed by calculation of a complex sensory quality assessment index for pea snacks with different dosages of pregelatinized corn starch (Figure 5).

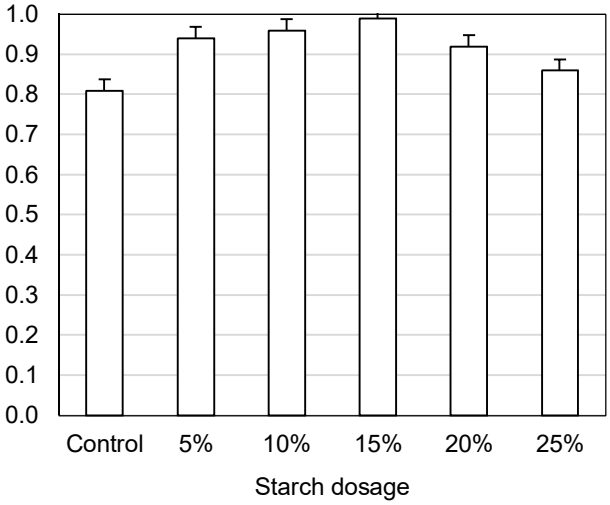

Figure 5. Complex sensory quality assessment index for pea snacks with different dosage of pregelatinized corn starch

Replacing native starch with pregelatinized corn starch with a subsequent increase in dosage to 15% contributed to an increase in complex indicator of sensory quality assessment which was closer to 1. The best result was obtained with a sample containing 15% of pregelatinized corn starch, the complex indicator of which was 0.99. Further increase in starch dosage reduced the complex indicator to 0.92 and 0.86 for 20 and 25 %, respectively.

The obtained data confirmed the results of studies by scientists (Chillo et al., 2007; Christaki et al., 2017; Fustier et al., 1998; Wang et al., 2019), who claimed that pregelatinized starches contributed to the structure formation of the dough by thickening it and increasing the adhesive (gluing) properties for thin wafers, crispy coating for nuts, molded chips, cookies, crackers, galettes, provided that its dosage was strictly controlled. Thus, based on the structural and mechanical properties of the dough, ready-made snacks based on pea flour and their sensory evaluation, it was recommend adding 15% of pregelatinized corn starch, which was the most optimal for achieving high quality of the finished product. In order to establish the quality of the finished product, nutritional and energy value of snacks made with the addition of 15% pregelatinized corn starch, the following indicators were calculated, which are presented in Table 2.

Table 2

Nutritional and energy value of pea snacks

Ingredient	Daily requirement	Control		Snacks with 15% pregelatinized corn starch	
		Content per 100 g of snack	Integral score, %	Contentper 100 g of snack	Integral score, %
Proteins, g	55–57	19.4	35.3	18.4	33.5
Fats, g	56–58	1.9	3.4	1.8	3.2
Carbohydrates, g	320–325	49.5	15.5	54.9	17.2
Energy value, kcal	2450–2500	280.3	-	295.0	-

The replacement of part of the pea flour with 15% pregelatinized corn starch led to a decrease in the protein content, the value of the integral score of which was reduced by only 6%, and for fat – by 5.3%. The carbohydrate content increased by 11%. And this, in turn, led to an increase in the energy value of snacks by 5%. Thus, the introduction of 15% starch reduced the nutritional value, increased the energy value, but these losses overlapped the effect on the structural and mechanical indicators of the finished snacks and their sensory characteristics.

Conclusions

The use of pregelatinized corn starch had a positive effect on the structure of gluten-free dough made from pea flour. Pregelatinized corn starch coused structural characteristics of a gel in pea dough, it became more elastic (the elasticity increased to a maximum of 37 g), and the viscosity increased (up to 171 cP). However, this pattern was observed when adding pregelatinized corn starch in an amount of up to 20%, and a further increase in the dosage of this ingredient led to a deterioration in the consistency of the dough. In addition, since increasing the dosage of the additive reduced the strength of finished products, they became more tender, crispy, but in the amount of 20 and 25% starch, the products had such a low strength (namely 130.5 g and 106 g, respectively) that they became thin and overdried.

The starch used had no taste and did not affect the flavor or aroma of the snacks, while improving their consistency (crispness) up to the addition limit of 15% pregelatinized corn starch.

It is recommended to add pregelatinized corn starch to pea snack formulations in amounts not exceeding 15%. This level ensures the production of gluten-free dough and finished snacks with favorable structural, mechanical, and textural properties. Furthermore, nutritional value assessments support the feasibility of incorporating starch at this level, as the reductions in protein and fat content were relatively minor – 5.2% and 5.3%, respectively – while the carbohydrate content increased by only 10.9%.

References

Agama-Acevedo E., Flores-Silva P. C., Bello-Perez L. A. (2019), Cereal starch production for food applications In: M. Clerici, M. Schmiele (Eds.), *Starches for Food Application*, pp.

71–102, Academic Press, USA, https://doi.org/10.1016/B978-0-12-809440-2.00003-4
Agudelo A., Varela P., Sanz T., Fiszman S. M. (2014), Native tapioca starch as a potential thickener for fruit fillings. Evaluation of mixed models containing low-methoxyl pectin, *Food Hydrocolloids*, 35, pp. 297–304, https://doi.org/10.1016/j.foodhyd.2013.06.004
Block A.E., Bolhuis D.P., Arnaudov L.N., Velikov K.P., Stieger M. (2023), Influence of thickeners (microfibrillated cellulose, starch, xanthan gum) on rheological, tribological and sensory properties of low-fat mayonnaises, *Food Hydrocolloids*, 136(2), 108242, https://doi.org/10.1016/j.foodhyd.2022.108242
Chehtman A. (2022), Top six trends shaping the global snacks industry, *Euromonitor International*, Available at: https://www.euromonitor.com/article/top-six-trends-shaping-the-global-snacks-industry
Chillo S., Laverse J., Falcone P.M., Del Nobile M.A. (2007), Effect of carboxymethylcellulose and pregelatinized corn starch on the quality of amaranthus spaghetti, *Journal of Food Engineering*, 83(4), pp. 492–500, https://doi.org/10.1016/j.jfoodeng.2007.03.037
Christaki M., Verboven P., Van Dyck T., Nicolai B., Goos P., Claes J. (2017), The predictive power of batter rheological properties on cake quality – The effect of pregelatinized flour, leavening acid type and mixing time, *Journal of Cereal Science*, 77, pp. 219–227, https://doi.org/10.1016/j.jcs.2017.07.001
Crocket R., Le P., Vodovotz Y. (2011), Effect of soy protein isolate and egg wite solids on the physicochemical properties of gluten-free bread, *Food Chemistry*, 129, pp. 84-91, https://doi.org/10.1016/j.foodchem.2011.04.030
Félix-Medina J.V., Montes-Ávila J., Reyes-Moreno C., Perales-Sánchez J.X.K., Gómez-Favela M.A., Aguilar-Palazuelos E., Gutiérrez-Dorad R. (2020), Second-generation snacks with high nutritional and antioxidant value produced by an optimized extrusion process from corn/common bean flours mixtures, *Lebensmittel- Wissenschaft & Technologie,* 124, 109172, https://doi.org/10.1016/j.lwt.2020.109172
Fonseca L.M., Halal S.L.M.E., Dias A.R.G., Zavareze E.D.R. (2021), Physical modification of starch by heat-moisture treatment and annealing and their applications: A review, *Carbohydrate Polymers*, 274, 118665, https://doi.org/10.1016/j.carbpol.2021.118665
Fustier P., Gélinas P. (1998), Combining flour heating and chlorination to improve cake texture, *Cereal Chemistry*, 75(4), pp. 568–570, http://dx.doi.org/10.1094/CCHEM.1998.75.4.568
Galenko O., Shevchenko A., Ceccanti C., Mignani C., Litvynchuk S. (2024), Transformative shifts in dough and bread structure with pumpkin seed protein concentrate enrichment, *European Food Research and Technology*, 250, 1177–1188, https://doi.org/10.1007/s00217-023-04454-z
Ivanov V., Shevchenko O., Marynin A., Stabnikov V., Gubenia O., Stabnikova O., Shevchenko A., Gavva O., Saliuk A. (2021), Trends and expected benefits of the breaking edge food technologies in 2021–2030, *Ukrainian Food Journal*, 10(1), pp. 7-36, https://doi.org/10.24263/2304-974X-2021-10-1-3
Lyu Z., Sala G., Scholten E. (2024), Texture of emulsion-filled pea protein-potato starch gels: Effect of processing conditions and composition, *International Journal of Biological Macromolecules*, 277(2), 133889, https://doi.org/10.1016/j.ijbiomac.2024.133889
Magallanes-Cruz P.A., Flores-Silva P.C., Bello-Perez L.A. (2017), Starch structure influences its digestibility: A review, *Journal of Food Science,* 82, pp. 2016–2023, https://doi.org/10.1111/1750-3841.13809
Marynin A., Shpak V. (2022), Influence of electrochemically activated water on the rheological indicators of starch suspensions, *Ukrainian Journal of Food Science*, 10(2), pp. 149-160, https://doi.org/10.24263/2310-1008-2022-10-2-5
Marynin A., Shpak V., Pasichnyi V., Svyatnenko R., Shubina Y. (2023), Physico-chemical and rheological properties of meat pates with corn starch suspensions prepared on electrochemically activated water, *Ukrainian Food Journal*, 12(2), pp. 207-226,

https://doi.org/10.24263/2304-974X-2023-12-2-5
Maskus H., Arntfield S. (2015), Extrusion processing and evaluation of an expanded, puffed pea snack product, *Journal of Nutrition & Food Sciences, 5*(4), 1000378, https://doi.org/10.4172/2155-9600.1000378
Meiselman H.L. (2013), The future in sensory/consumer research: evolving to a better science, *Food Qual Prefer*, 27(2), pp. 208-214, https://doi.org/10.1016/j.foodqual.2012.03.002
Morales-Polanco E., Campos-Vega R., Gaytán-Martínez M., Enriquez L.G., Loarca-Piña G. (2017), Functional and textural properties of a dehulled oat (*Avena sativa* L) and pea (*Pisum sativum*) protein isolate cracker, *LWT – Food Science and Technology,* 86, pp. 418-423, https://doi.org/10.1016/j.lwt.2017.08.015
Naseer B., Naik H.R., Hussain S.Z., Bhat T., Nazir N. (2021), Development of instant *phirni* mix (a traditional dairy dessert) from high amylose rice, skim milk powder and carboxymethyl cellulose-resistant starch, predicted glycemic index and stability during storage, *Food Bioscience*, 42, 101213, https://doi.org/10.1016/j.fbio.2021.101213
Oliver G., Sahi S.S. (1995), Wafer batters: A rheological study, *Journal of Science Food Agriculture*, 67, pp. 221–227, https://doi.org/10.1002/jsfa.2740670212
Farshi P., Mirmohammadali S.N., Rajpurohit B., Smith J.S., Li Y. (2024), Pea protein and starch: Functional properties and applications in edible films, *Journal of Agriculture and Food Research*, 15, 100927, https://doi.org/10.1016/j.jafr.2023.100927
Rubanka K., Shevchenko O. (2022), Application of potato pulp in technology of snacks, *Scientific Works of National University of Food Technologies,* 28(2), pp. 132–141, https://doi.org/10.24263/2225-2924-2022-28-2-12
Shevkani K. (2023), Protein from land—legumes and pulses Author links open overlay panel. In: B.K. Tiwari., L.E. Healy (Eds.), *Future Proteins Sources, Processing, Applications and the Bioeconomy*, pp. 35-68, Academic Press, USA, https://doi.org/10.1016/B978-0-323-91739-1.00003-9
Singh G.D., Bawa A.S., Riar C.S., Saxena D.C. (2009), Influence of heat-moisture treatment and acid modifications on physicochemical, rheological, thermal and morphological characteristics of Indian water chest nut (*Trapa natans*) starch and its application in biodegradable films, *Starch,* 61, pp. 503–513, https://doi.org/10.1002/star.200900129
Sobczyk A., Pycia K., Stankowski S., Jaworska G., Kuźniar P. (2017), Evaluation of the rheological properties of dough and quality of bread made with the flour obtained from old cultivars and modern breeding lines of spelt (*Triticum aestivum* ssp. spelta), *Journal of Cereal Science*, 77, pp. 35-41, https://doi.org/10.1016/j.jcs.2017.07.013
Sugiura F., Ito S., Arai E., (2017), Effect of pregelatinized starch paste on the ease of swallowing high-moisture content bread, *Journal of Food Engineering*, 214, pp. 209-217, https://doi.org/10.1016/j.jfoodeng.2017.06.021
Tsykhanovska I., Lazarieva T., Stabnikova O., Kupriyanov O., Litvin O., Yevlash V. (2023), Potential benefits of functional antianemic energy bars, *Ukrainian Food Journal*, 12(4), pp. 578-598, https://doi.org/10.24263/2304-974X-2023-12-4-7
Torrico D., Mehta A., Borssato A.B. (2023), New methods to assess sensory responses: a brief review of innovative techniques in sensory evaluation, *Current Opinion in Food Science*, 49, 100978, https://doi.org/10.1016/j.cofs.2022.100978
Varghese S., Awana M., Mondal D., Rubiya M.H., Melethil K., Singh A., Krishnan V., Thomas B. (2022), Amylose–amylopectin ratio. In: S. Thomas, A. Ar, C.J. Chirayil, B. Thomas (Eds.), *Handbook of Biopolymer*, pp. 1305–1334, Springer, Singapore, https://doi.org/10.1007/978-981-16-6603-2_48-1
Venkatachalam A., Wilms P.F.C., Tian B., Bakker E.J., Schutyser M.A.I., Zhang L. (2025), Customizing fracture properties of pea-based snacks using 3D printing by varying composition and processing parameters, *Food Research International*, 202, 115715, https://doi.org/10.1016/j.foodres.2025.115715

Wang H., Xiao N., Wang X., Zhao X., Zhang H. (2019), Effect of pregelatinized starch on the characteristics, microstructures, and quality attributes of glutinous rice flour and dumplings, *Food Chemistry*, 283(4), pp. 248-256, https://doi.org/10.1016/j.foodchem.2019.01.047

Wani S.A., Kumar P. (2018), Influence on the antioxidant, structural and pasting properties of snacks with fenugreek, oats and green pea, *Journal of the Saudi Society of Agricultural Sciences*, 18, pp. 389–395, https://doi.org/10.1016/j.jssas.2018.01.001

Yifei F., Francesco P. (2020), Modification of starch: A review on the application of «green» solvents and controlled functionalization, *Carbohydrate Polymers,* 241, 116350, https://doi.org/10.1016/j.carbpol.2020.116350

Yousif E.I., Gadallah M.G.E., Sorour A.M. (2012), Physico-chemical and rheological properties of modified corn starches and its effect on noodle quality, *Annals of Agricultural Science*, 57(1), pp. 19-27, https://doi.org/10.1016/j.aoas.2012.03.008

Cite:

UFJ Style

Rubanka K., Pysarets O., Levkivska T., Samoilik O., Shpak V. (2025), Effect of pregelatinized corn starch on the technological and quality properties of pea dough and snacks, *Ukrainian Journal of Food Science*, 13(1), pp. 55–66, https://doi.org/10.24263/2310-1008-2025-13-1-7

APA Style

Rubanka, K., Pysarets, O., Levkivska, T., Samoilik, O., & Shpak, V. (2025). Effect of pregelatinized corn starch on the technological and quality properties of pea dough and snacks. *Ukrainian Journal of Food Science, 13*(1), 55–66. https://doi.org/10.24263/2310-1008-2025-13-1-7

Operational improvement of the technological process in instant noodle production

Serhii Yakymenko, Bohdan Pashchenko, Oksana Vasheka

National University of Food Technologies, Kyiv, Ukraine

Keywords:

Production
Noodles
Lean-thinking
Power
Improvement
Blackout

Article history:

Received 21.12.2024
Received in revised form 26.02.2024
Accepted 30.06.2024

Corresponding author:

Serhii Yakymenko
E-mail: serjozhayakimenko@gmail.com

DOI:
10.24263/2310-1008-2025-13-1-8

Abstract

Introduction. The aim of the study is to improve the technological process of instant noodle production, ensuring stable and uninterrupted operation in the absence of electricity supply.

Materials and methods. To assess the effectiveness of the proposed backup power solutions, the Lean thinking methodology was applied. The analysis was based on overall equipment effectiveness (OEE), downtime duration, and seasonal blackout frequency. Modeling was performed using mathematical matrices, histograms, box plots, and combined graphs with dual Y-axes.

Results and discussion. It was found that power outages cause significant disruptions to the continuity of the instant noodle production process. Calculations showed that the recovery time after a power outage exceeds the working cycle by a factor of 2.3: 2100 > 937 seconds. This, in turn, leads to reduced production line performance and increased risk of defects. By modeling several blackout scenarios (short-term, medium-duration, and long-term), the seasonal dynamics of outages over a 12-month period were analyzed. It was revealed that the highest number of outages occurred in June-July, while the longest outages were observed in November-December.

Analysis of the results and validation of the effectiveness of the proposed solutions to ensure uninterrupted operation of the instant noodle production line indicate that the choice of backup power type should be based on the intensity and nature of power outages. In the case of short and infrequent outages (100-25 hours / year), the implementation of a manually started generator is sufficient, significantly improving the situation: the production cycle is reduced to 0.287 seconds, and overall equipment effectiveness (OEE) increases to 76.36 %.

In contrast, under medium-duration outages (350-380 hours / year), the implementation of a comprehensive solution proves most effective, achieving an overall OEE of 78.96 % and minimizing deviations from the nominal cycle (0.288 seconds), which significantly shortens the production cycle duration, minimizes productivity losses, and maintains process stability. During prolonged outages (over 600 hours / year), the highest performance indicators are also achieved with the comprehensive approach, ensuring stable equipment operation at an OEE level of 78.96 % and restoring the nominal cycle time to 0.288 seconds, which is equivalent to uninterrupted power supply conditions.

Conclusions. The research has shown that the rationality of choosing a technical solution is determined by the frequency, duration, and nature of power outages. If the intensity of external power outages increases, a solution consisting of a generator + ATS + UPS is needed to maintain process stability and minimize losses.

Introduction

The efficiency of the food industry is recognized as one of the key components of food security for the population in any country (Mbow et al., 2019). This issue becomes particularly critical under martial law conditions, where ensuring access to food in crisis situations – such as resource supply disruptions, power outages, and security threats – is essential. Therefore, addressing the challenges faced by food industry operators and developing solutions to overcome or mitigate them is a crucial task. It has been identified that production-related costs account for a significant share of the total expenditures in the food industry (Womack et al., 2018). Reducing these costs through operational improvements has a direct impact on the ability to sustain production activities (Anderson et al., 2020).

One of the most effective tools to achieve this goal is the application of Lean-Thinking – a comprehensive management and improvement concept aimed at eliminating waste and optimizing all stages of production processes: from technological operations to interactions with suppliers and consumers (Womack et al., 2018). Research in this field is focused on maximizing process value for the consumer while minimizing the manufacturer's resource expenditure, including human effort, equipment usage, and especially downtime (Eskandari, Hamid, Masoudian, Rabbani, 2022).

While it is impossible to completely eliminate losses in the production process, ensuring its stable and uninterrupted operation under any conditions is essential (Pereira et al., 2022). A literature review revealed a lack of research specifically addressing the issue of uninterrupted production line operation during power outages at the global level, making direct comparisons of research outcomes currently unavailable. This is primarily due to the previously low relevance of such studies in countries with stable security and economic environments. However, with the rapid growth of global threats in recent years, this issue is gaining increasing importance, particularly in EU countries (Pereira et al., 2022).

It is also worth noting that under conditions of stable power supply, the control of technological parameters is carried out continuously – both manually and automatically. However, power outages directly affect all critical points in production (Haes Alhelou et al., 2019), as they disrupt temperature conditions during various process stages; halt production lines when the product is in critical zones (thermal treatment, cooling, forming); and create situations where parameter control becomes either impossible or irrelevant, since even short power interruptions require complete system reinitialization and repeated control procedures (Salman et al., 2023).

The scientific value lies in developing an effective theoretical tool based on mathematical and digital methods that can solve practical problems related to the stable functioning of technological processes and reduce production costs for food industry operators.

Based on the above, the object of this research is the technological process of instant noodle production, chosen due to the sufficient number of operations and process parameters that allow for more accurate and relevant results under power outage conditions. It is important to note that the results of operational improvements obtained in this research can be scaled to other sectors of the food industry, as one of the key advantages of Lean-Thinking is the universality of its tools, which can be applied to any production or process (Bittencourt et al., 2021).

The aim of the research is to justify operational improvement measures for food production processes in order to ensure stable and uninterrupted operation in the face of external disturbances – specifically, power supply disruptions.

Materials and methods

Materials

The research focused on the technological process of producing instant noodles – a pre-cooked and dried product typically sold in brick form with seasoning sachets. The production process consists of the following main operations: sifting and weighing flour and other ingredients, dough mixing, resting, rolling, cutting, steaming, separation, frying, cooling, packaging, rejection of defective products, manual packaging, palletizing, transportation to the warehouse, and storage.

The research was conducted at the facilities of a food market operator located in the Kyiv region. The operating time was based on the durations of production stages as defined in the technological guidelines under a three-shift schedule, 24 hours a day, 360 days a year. The total production period duration was 8.760 hours, of which 8.640 hours were allocated to operational cycles, and 120 hours were reserved for planned downtime not related to technical needs (e.g., holidays).

Given the stated production duration, the planned output was 125 million units. However, the actual output reached 107 million units, of which 104 million met quality standards.

Methods

Duration of technological stages in instant noodle production

The duration of each production operation (carried out according to technological instructions for the specific product) was measured manually using an electronic chronograph. The total production time for instant noodles was calculated using formula 1: (Varsha et al., 2025):

$$\sum_{n=1}^{1} TO \tag{1}$$

where n – number of technological operations;

TO – duration of a technological operation, s.

Production Takt Time and Production Cycle Time

The production takt time and the production cycle time were calculated using formulas 2 and 3 (Taifa et al., 2019):

$$T_{takt} = \frac{T_p}{N} \tag{2}$$

$$T_{cycle} = \frac{T_{a.p.}}{N_{n.d.p.}} \tag{3}$$

where T_p is planned production time, s;

N is ordered product batch, units;

$T_{a.p.}$ is actual production time, s;

$N_{n.d.p.}$ is ordered batch of non-defective products, units.

Calculation of overall equipment effectiveness

The concept of Overall Equipment Effectiveness (OEE) was proposed by Japanese engineer Seiichi Nakajima (Corrales et al., 2020). OEE provides a systematic way to evaluate losses related to downtime, speed reduction, and defects, based on three components: availability, performance, and quality (Biswas, 2024).

OEE is calculated as the product of these three components using formula 4:

$$\text{OEE} = Av \cdot Pr \cdot Ql \tag{4}$$

Availability Av (represents losses due to downtime, %), line Performance Pr (expressed as % %), Quality Ql (share of good-quality products without defects, %) are calculated using formulas 5–7, respectively:

$$Av = \frac{T_{a.p.}}{T_{p.}} \cdot 100\% \tag{5}$$

$$Pr = \frac{N_a}{N_{t.p.}} \cdot 100\% \tag{6}$$

$$Ql = \frac{N_{f.w.d.}}{N_{a.d.p.}} \cdot 100\%, \tag{7}$$

where N_a is actual product output, units;

$N_{t.p.}$ is theoretical production output, units;

$N_{a.d.p.}$ is actual output of non-defective products, units.

Power supply modeling

Three power outage duration scenarios were selected for modeling, based on the average annual duration of electricity supply interruptions. Subsequently, their impact on production process losses and equipment efficiency of the production line was evaluated.

Each scenario was assigned a corresponding designation: short-term outages (approximately 100–125 hours per year) – Scenario 1; medium-duration outages (approximately 350–380 hours per year) – Scenario 2; long-term outages (over 600 hours per year) – Scenario 3 (Table 1). These values were obtained through monitoring, recording, and summing the durations of outages throughout the calendar working year (Pereira et al., 2022).

Table 1

Modeling scenarios of downtime duration for the instant noodle production line during the calendar working year

Scenario Name	Type of Outage	Outage Duration, hours / year
Scenario 1	Short-term	100-125
Scenario 2	Medium-term	350-380
Scenario 3	Long-term	≤ 600

Backup power supply solutions

Two possible backup power solutions were identified for assessing response effectiveness during outages:

Simple solution – "Generator (manual start)": purchasing and installing a diesel generator with appropriate power capacity. The downside of this option is the need for manual startup (time loss due to extra actions) and generator startup time (7–15+ minutes on average for a 10 kW model (Salman et al., 2023)), along with the risk of failure to start in advance.

Comprehensive solution – "Generator + ATS + UPS (instant switchover)": a long-term, efficient solution combining a generator, automatic transfer switch (ATS), and uninterruptible power supply (UPS with a battery set). This combination provides an immediate switchover without voltage drop or equipment damage, minimizing time loss, increasing quality and productivity, and practically eliminating defects caused by power fluctuations. As a result, OEE approaches its potential maximum, annual losses become minimal, and energy independence is ensured under various power supply conditions.

Mathematical analysis

To improve the accuracy of calculations, outages were compared and classified as follows: planned outages (those that match the outage schedules provided by the relevant regulatory authority) and emergency outages, which occur unscheduled. Following the established methodology (Erdős et al., 2020), mathematical matrices of outage frequency and average duration were constructed to identify characteristic seasonal and daily patterns of interruptions across each of the three scenarios. The columns represented months of the year (1 to 12), while the rows denoted hours of the day (0 to 24). From the data array and matrices, the number and duration of outages were extracted accordingly.

To research the similarities and differences in the behavior of simulated power scenarios 1, 2, and 3, several visual tools were employed using well-known methodologies. A histogram (Devore et al., 2021) was created to show the duration and frequency of outages for all scenarios. A box plot was used to analyze outliers, spreads, and medians for each scenario, and a combined chart displaying seasonal outage frequency and average duration with dual y-axes was built (Babura et al., 2018).

Results and discussion

Time losses in the instant noodle production process

The total production time of instant noodles, calculated using formula (1), from the delivery of flour and dry mixes for dough preparation to the completion of the first pallet's movement to storage, amounted to 836 seconds (T_{lead}). The actual time was 971 seconds ($T_{lead\ fact}$ = 836 s + 135 s = 971 s, where 135 seconds represent losses due to additional movements, operator actions, etc.).

The calculated values for production takt time and production cycle time were 0.249 s and 0.289 s, respectively (according to formulas 2 and 3), under stable line operation without power outages. Thus, the actual production speed lagged behind the planned one by 0.04 seconds per unit, resulting in underproduction within a shift. The drop in productivity is primarily recorded at the production stage, which takes 971 seconds instead of the planned 836 seconds (based on formula 1).

In the event of a prolonged power outage, the line must be cleaned, and all products at intermediate processing stages at the time of the stoppage must be discarded (Haes Alhelou, 2019). It is practically impossible to restore the uniformity of the technological process after such a stoppage without complete cleaning and a restart ("cold start"), which results in the loss of both time and raw materials (Pereira et al., 2022). The duration of each operation during the restart of the production line was also manually timed with a stopwatch to obtain accurate and reliable data. The total time for a cold start ($T_{lead\ cold}$) amounted to 2100 seconds (calculated analogously to $T_{lead\ fact}$).

A comparison of $T_{lead\ fact}$ and $T_{lead\ cold}$ shows that $T_{lead\ fact}$ (937 c) < $T_{lead\ cold}$ (2100), meaning that the time required to restart the line exceeds the normal cycle by 2.3 times. Additionally, the downtime during the actual power outage itself can further increase the total loss. Based on this, it can be concluded that the presence and duration of power outages are the key destabilizing factors in production.

In 2024, the planned production time for an average food industry operator (Kudriavtseva, 2025) was 8224 hours, of which 416 hours were allocated for scheduled stops for cleaning and maintenance, conducted weekly. At the same time, an additional 419 hours of unplanned downtime were recorded due to disruptions in external power supply or failures in specific equipment units. As a result, the actual net operating time totaled 7805 hours (according to formula 1).

Overall equipment effectiveness

Losses at the quality control stage amounted to approximately 2.8 %, which is considered an acceptable level for high-volume continuous production in the food industry (Vasylyk, 2018).

In this regard, the impact of emergency and planned power outages on the Overall Equipment Effectiveness (OEE) was simulated.

Based on the research, the calculated performance indicators of OEE components (according to formulas 4-7) are as follows: availability – 94.9 %, performance – 85.6 %, quality – 97.2 %, resulting in an overall OEE value of approximately 78.96 % (Figure 1). This value classifies equipment performance as acceptable (Tsarouhas, 2019), though it still demonstrates a notable potential for improvement. The main losses are caused by unplanned downtime due to power outages.

Pattern and Seasonality of Outage Durations

Based on the above, it follows that due to emergency power supply interruptions, the equipment operates at approximately 79 % of its potential capacity. Further efficiency improvements can be achieved through the implementation of automated monitoring systems and the introduction of backup power systems (Arshad et al., 2021).

The results of the outage classification, calculated using matrices of the number and average duration of outages, are presented in Table 2.

In all three networks, the distributions of outages differ according to the following trends:

- Scenario 1 is the most "stable" (125 hours);
- Scenario 2 combines a large number of short and a considerable share of medium-duration outages (375 hours);
- Scenario 3 features significantly longer durations (616 hours), indicating systematic prolonged interruptions.

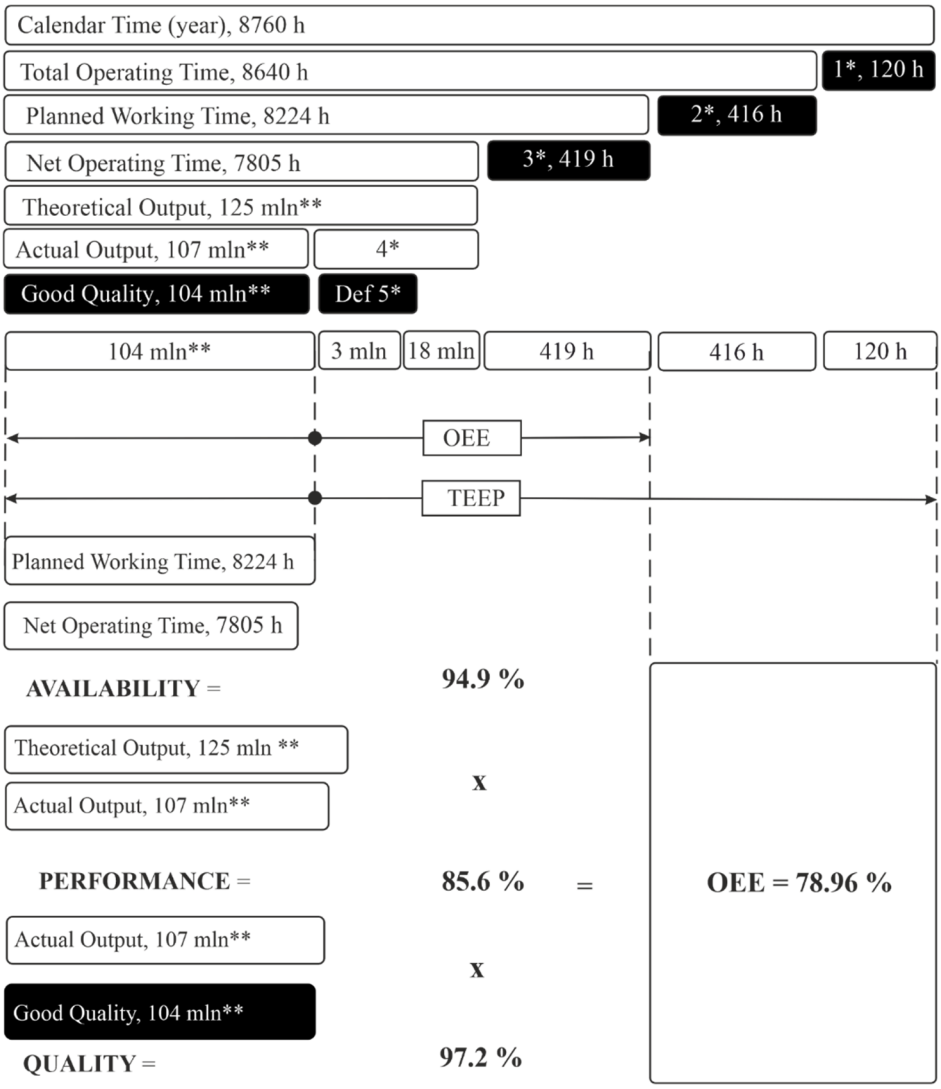

Figure 1. Calculation of overall equipment effectiveness (OEE):
1* – scheduled idle time, 2* – planned downtime,
3* – unplanned downtime, 4* – speed losses,
5* – defects, ** – units

Table 2

Classification of outages into planned (scheduled) and unplanned (emergency)

	Scenario 1	Scenario 2	Scenario 3
Number of Outages			
Total	76	235	161
Scheduled	45 (59.2 %)	132 (56.2 %)	70 (43.5 %)
Unplanned	**20 (26.3 %)**	**54 (23.0 %)**	**61 (37.9 %)**
Duration			
Total	7 429 min (125 h)	22 246 min (375 h)	36 796 min (616 h)
Scheduled, h	67 (54 %)	204 (55 %)	263 (42.9 %)
Unplanned, h	**38 (30.6 %)**	**94 (25.3 %)**	**232 (37.9 %)**

The data obtained from the matrices of outage frequency and average duration, as well as from Table 2, were visualized using a histogram (Figure 2) and a box plot (Figure 3) to simplify the interpretation of results.

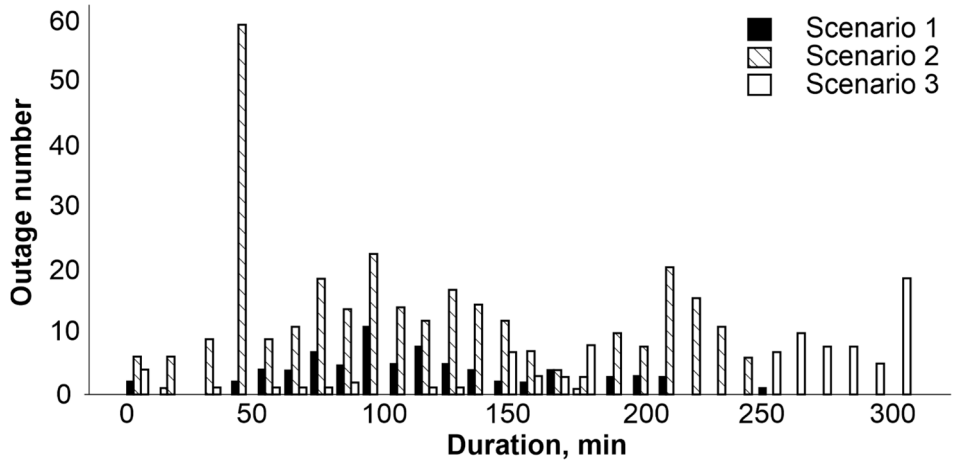

Figure 2. Histogram of outage durations (data is taken every 10 minutes)

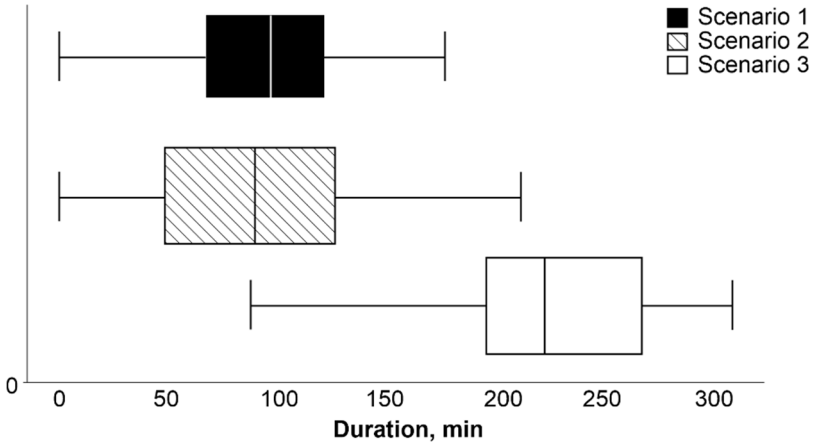

Figure 3. Box plot comparing the distribution of outage durations (data is taken every 10 minutes)

The histogram of outage durations (Figure 2) shows that Scenario 1 and 2 have similar distribution patterns (Devore et al., 2021): the majority of outages last less than 150 minutes, with the frequency peaks of scenario 2 slightly shifted to the right compared to Scenario 1, indicating a general tendency toward somewhat longer downtimes in the second case. In contrast, Scenario 3 is characterized by a distinct pattern with a prevalence of both short outages (up to 100 minutes) and very long ones exceeding 200 minutes.

From the box plot analysis (Figure 3), it can be seen that the medians of Scenario 1 and 2 fall within approximately 70–120 minutes, and their interquartile ranges are relatively narrow, indicating fairly stable short-duration outages.

For Scenario 3, the median (Figure 3) rises to approximately 230 minutes, with interquartile range boundaries stretching from 190 to 265 minutes, demonstrating a significantly wider spread and high variability (Babura et al., 2018), which highlights the instability of the third scenario and the need for further backup power using one of the response scenarios.

After comparing the distribution of outage durations using the histogram and box plot, which provide insight into the wide range and presence of outliers for each scenario, the next step was to analyze the temporal pattern of these events. The chart of the seasonal distribution of the number and average duration of outages by month (Figure 4) shows that the highest number of outages and the longest interruptions are concentrated in the summer months (June-July) and peak winter months (November-January), while in the off-season (September-October, March-April) the indicators practically drop to zero. Scenario 2 records the highest number of outages in July–August, while the duration of interruptions remains relatively stable (≈30-40 minutes). In contrast, Scenario 3 experiences not only high frequency during July-August but also a significant increase in average outage duration (over 220 minutes in August). Scenario 1 shows less seasonality: the number of incidents in July is small (≈33), but the average duration gradually increases, reaching its maximum in November-December.

This indicates a clear seasonal nature of the network's performance and varying loads during warm and cold seasons (Chojnacki, 2023).

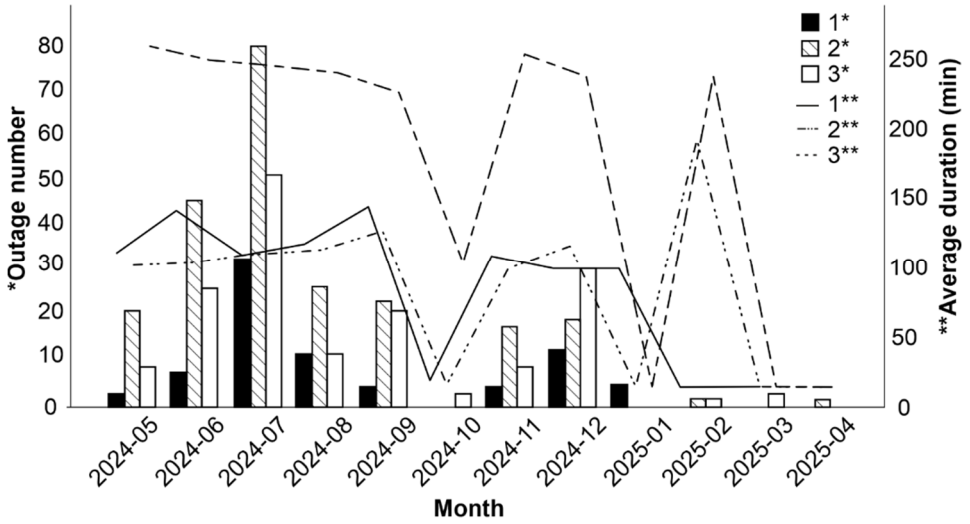

Figure 4. Seasonal distribution chart of outage frequency and average duration by month for Scenarios 1, 2, and 3 respectively (mark 1, 2, 3 on the chart)

Thus, in summer, network loads result in a high number of short outages (especially for scenarios 1 and 2), while scenario 3 is characterized by both frequent and prolonged interruptions. In winter, the effects of cold or precipitation likely lead to less frequent but extremely prolonged outages in scenario 1 and 3. This suggests a focus on preventive measures: during the summer period, rapid elimination of short-term outages should be prioritized, whereas in the cold season, preparation for large-scale long-term downtimes is necessary.

Effectiveness of backup power solutions within operational improvement measures

After performing calculations using the described methods for all selected scenarios (1, 2, 3) and the proposed response options to power outages – "Generator (manual start)" and "Generator + ATS + UPS (instant switching)" – the results were obtained and summarized in Table 3.

For Scenario 1 (short-term outages – 100-125 hours / year), the implementation of a simple generator significantly improves the situation: cycle time is reduced to 0.287 s, and overall equipment effectiveness (OEE) increases to 76.36 %. The comprehensive solution (generator with ATS and UPS) further optimizes operations, reducing the cycle time to 0.288 s and bringing performance and quality indicators close to the standard (OEE = 78.96 %). This indicates full compliance of the backup system with the requirements of stable production cycle support (Van De Ginste, 2022).

For Scenario 2 (medium-duration outages – 350-380 hours / year), a simple generator considerably stabilizes the process indicators: cycle time is reduced to 0.294 s, availability increases to 91.84 %, and performance to 82.37 %. The comprehensive solution ensures the highest stability and efficiency, nearly reaching normative parameters (OEE = 78.96 %). Due to reduced downtime and emergency stops, the production process approaches the nominal cycle (0.288 s).

Table 3

Testing the effectiveness of proposed backup power solutions for simulated scenarios 1, 2, 3

Scenario	Solution	OEE	Availability	Productivity	Quality	Model T_{cycle}, s***
1*	Gen.	76.4	93.78	84.42	96.46	0.287
1*	Gen.++**	78.9	94.9	85.6	97.2	0.288
2*	Gen.	71.8	91.84	82.37	94.92	0.294
2*	Gen.++**	78.9	94.9	85.6	97.2	0.288
3*	Gen.	71.8	91.54	82.06	95.64	0.295
3*	Gen.++**	78.9	94.9	85.6	97.2	0.288

1* – (125 hours / year, 76 outages, 26 % unplanned, average duration 98 min);
2* – (375 hours / year, 235 outages, 23 % unplanned, average duration 91 min);
3* – (616 hours / year, 161 outages, 38 % unplanned, average duration 224 min);
**Generator + ATS + UPS;
***The production takt time and production cycle time are 0.249 s and 0.289 s, respectively, under conditions without power outages.

For Scenario 3 (600 hours / year of outages), generator implementation significantly improves efficiency indicators (OEE = 71.83 %), reducing the cycle time to 0.295 s. However, a notable gap remains compared to nominal parameters. The best results are shown by the comprehensive solution (generator + ATS + UPS), achieving nearly standard indicators (OEE = 78.96 %). The calculated cycle time is reduced to 0.288 s, matching the cycle time under stable conditions.

A comparative analysis of the two scenario results suggests that the optimal solution depends on the intensity and nature of outages (Haes Alhelou, 2019). Under conditions of fewer outages (125 hours/year), a simple generator is a sufficient solution, as its impact significantly improves the main process parameters.

For medium and high outage levels (375-600 hours / year), the most optimal solution is the comprehensive one (generator + ATS + UPS), which minimizes cycle time, productivity losses, and provides the highest production process stability.

Conclusions

1. The research revealed that the optimal solution depends on the frequency, duration, and type of power outages. The higher the intensity of external disruptions, the more comprehensive the solution must be to ensure production cycle stability, maximize equipment efficiency, and minimize unproductive time losses. Solutions proposed to ensure uninterrupted operation and improve the efficiency of the instant noodle production line include the use of a manual generator and a comprehensive solution (generator + ATS + UPS).
2. It was determined that under conditions of short and infrequent outages (short-term outages – 100–125 hours / year), a manual generator reduces the production cycle to 0.287 s and increases the overall equipment effectiveness (OEE) to 76.36 %.

3. In the case of medium-duration outages (350-380 hours / year), the generator reduces the cycle to 0.294 s, while availability and performance increase to 91.84 % and 82.37 %, respectively.
4. It was established that the comprehensive solution (consisting of a generator + ATS + UPS) demonstrated the highest efficiency under long-term outages (over 600 hours / year) in all three scenarios. This solution stabilizes the production cycle at 0.288 s and brings overall equipment effectiveness (OEE) to the target value of 78.96 %. This is especially relevant when a simple generator provides only partial compensation for losses (OEE = 71.83 %, cycle = 0.295 s).

Thus, applying Lean-Thinking tools not only helps optimize resources and reduce production losses but also increases the adaptability of food enterprises to external challenges, particularly under conditions of energy instability. The proposed approach is universal and can be scaled to other technological processes in the industry.

References

Anderson K., Yoshino I., Shook J. (2020), *Learning to Lead, Leading to Learn: Lessons from Toyota Leader Isao Yoshino on a Lifetime of Continuous Learning*, Integrand Press, Cleveland.

Arshad R.N., Abdul-Malek Z., Roobab U., Aadil R.M. (2021), Pulsed electric field: a potential alternative towards a sustainable food processing, *Trends in Food Science & Technology*, 111, pp. 43–54, https://doi.org/10.1016/j.tifs.2021.02.041

Babura B.I., Adam M.B., Samad A.R., Fitrianto A., Yusif B. (2018), Analysis and assessment of boxplot characters for extreme data, *Journal of Physics: Conference Series*, 1132(1), 012078, https://doi.org/10.1088/1742-6596/1132/1/012078

Bicheno J.R., Holweg M. (2016), *The Lean Toolbox 5th Edition: a Handbook for Lean Transformation*, Picsie Books, Johannesburg.

Biswas J. (2024), Total productive maintenance: an in-depth review with a focus on overall equipment effectiveness measurement, *International Journal of Research in Industrial Engineering*, 13(4), pp. 376–383, https://doi.org/10.22105/riej.2024.453380.1436.

Bittencourt V.L., Alves A.C., Leão, C.P. (2021), Industry 4.0 triggered by Lean Thinking: Insights from a systematic literature review, *International Journal of Production Research*, 59(5), pp. 1496–1510, https://doi.org/10.1080/00207543.2020.1832274

Chojnacki A.L. (2023), Analysis of seasonality and causes of equipment and facility failures in electric power distribution networks, *Przeglad Elektrotechniczny*, 99(1), pp. 157–163, https://doi.org/10.15199/48.2023.01.30

Corrales L., Lambán M., Hernandez M., Royo J. (2020), Overall equipment effectiveness: Systematic literature review and overview of different approaches, *Applied Sciences*, 10(18), pp. 6469–6489, https://doi.org/10.3390/app10186469

Devore J.L., Berk K.N., Carlton M.A. (2021), *Modern Mathematical Statistics with Applications*. Springer Nature, Cham.

Erdős L., Götze F., Guionnet, A. (2020), Random matrices, *Oberwolfach Reports*, 16(4), pp. 3459–3527, https://doi.org/10.4171/owr/2019/56

Eskandari M., Hamid M., Masoudian M., Rabbani M. (2022), An integrated Lean production-sustainability framework for evaluation and improvement of the performance of pharmaceutical factory, *Journal of Cleaner Production*, 376, 134132, https://doi.org/10.1016/j.jclepro.2022.134132

Haes Alhelou H., Hamedani-Golshan M., Njenda T., Siano P. (2019), A survey on power system blackout and cascading events: research motivations and challenges, *Energies*, 12(4), pp. 682–710, https://doi.org/10.3390/en12040682

Kudriavtseva O.V. (2025), Teoretychni aspekty vyrobnychoho planuvannia na pidpryiemstvi, *Science and Technology: Challenges, Prospects and Innovations*: *Proceedings of the 6th International*

Scientific and Practical Conference, January 29–31, 2025, CPN Publishing Group, Osaka, pp. 443-451.
Markina I., Diachkov D., Bodnarchuk T., Paschenko P., Chernikova N. (2022), Management of resource-saving and energy-saving technologies as an innovative direction of agri-food enterprise restructuring, *International Journal of Innovation and Technology Management*, 19(02), 2150047, https://doi.org/10.1142/S0219877021500474
Mbow C., Rosenzweig C., Barioni L., Benton T., Herrero M., Krishnapillai M. (2019), *Food Security*, University of Tasmania, Melbourne.
Pereira P., Bašić F., Bogunovic I., Barcelo D. (2022), Russian-Ukrainian war impacts the total environment, *Science of the Total Environment*, 837, 155865, https://doi.org/10.1016/j.scitotenv.2022.155865
Salman H., Pasupuleti J., Sabry, A. (2023), Review on causes of power outages and their occurrence: mitigation strategies, *Sustainability*, 15(20), 15001, https://doi.org/10.3390/su152015001
Taifa I., Vhora T. (2019), Cycle time reduction for productivity improvement in the manufacturing industry, *Journal of Industrial Engineering and Management Studies*, 6(2), pp. 147–164, https://dx.doi.org/10.22116/jiems.2019.92695
Tsarouhas P. (2019), Improving operation of the croissant production line through overall equipment effectiveness (OEE). A case study, *International Journal of Productivity and Performance Management*, 68(1), pp. 88–108, https://doi.org/10.1108/IJPPM-02-2018-0060
Van De Ginste L., Aghezzaf E., Cottyn J. (2022), The role of equipment flexibility in Overall Equipment Effectiveness (OEE)-driven process improvement, *Procedia CIRP*, 107, pp. 289–294, https://doi.org/10.1016/j.procir.2022.04.047
Varsha L., Sudheesh C., Sunooj K. (2025), Technology of pasta making, *Advances in Pasta Technology,* 1, pp. 43–69, https://doi.org/10.1007/978-3-031-84497-3_3
Vasylyk N. (2018), Estimation of efficiency of resource potential management of enterprise, *Economic Analysis*, 28(3), pp. 154–161, http://dx.doi.org/10.35774/econa2018.03
Womack J., Jones D. (2018), *Lean Manufacturing*, Fabula, Kyiv.

Cite:

UFJ Style

Yakymenko S., Pashchenk B., Vasheka O. (2025), Operational improvement of the technological process in instant noodle production, *Ukrainian Journal of Food Science*, 13(1), pp. 67–79, https://doi.org/10.24263/2310-1008-2025-13-1-8

APA Style

Yakymenko, S., Pashchenk, B., & Vasheka, O. (2025). Operational improvement of the technological process in instant noodle production. *Ukrainian Journal of Food Science, 13*(1), 67–79. https://doi.org/10.24263/2310-1008-2025-13-1-8

Rapid spectrophotometric method for the determination of iron content in yeast

Hanna Bondar, Viktoriia Krasinko

National University of Food Technologies, Kyiv, Ukraine

Keywords:

Yeast
Iron
Spectrophotometry
Absorption
Chelator

Article history:

Received 12.01.2025
Received in revised form 16.06.2024
Accepted 30.06.2024

Corresponding author:

Hanna Bondar
E-mail:
abn2292@gmail.com

DOI:
10.24263/2310-1008-2025-13-1-9

Abstract

Introduction. The development of a rapid method for the determination of iron in yeast has become especially important due to the growing demand for functional foods with increased content of this bioavailable microelement.

Materials and Methods. *Saccharomyces cerevisiae* M437 yeast enriched with iron. The determination of total iron content was carried out using a spectrophotometric method based on a colorimetric reaction between ferrous iron Fe (II) and the iron-specific chelator bathophenanthroline disulfonate (BPS). To ensure complete conversion of iron into the Fe (II) form, ferric ions Fe (III) were reduced using sodium ascorbate prior to the reaction.

Results and discussion. The optimal sample preparation conditions for the release of absorbed iron involved treating yeast biomass with 3% HNO_3 at 97 °C. The Fe^{2+}-BPS complex formed stably at pH 5.3–5.4, reaching equilibrium within 3 minutes. A citrate-based buffer system maintained the optimal pH, which is critical for chelate complex stability. The resulting complex solutions remained stable for up to 45 minutes, enabling batch analysis without compromising measurement accuracy.

The method's reproducibility was assessed using three parallel solutions with iron concentrations ranging from 110 to 360 μM; the relative standard deviation (RSD) did not exceed 1.4% across the entire range. Notably, for the 360 μM solution, the RSD was 0.4%, indicating high signal stability at elevated analyte concentrations. Linearity was confirmed over the range of 20–950 μM ($R^2 > 0.99$), allowing for accurate quantification of both low and high iron concentrations.

The iron content in yeast enriched with $FeSO_4$ was 9.7 ± 0.2 mg/g, while enrichment with $FeCl_3$ resulted in 5.2 ± 0.5 mg/g. These values were in good agreement with those obtained using atomic absorption spectrometry (9.3 ± 0.4 mg/g and 5.7 ± 0.6 mg/g, respectively). ANOVA analysis confirmed a statistically significant difference in iron content depending on the type of salt used ($FeSO_4$ vs. $FeCl_3$), whereas the difference between measurement methods (spectrophotometry vs. atomic absorption spectrometry) was not significant ($p = 0.8522$), indicating analytical equivalence between the two methods.

Conclusions. A method for determining iron content in yeast demonstrating high accuracy, reproducibility, and ease of implementation in food quality control and yeast-based biotechnological processes.

Introduction

Iron is one of the key trace elements necessary for the normal functioning of the human body (Piskin et al., 2021). Meanwhile, iron deficiency is the most common cause of anemia worldwide, affecting more than 2 billion people, according to the World Health Organization (World Health Organization, 2008). Therefore, the content of iron in food products is crucial for maintaining public health and forming a balanced diet. There are a number of studies devoted to the issue of functional food fortification with iron to prevent anemia in the population (Hamad and Singh, 2025; Jarzębski et al., 2023; Tsykhanovska et al., 2022, 2023, 2024; Xing et al., 2022; Zielińska-Dawidziak et al., 2023). Yeast enriched with iron is considered a promising source of this trace element, as it is commonly used as a food additive (Jach et al., 2022).

The determination of iron content in biological samples and food products is a multi-stage process. Preliminary sample processing, including deproteinization and the release of iron from protein complexes, is a crucial step that must be optimized depending on the specific characteristics of the sample. Classical approaches involve the use of mixtures of hydrochloric acid and potassium permanganate (Fish, 1988), burning samples to obtain ash with iron (Hailu et al., 2019), but to ensure complete extraction of iron from yeast cells with a strong cell wall, it has been proposed to use more aggressive reagents, such as a 3% solution of nitric acid (Tamarit et al., 2006), a mixture of nitric and perchloric acids (Chen et al., 2024), a 65% solution of nitric and hydrochloric acids (Tafazzoli et al., 2024).

There are several analytical methods for the quantitative determination of iron, each of which is characterized by certain advantages and limitations. Atomic absorption spectrometry (AAS) is one of the most common methods for determining iron content in biological samples, particularly in yeast (Kyyaly et al., 2015; Pirman and Orešnik, 2012). The main advantages of this method are high sensitivity and specificity, as well as the ability to analyze iron concentrations in a wide range. Inductively coupled plasma optical emission spectrometry (ICP-OES) is a highly accurate and sensitive technique that enables the quantitative determination of iron in various biological samples (Mier-Alba et al., 2024; Orlowska et al., 2023). Despite its analytical advantages, including high precision at low analyte concentrations, the practical application of ICP-OES is limited by its technical complexity and the need for specialized laboratory infrastructure. In contrast to the above-mentioned methods, spectrophotometric and colorimetric analyses are more accessible and cost-effective for determining high iron concentrations (over 1 mg/kg), which provide reliability and sufficient sensitivity of the analysis. In colorimetric determinations of iron, methods using colored complexes formed by iron are most often used. Among the most effective chelators used for determining iron in biological objects, ferrozine (Riemer et al., 2004), bathophenanthrolinedisulfonic acid (Gaensly et al., 2014; Tamarit et al., 2006), 1,10-phenanthroline (Herrera et al., 2007), and 2,2'-bipyridyl (Niedzielski et al., 2014) can be highlighted. The application of these reagents provides high sensitivity of the analysis, which makes the spectrophotometric method an optimal choice for routine determination of iron in yeast.

This article presents a rapid and simple spectrophotometric method for determining iron content in yeast, based on the formation of a colored iron complex with the chelator BPS. The main advantages of this method are high sensitivity, ease of implementation, short analysis time and the use of available reagents.

The proposed method for determining iron in yeast can be used for routine control of raw materials and finished products in the food industry, as well as for assessing the effectiveness of iron enrichment of yeast biomass in the process of developing and

implementing biotechnology for obtaining iron-containing biopreparations. This approach is promising for the creation of functional food additives and products with increased content of bioavailable iron, which can potentially contribute to solving the problem of deficiency of this element in the human diet.

Materials and Methods

Equipment

For spectrophotometric analyses, a Specord 210 spectrophotometer (Analytik Jena, Austria) was used, ensuring accurate measurement of the optical density of the iron-chelator complex at a wavelength of 536 nm. To validate the iron content determination, an atomic absorption spectrometer Shimadzu AA-7000 (Shimadzu, Turkey) with flame atomization in an air–acetylene environment was additionally used. The device was equipped with a hollow cathode lamp, and measurements were carried out at a wavelength of 248.3 nm, corresponding to the maximum absorption of iron.

Reagents

The following reagents were used: ferrous sulfate heptahydrate and ferric chloride hexahydrate (Carlo Erba), anhydrous citric acid (Sigma Aldrich), sodium citrate dihydrate (Sigma Aldrich), sodium ascorbate (Sigma Aldrich), 4,7-diphenyl-1,10-phenanthroline disulfonate (bathophenanthroline disulfonate sodium salt, BPS), and Certipur® for MS multi-element standard (Sigma Aldrich) containing iron at a concentration of 1000 ppm, and chromatography-grade water (Millipore).

BPS (bathophenanthroline disulfonic acid) is a water-soluble chelator that specifically binds ferrous ions (Fe^{2+}), forming an intensely colored complex with maximum absorption in the visible spectrum (536 nm). The stoichiometry of BPS binding with iron (Fe^{2+}) is 3:1, meaning that three BPS molecules bind to one Fe^{2+} ion, forming a stable complex $[Fe(BPS)_3]^{6-}$.

Microorganism

The object of the study was *Saccharomyces cerevisiae* M437 yeast, obtained from the Collection of Live Microbial Cultures of the Department of Biotechnology and Microbiology, National University of Food Technologies, and enriched with iron.

Culture preparation

The yeast culture was stored in test tubes on slanted agarized unhopped beer wort (wort agar, WA) at 4 ± 1°C. Before inoculum preparation, the yeast was streaked onto Petri dishes with WA using the depletion method to obtain isolated colonies and cultivated at 30 ± 1°C for 48 hours. Colonies that grew at least 1 cm apart were used for inoculum preparation. These colonies were transferred to tubes with slanted WA and incubated at 30 ± 1°C for 24 hours. All transfers were carried out under aseptic conditions.

Culture medium composition

Saccharomyces cerevisiae M437 was cultivated in a liquid nutrient medium with the following composition (g/L): ammonium sulfate – 1.0, ammonium phosphate – 5.5, potassium dihydrogen phosphate – 5.5, calcium chloride – 0.021, magnesium sulfate – 0.025, glucose – 15.0, yeast extract – 0.5, and casein peptone – 1.5; pH 4.5.

Iron salts (ferric chloride and ferrous sulfate) were added to the medium to reach a final concentration of 100 mM. The control variant consisted of the base medium without the addition of iron compounds.

Cultivation conditions

The inoculum for all variants was prepared by washing a one-day-old culture with sterile saline. Specifically, 5 ml of sterile saline was added to a test tube containing the culture, and a sterile inoculating loop was used to suspend the yeast cells. The resulting inoculum was then transferred with a sterile pipette into a flask containing 50 ml of sterile nutrient medium. The inoculum volume constituted 10% of the medium volume, with an initial cell concentration of 10^4–10^5 CFU/ml. All manipulations were performed under aseptic conditions.

Cultivation was carried out in 250 ml flasks under static microaerophilic conditions at 30°C for 48 hours, until the late exponential growth phase typical of yeast was reached.

Preparation of test solutions

After 48 hours of cultivation, yeast biomass samples were taken from each culture flask. The sample was washed three times with distilled water (centrifuged three times for 10 minutes at 6000 rpm) to remove weakly bound iron fractions from the yeast cell surface. The washed yeast biomass was dried at 80°C for 8 hours and then weighed. To 100.0 mg of biomass, 2.0 mL of 3% (v/v) nitric acid was added, sealed tightly, and heated for 16 hours at 97°C to break down the yeast cell wall and release intracellular iron. After cooling the samples, 8 mL of 3% (v/v) nitric acid was added, and the solution was filtered through a "Red Stripe" filter. 4.0 mL of the filtered solution was diluted to a final volume of 20.0 mL with 3% nitric acid.

Preparation of reference solutions

Iron reference solutions for the calibration curve were prepared by diluting 0.02 M stock solutions of ferrous sulfate (Fe(II)) or ferric chloride (Fe(III)) in 3% nitric acid solution.

Spectrophotometric determination of iron in yeast biomass

0.5 mL of the test solution from the yeast sample or the iron reference solutions was mixed with 4 mL of citrate buffer, followed by the addition of 0.5 mL of 40 mg/mL sodium ascorbate solution and 0.5 mL of 2.0 mg/mL iron chelator (BPS). After 5 minutes, the specific absorbance of the iron-chelator complex was recorded at 536 nm on a spectrophotometer. A compensation solution was prepared similarly using the yeast biomass sample without exogenous iron addition.

Results and discussion

Sample preparation

To break down the yeast cell wall and release iron, solutions of nitric acid with concentrations of 2%, 3%, and 5%, as well as a 2 M hydrochloric acid solution, were tested. Increasing the nitric acid concentration from 2% to 3% resulted in a higher total iron concentration in the samples. However, the use of a 5% nitric acid solution did not lead to further iron release and complicated achieving the optimal pH (5.3-5.4) when adding the buffer solution due to the excessively acidic environment. The high acidity of the 5% solution may reduce the method's sensitivity and also cause corrosion and damage to the equipment. For the same reason, the use of a 2 M hydrochloric acid solution for iron release was also excluded.

Using a 3% nitric acid solution improved the efficiency of iron extraction, allowing more accurate results and enabling simultaneous analysis of the samples using both atomic absorption spectrometry and spectrophotometry.

Choice of iron chelator

BPS (4,7-diphenyl-1,10-phenanthroline-disulfonic acid) was preferred as the iron chelator due to its high solubility in aqueous media, owing to the presence of sulfonate groups, while 1,10-phenanthroline requires organic solvents (e.g., ethanol) for effective dissolution. Moreover, the Fe(II)-BPS complex is highly stable in aqueous solutions, ensuring reproducibility of results. Another important feature of BPS is its lower sensitivity to foreign ions, reducing potential interference when analyzing complex biological samples. The formation of the Fe(II)-BPS complex with 1,10-phenanthroline required heating to 80°C for 10 minutes to achieve sufficient reaction speed. However, BPS also has certain drawbacks. In particular, the formation of the Fe(II)-BPS complex is more sensitive to changes in pH, requiring careful control of this parameter during analysis. However, the chosen buffer solution ensures that the pH remains within the range of 5.3–5.4.

Influence of other metals on iron-BPS complex formation

According to literature (Nilsson et al., 2002; Tamarit et al., 2006), the impact of other metals potentially present in yeast on the formation of the iron-BPS complex was analyzed, specifically manganese, zinc, and copper. The reactivity of BPS with copper was significantly lower than with iron, and no complex formation with zinc or manganese was observed.

Effect of pH on the formation of the iron-BPS complex

The pH of the solution is a key factor affecting the effectiveness of the iron complexation with BPS. The optimal pH range, according to literature, is 5.3–5.4. Experimentally, it was determined that under these conditions, the absorbance of the iron-BPS complex was 0.6010, confirming the stability of the complex and effective chelation. A significant decrease in absorbance to 0.0143 was observed when the pH dropped to 2.3. This can be explained by the oxidation of Fe^{2+} to Fe^{3+} in the strongly acidic environment, which has a lower affinity for BPS. Additionally, protonation of BPS, which reduces its chelation ability, and the competitive binding of hydrogen ions with the chelator may contribute to this decrease.

When the pH was increased to 10.0, the absorbance increased to 0.1052 but remained significantly lower than at the optimal pH. This could be attributed to partial precipitation of iron as $Fe(OH)_2$ or $Fe(OH)_3$, reducing the number of available iron ions for interaction with BPS. In alkaline conditions, the formation of other hydroxy complexes that compete with BPS for iron ions may also reduce the efficiency of the target complex formation.

Thus, the results confirm that the pH range of 5.3–5.4 is the most favorable for stable Fe^{2+}-BPS complex formation, while significant deviations toward acidic or alkaline environments negatively affect the chelation process, as demonstrated by the sharp decrease in absorbance. Citrate buffer solution was added to the aliquot of reference or test solution to achieve a pH of 5.3–5.4, where BPS absorption is maximal.

Method validation

The proposed analytical method for determining iron was validated in terms of specificity, linearity, precision, and stability.

Specificity. The specificity of the method was assessed by recording the spectra of a yeast biomass sample without exogenous iron (control solution) and the test solution (yeast enriched with iron). The spectra are shown in Figure 1. At a wavelength of 536 nm, the formation of the iron-BPS complex was observed, with an optical density value of 0.8418. For the control solution, which did not contain iron, the optical density was 0.0425, indicating no significant background spectral interference. These results confirm the high specificity of the method for determining iron in the analyzed solutions. The control solution was used as a compensation solution in subsequent tests.

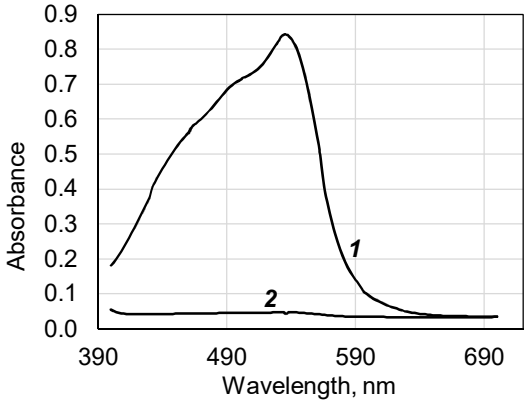

Figure 1. Spectral confirmation of iron-BPS complex formation:
1 – with complex formation (yeast enriched with iron);
2 – without complex formation (control solution).

Linearity. The linearity of the method was assessed based on the calibration curve constructed using a range of analyte concentrations from 20 to 950 μM iron. The corresponding optical density values were recorded in three parallel measurements, confirming the reproducibility of the method. Figure 2 and Figure 3 show the correlation between iron content and light absorbance after complete reaction of iron with BPS. The analysis demonstrated a linear dependence of absorbance on iron content in the range of 20 μM – 950 μM and could accurately determine 20 μM of iron, regardless of whether the iron was in the +2 oxidation state ($FeSO_4$) or +3 oxidation state ($FeCl_3$). This indicates that sodium ascorbate was capable of effectively reducing iron under these conditions.

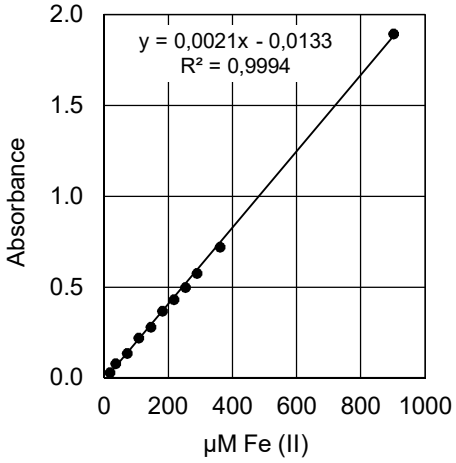

Figure 2. Linear dependence of optical density on iron concentration (from reference solutions of iron (II) sulfate after complex formation with BPS)

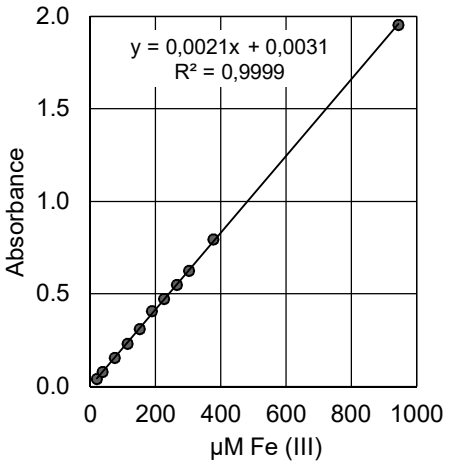

Figure 3. Linear dependence of optical density on iron concentration (from reference solutions of iron (III) chloride after complex formation with BPS)

Stability of the solutions. Previous studies (Nilsson et al., 2002; Tamarit et al., 2006) demonstrated that the formation of the iron complex with 2,2'-bipyridyl-5,5'-sulfonic acid (BPS) occurs within one minute. However, considering that smaller sample volumes were used in those studies, it became necessary to assess the rate of complex formation in a final solution volume of 5.5 mL.

The rate of formation of the iron–BPS complex was evaluated by measuring the optical density of a reference iron solution with a concentration of 300 μM and of the test solution (iron-enriched yeast) over a 5-minute period. The obtained optical density values at different time intervals are presented in Table 1.

Analysis of the data indicates rapid complex formation, as a significant increase in optical density occurs within the first two minutes. From the third minute onwards, the values stabilize, indicating that complexation equilibrium has been reached. Minor fluctuations in optical density after the third minute (0.6239–0.6240) suggest high reproducibility of the process and stability of the formed complex. Thus, the iron–BPS complex forms quickly, and equilibrium is established within 3 minutes, allowing a 5-minute incubation period to be recommended for subsequent measurements in analytical studies.

Table 1

Absorbance values depending on the incubation time of the solution after BPS addition (complex formation study)

Time, min	Absorbance of reference solution	Absorbance of test solution
0	0.5726	0.6765
1	0.6067	0.6877
2	0.6227	0.6963
3	0.6239	0.6983
4	0.6240	0.6984
5	0.6239	0.6984

The stability of the iron-BPS complex solutions was evaluated over time by storing a reference solution containing 360 μM iron and the test solution (iron-enriched yeast) for periods ranging from 5 to 45 minutes. The measurement results are presented in Table 2. Optical density measurements showed only minor changes. Minimal fluctuations in absorbance indicate high stability of the complex within the investigated time range, which allows its use in further analytical studies without significant errors related to the decomposition or transformation of the complex.

Table 2

Absorbance values depending on the incubation time of the solution after BPS addition (stability study)

Time, min	Absorbance of reference solution	Absorbance of test solution
5	0.7276	0.6984
15	0.7245	0.6988
25	0.7275	0.6986
35	0.7280	0.6986
45	0.7286	0.6988

Reproducibility. The reproducibility of the analysis was evaluated by preparing three reference solutions in triplicate on the same day. The measurement results are presented in Table 3.

Table 3

Results of repeated optical density measurements for samples with different iron concentrations

Test number	360 μM Fe	190 μM Fe	110 μM Fe
Measurement 1	0.6010	0.3759	0.2267
Measurement 2	0.5971	0.3710	0.2203
Measurement 3	0.6006	0.3774	0.2231
Average	0.5996	0.3748	0.2234
RSD,%	0.4	0.9	1.4

The obtained values of relative standard deviation (RSD) did not exceed 1.4%, indicating high reproducibility of the method across the entire studied concentration range. The lowest deviation (0.4%) was observed at an iron concentration of 360 μM, which reflects signal stability at higher analyte content. RSD values below 2% generally indicate the reliability and robustness of the method under routine analytical conditions.

To further confirm the accuracy of the spectrophotometric method described in this study, the results were compared with those obtained using atomic absorption spectrometry (AAS). Iron reference solutions for the calibration curve were prepared by diluting a Certipur® multi-element standard for MS. The test samples (solutions obtained from biomass of yeast enriched with iron via the addition of iron (II) sulfate and iron (III) chloride), prepared according to the described procedure, and were analyzed by both methods. The obtained results are presented in Table 4.

Table 4

Comparative table of iron content in yeast determined by spectrophotometry and atomic absorption spectrometry

Sample	Iron content, mg/g DW of yeast, determined by	
	method 1	method 2
Sample (iron enrichment source – $FeSO_4$)	9.7 ± 0.2	9.3 ± 0.4
Sample (iron enrichment source – $FeCl_3$)	5.2 ± 0.5	5.7 ± 0.6

Note:
Method 1 – spectrophotometric method;
Method 2 – atomic absorption spectrometry;
DW, dry weight

The results of the analysis of variance (ANOVA) revealed a significant difference between the two iron sources – iron sulfate ($FeSO_4$) and iron chloride ($FeCl_3$). The F-value for the iron sources was high ($F(1,8) = 243.00$, $p < 0.0001$), indicating a significant difference in iron content depending on the type of compound. This suggests that the form of iron affects its availability or effectiveness under different conditions. Iron in the form of $FeSO_4$ (Fe (II)) is likely better absorbed, as confirmed by the high F-value, compared to $FeCl_3$ (Fe (III)), which requires additional reduction before absorption.

At the same time, no statistically significant difference was found between the measurement methods – spectrophotometry and atomic absorption spectrometry (AAS) ($F(1,8) = 0.037$, $p = 0.8522$). This means that both methods provided similar results, and the choice of measurement method had no substantial effect on determining the iron content in both types of samples. Therefore, under the studied conditions, the choice of method for measuring iron content is not a critical factor.

Conclusions

This study presents a simple and accessible approach for determining iron content in yeast. An effective extraction method was developed that does not require complex or specialized equipment. The proposed method is characterized by ease of execution, reproducibility of results, and suitability for application in a standard laboratory setting. The use of a 3% nitric acid solution was identified as the optimal option for releasing iron from yeast cells, providing high extraction efficiency and compatibility with both spectrophotometric and atomic absorption analyses.

The obtained results highlight the practical value of the proposed method for routine monitoring of iron content in food products, as well as for evaluating the effectiveness of biotechnological processes for yeast iron enrichment and investigating the forms and bioavailability of iron in the development of functional food products.

References

Chen Y., Pang Y., Wan H., et al. (2024), Production of iron-enriched yeast and its application in the treatment of iron-deficiency anemia, *Biometals*, 37, pp. 1023–1035. https://doi.org/10.1007/s10534-024-00592-3.

Fish W.W. (1988), Rapid colorimetric micromethod for the quantitation of complexed iron in biological samples, *Methods in Enzymology*, 158, pp. 357–364. https://doi.org/10.1016/0076-6879(88)58067-9.

Gaensly F., Picheth G., Brand D., Bonfim T.M. (2014), The uptake of different iron salts by the yeast *Saccharomyces cerevisiae*, *Brazilian Journal of Microbiology*, 45(2), pp. 491–494. https://doi.org/10.1590/s1517-83822014000200016.

Jach M.E., Serefko A., Ziaja M., Kieliszek M. (2022), Yeast protein as an easily accessible food source, *Metabolites*, 12(1), 63. https://doi.org/10.3390/metabo12010063.

Hailu T., Solomon D., Worku E., Sisay S., Demissie K. (2019), Determination of iron and moisture content in commonly consumed vegetable samples of Gubrie and Wolkite Town, Southern Ethiopia, *Journal of Analytical & Bioanalytical Techniques*, 10(4), 10000198. https://doi.org/10.4172/2150-3494.10000198.

Herrera L., Ruiz P., Aguillon J. C., Fehrmann A. (2007), A new spectrophotometric method for the determination of ferrous iron in the presence of ferric iron, *Journal of Chemical Technology & Biotechnology*, 44(3), pp. 171–181. https://doi.org/10.1002/jctb.280440302.

Hamad A., Singh P. (2025), Boosting nutritional value: The role of iron fortification in meat and meat products, *Biometals*, 38(2), pp. 337-355. https://doi.org/10.1007/s10534-024-00659-1.

Jarzębski M., Wieruszewski M., Kościński M., Rogoziński T., Kobus-Cisowska J., Szablewski T., Perła-Kaján J., Waszkowiak K., Jakubowicz J. (2023), Heme iron as potential iron fortifier for food application – characterization by material techniques, *Reviews on Advanced Materials Science*, 62, pp. 20230128–20230142. https://doi.org/10.1515/rams-2023-0128.

Kyyaly M. A., Powell C., Ramadan E. (2015), Preparation of iron-enriched baker's yeast and its efficiency in recovery of rats from dietary iron deficiency, *Nutrition*, 31(9), pp. 1155–1164. https://doi.org/10.1016/j.nut.2015.04.017.

Mier-Alba E., Martiniano S. E., Sánchez-Muñoz S., de Oliveira G., Santos J., da Silva S. (2024), Sustainable production of nutritional iron-enriched yeast from low-cost bran sources: A valuable feedstock for circular economy, *Sustainable Chemistry One World*, 3, 100021. https://doi.org/10.1016/j.scowo.2024.100021.

Niedzielski P., Zielinska-Dawidziak M., Kozak L., Kowalewski P., Szlachetka B., Zalicka S., Wachowiak W. (2014), Determination of iron species in samples of iron-fortified food, *Food Analytical Methods*, 7, pp. 2023–2032. https://doi.org/10.1007/s12161-014-9843-5.

Nilsson U.A., Bassen M., Sävman K., Kjellmer I. (2002), A simple and rapid method for the determination of "free" iron in biological fluids, *Free Radical Research*, 36(6), pp. 677–684. https://doi.org/10.1080/10715760290029128.

Orlowska A., Proch J., Niedzielski P. (2023), A fast and efficient procedure of iron species determination based on HPLC with a short column and detection in high resolution ICP OES, *Molecules*, 28(11), 4539. https://doi.org/10.3390/molecules28114539.

Pirman T., Orešnik A. (2012), Fe bioavailability from Fe-enriched yeast biomass in growing rats, *Animal*, 6(2), pp. 221–226. https://doi.org/10.1017/S1751731111001546.

Piskin E., Cianciosi D., Gulec S., Tomas M., Capanoglu E. (2022), Iron absorption: Factors, limitations, and improvement methods, *ACS Omega*, 7(24), pp. 20441–20456. https://doi.org/10.1021/acsomega.2c01833.

Riemer J., Hoepken H. H., Czerwinska H., Robinson S. R., Dringen R. (2004), Colorimetric ferrozine-based assay for the quantitation of iron in cultured cells, *Analytical Biochemistry*, 331(2), pp. 370–375. https://doi.org/10.1016/j.ab.2004.03.049.

Tafazzoli K., Ghavami M., Khosravi-Darani K. (2024), Production of iron-enriched *Saccharomyces boulardii*: impact of process variables, *Scientific Reports*, 14(1), 4844. https://doi.org/10.1038/s41598-024-55433-7.

Tamarit J., Irazusta V., Moreno-Cermeño A., Ros J. (2006), Colorimetric assay for the quantitation of iron in yeast, *Analytical Biochemistry*, 351(1), pp. 149–151. https://doi.org/10.1016/j.ab.2005.12.001.

Tsykhanovska I., Evlash V., Alexandrov O., Riabchykov M., Lazarieva T., Nikulina A., Blahyi O. (2022), Technology of bakery products using magnetofood as a food additive. In: O. Paredes-López, O. Shevchenko, V. Stabnikov, V. Ivanov, (Eds.), *Bioenhancement and Fortification of Foods for a Healthy Diet,* pp. 3-28, CRC Press, Boca Raton, https://doi.org/10.1201/9781003225287-2.

Tsykhanovska I., Lazarieva T., Stabnikova O., Kupriyanov O., Litvin O., Yevlash V. (2023), Potential benefits of functional antianemic energy bars, *Ukrainian Food Journal*, 12(4), pp. 578-598. https://doi.org/10.24263/2304-974X-2023-12-4-7.

Tsykhanovska I., Stabnikova O., Oliinyk S., Lazarieva T., Gubsky S. (2024), Application of combined food additive based on iron oxide nanoparticles and kombu in a rye-wheat bread technology, *Ukrainian Food Journal*, 13(3), pp. 576-596. https://doi.org/10.24263/2304-974X-2024-13-3-10.

World Health Organization. (2008), Worldwide prevalence of anaemia 1993-2005: WHO global database on anaemia, Geneva, 2008.

Xing Y., Gao S., Zhang X., Zang J. (2022), Dietary heme-containing proteins: Structures, applications, and challenges, *Foods*, 11(22), pp. 3594–3614. https://doi.org/10.3390/foods11223594.

Zielińska-Dawidziak M., Białas W., Piasecka-Kwiatkowska D., Staniek H., Niedzielski P. (2023), Digestibility of protein and iron availability from enriched legume sprouts, *Plant Foods for Human Nutrition*, 78(2), pp. 270-278. https://doi.org/10.1007/s11130-023-01045-x.

Cite:

UFJ Style

Bondar H., Krasinko V. (2025), Rapid spectrophotometric method for the determination of iron content in yeast, *Ukrainian Journal of Food Science*, 13(1), pp. 80–90, https://doi.org/10.24263/2310-1008-2025-13-1-9

APA Style

Bondar, H., & Krasinko, V. (2025). Rapid spectrophotometric method for the determination of iron content in yeast. *Ukrainian Journal of Food Science, 13*(1), 80–90. https://doi.org/10.24263/2310-1008-2025-13-1-9

Biosynthesis and characterization of selenium nanoparticles by *Saccharomyces cerevisiae* M437

Oksana Skrotska, Maria Protsenko, Oleksandr Zholobko, Andrii Marynin

National University of Food Technologies, Kyiv, Ukraine

Keywords:

Selenium
Nanoparticle
Yeast
Saccharomyces cerevisiae
Biosynthesis
Characteristics

Article history:

Received 12.01.2025
Received in revised form 16.06.2024
Accepted 30.06.2024

Corresponding author:

Oksana Skrotska
E-mail: skrotskaoi@nuft.edu.ua

DOI: 10.24263/2310-1008-2025-13-1-10

Abstract

Introduction. Biosynthesized selenium nanoparticles (SeNPs) hold significant promise for applications in the food industry due to their antimicrobial and antioxidant properties.

Materials and methods. The yeast strain *Saccharomyces cerevisiae* M437 was cultivated in yeast peptone dextrose medium. The SeNPs biosynthesis conditions included: *Saccharomyces cerevisiae* M437 biomass, 1 mM sodium selenite (Na_2SeO_3), 30°C, 250 rpm, for 7 days. Nanoparticle formation was assessed using light microscopy, UV-visible spectroscopy, and dynamic light scattering (DLS) analysis.

Results and discussion. A sodium selenite concentration of 1 mM was selected as optimal, as it ensured high bioreduction efficiency with minimal cytotoxic effects on *Saccharomyces cerevisiae* M437 cells. Throughout the 7-day biosynthesis process, a visible color shift of the biomass was observed from milky white to pink, and finally to deep red, serving as a visual indicator of intracellular SeNPs formation *via* the biological reduction of selenite ions to elemental selenium, one of the allotropes of which exhibits a red color. Light microscopy confirmed the presence of fine particulate inclusions both inside and outside the cells, indicating efficient nanoparticle formation. For more detailed characterization of SeNP morphology and internal structure, scanning transmission electron microscopy (STEM) are planned in future studies.

UV-Vis spectral analysis of the biogenic SeNPs revealed a distinct absorption peak at 252 nm, associated with electronic transitions and surface plasmon resonance. DLS measurements showed an average hydrodynamic diameter of 179.3 nm. The zeta potential value of –16.2 mV suggests moderate colloidal stability, while the polydispersity index of 0.229 indicates a narrow size distribution and low tendency toward agglomeration. The organic capping layer, likely composed of biomolecules derived from yeast cells, contributes to the stability and bioactivity of the nanoparticles. The obtained results are consistent with literature reports on SeNPs synthesized by microorganisms and demonstrate the promise of this biotechnological approach.

Conclusions. The intracellular biosynthesis of selenium nanoparticles by *Saccharomyces cerevisiae* M437 was confirmed. The core physicochemical properties of the synthesized nanoparticles were characterized, demonstrating their potential suitability for applications in the food industry.

Introduction

Selenium nanoparticles (SeNPs) exhibit significant potential for applications in the food industry due to their antimicrobial and antioxidant properties. SeNPs are effective against a broad spectrum of foodborne pathogenic microorganisms, including *Bacillus cereus*, *Escherichia coli*, *Staphylococcus aureus* (Hussein et al., 2022), *Listeria monocytogenes*, *Salmonella enterica* (Abdel-Moneim et al., 2022), *Vibrio parahaemolyticus* (Vinu et al., 2021; Zhang et al., 2021), *Pseudomonas aeruginosa*, *Enterococcus faecalis*, *Klebsiella pneumoniae* (Huang et al., 2020), as well as fungi such as *Fusarium verticillioides*, *Fusarium graminearum,* and *Alternaria alternata* (Hu et al., 2019). These antimicrobial properties enable the use of SeNPs in the production of active food packaging, which can potentially extend the shelf life of food products.

Biopolymers are commonly used as carriers for SeNPs due to their biocompatibility and eco-friendliness (Ao et al., 2023; Ndwandwe et al., 2021). Biopolymer films serve as an alternative to synthetic packaging materials (Jamróz et al., 2019a). For instance, films incorporating SeNPs have been shown to extend the shelf life of hazelnuts, walnuts, potato chips, ham, chicken, and ready-to-eat vegetable mixes (Vera et al., 2018). Similarly, the preservation of freshness of mini-kiwi (Jamróz et al., 2019a) and fish products (Jamróz et al., 2019b) has been demonstrated. SeNPs embedded in polymer matrices damage bacterial cell walls, disrupt DNA structure, and induce apoptosis, exhibiting biocidal activity even against multidrug-resistant strains. Additionally, SeNPs demonstrate the antioxidant activity by reducing oxidative processes in food products, thereby preventing spoilage. Although no specific regulatory framework exists for SeNPs in food packaging, their biocompatibility and efficacy warrant further research in this field (Ndwandwe et al., 2021).

Beyond food packaging, selenium nanoparticles are actively investigated as feed supplements for livestock (Zhang et al., 2023). This approach not only supports animal health and productivity but also enhances selenium intake in human diets through increased selenium content in meat, milk, and eggs (Malyugina et al., 2021). Positive effects of SeNPs on weight gain in broiler chickens (Nabi et al., 2020) and growth in various fish species (Jahanbakhshi et al., 2021), including Nile tilapia (Ghazi et al., 2021; Ibrahim et al., 2021) and grass carp (Zhang et al., 2022), have been reported.

Selenium nanoparticles can be synthesized *via* physical, chemical, or biological methods (Zhang et al., 2023). For biogenic synthesis, microorganisms such as fungi, bacteria, and yeast are utilized (Dutta and Ray, 2024; Gregirchak et al., 2024; Stabnikova et al., 2023).

Selenium nanoparticle biosynthesis has also been explored using different yeast species (Table 1). For example, *Kluyveromyces lactis* GG799 (Song et al., 2021), *Candida utilis* ATCC 9950 (Kieliszek et al., 2020), marine yeast *Yarrowia lipolytica* NCIM 3589 (Hamza et al., 2017), and genetically modified yeast *Pichia pastoris* (Elahian et al., 2017) have been utilized. Lashani et al. investigated SeNPs biosynthesis using *Yarrowia lipolytica* ATCC 18942, demonstrating antimicrobial activity against *Serratia marcescens*, *Klebsiella pneumoniae*, *Escherichia coli*, *Pseudomonas aeruginosa*, and *Candida albicans*, as well as anti-biofilm activity against *Klebsiella pneumoniae*, *Acinetobacter baumannii*, *Staphylococcus aureus*, and *Pseudomonas aeruginosa*. The biogenic SeNPs also exhibited antioxidant activity (Lashani et al., 2024). SeNPs produced using the supernatant of *Candida albicans* TIMML-1306 showed significant antifungal effects against *Candida albicans* and *Candida glabrata* (Bafghi et al., 2022). In the case of selenium nanoparticles biosynthesis using cell-free aqueous extracts of *Magnusiomyces ingens* LH-F1, inhibition of *Arthrobacter* sp. W1 growth was observed (Lian et al., 2019).

Table 1

Biosynthesis of selenium nanoparticles using yeast species

Yeast	SeNPs biosynthesis parameters	SeNPs characteristics	Source
Pichia pastoris	YPD broth, 4 mM SeO_2, 30°C, 96 h	Intracellular, spherical, size 70–180 nm	Elahian et al., 2017
Yarrowia lipolytica NCIM 3589	MGYP broth, 4 mM Na_2SeO_3, 30°C, 120 rpm, 48 h	Intracellular, spherical, size 30–60 nm	Hamza et al., 2017
Yarrowia lipolytica ATCC 18942	GYP broth medium, 2.5 mM Na_2SeO_3, 30°C, 160 rpm, 48 h	Intracellular, spherical, size 37–180 nm	Lashani et al., 2024
Candida albicans TIMML-1306	Supernatant after yeast cultivation was added to 5 mM Na_2SeO_4, 28°C, 24 h	Spherical, average diameter size 38 nm	Bafghi et al., 2022
Candida utilis ATCC 9950	YPD medium, 30 mg Na_2SeO_3, 200 rpm, 24 h	Intracellular, spherical, size 20–40 nm	Kieliszek et al., 2020
Magnusiomyces ingens LH-F1	Cell-free extract from cell lysate, 2 mM SeO_2, pH 7, 30°C	Spherical/quasi–spherical, size 70–90 nm	Lian et al., 2019
Nematospora coryli	Yeast biomass, 1 mM Na_2SeO_3, 28°C, 130 rpm, 48 h	Intracellular, spherical, size 50–250 nm	Rasouli, 2019
Kluyveromyces lactis GG799	YPD broth with yeast biomass, 1.2 mM Na_2SeO_3, 30°C, 200 rpm, 24 h	Intracellular, spherical, size 80–150 nm	Song et al., 2021

Note: YPD, Yeast extract, peptone, dextrose; MGYP, Malt extract, glucose, yeast extract, peptone; GYP, Glucose, yeast, peptone.

However, each microbial system has its advantages and limitations. One of the key advantages of using yeast, particularly *Saccharomyces species*, is their ease of handling and inherent safety, as they do not require specialized biosafety measures unlike many bacterial and fungal strains (Ao et al., 2023; Grasso et al., 2020).

Saccharomyces cerevisiae yeast is one of the most widely used organisms for SeNPs biosynthesis (Table 2) due to its availability and metabolic versatility. The intracellular biosynthesis of SeNPs has been studied using baker's yeast *Saccharomyces cerevisiae* and their antioxidant activity has been confirmed (Faramarzi et al., 2020; Fath-Alla et al., 2024). Cultivation of *Saccharomyces cerevisiae* GVT263 on agricultural waste resulted in the biosynthesis of crystalline rod-shaped SeNPs (Goud et al., 2016). SeNPs with antibacterial activity against *Escherichia coli*, *Pseudomonas aeruginosa*, *Klebsiella pneumoniae*,

Salmonella typhimurium, *Staphylococcus aureus*, and *Bacillus subtilis* were produced using *Saccharomyces cerevisiae* MTCC 36. The antibacterial activity of SeNPs is attributed to their ability to disrupt bacterial cell walls and generate reactive oxygen species, inducing oxidative stress in microorganisms (Hariharan et al., 2012). Controlled intracellular SeNPs biosynthesis, followed by their release from cells, was studied using *Saccharomyces cerevisiae* BY4741. SeNPs transport out of cells occurs via exocytosis or vesicular secretion (Pereira et al., 2018). Additionally, the biosynthesis of SeNPs under oxygen-limited conditions using *Saccharomyces cerevisiae* yielded nanoparticles with a protein coating containing carbonyl and hydroxyl groups, thereby enhancing their hydrophilicity and stability (Zhang et al., 2012).

Table 2

Biosynthesis of selenium nanoparticles using yeast *Saccharomyces cerevisiae*

Yeast	SeNPs biosynthesis parameters	SeNPs characteristics	Reference
S. cerevisiae	SDB medium, 25 µg Na_2SeO_3, 32°C, 120 rpm, 96 h	Intracellular, spherical, size 709 nm	Faramarzi et al., 2020
S. cerevisiae	SDB medium, 0.025 g Na_2SeO_3, 30°C, 24 h	Intracellular, spherical, size 34-125 nm	Fath-Alla et al., 2024
S. cerevisiae GVT263	Agro-waste based yeast fermented broth, 2 mM Na_2SeO_3, 18-20°C, 24 h	Intracellular, rod-shaped, size 170-240 nm	Goud et al., 2016
S. cerevisiae BY4741	YNB medium, 1 mM Na_2SeO_3, 30°C, 150 rpm, 48 h	Intracellular, spherical, size 20-30 nm	Pereira et al., 2018
S. cerevisiae	Malt juice, 100 mg Na_2SeO_3, pH 4, 30°C, 36 h	Intracellular, spherical, size 71.14 ± 18.17 nm	Wu et al., 2021
S. cerevisiae	YPD medium, 0.5 mM Na_2SeO_3, 30°C, 120 rpm, 36 h	Extracellular, spherical, size 100 nm	Zhang et al., 2012
S. cerevisiae MTCC 36	MY medium, 2 mM Na_2SeO_3, 30°C, 200 rpm, 24 h	Crystalline, size 30-100 nm	Hariharan et al., 2012

Note: SDB, Sabouraud dextrose broth; YNB, Yeast nitrogen base; MY, Malt yeast.

The aim of the present study was to investigate the characteristics of selenium nanoparticles produced using *Saccharomyces cerevisiae* M437 for potential applications in the food industry.

Materials and methods

Culture media for storage and cultivation of *Saccharomyces cerevisiae* M437

Medium 1 for storage in slant agar tubes and subculturing of *Saccharomyces cerevisiae* M437: Sabouraud medium, consisting of 9 g/L enzymatic peptone, 1 g/L yeast extract, 40 g/L glucose, and 15 g/L microbiological agar, pH 5.6.

Medium 2 for cultivating *Saccharomyces cerevisiae* M437 for intracellular SeNPs biosynthesis: YPD (Yeast Peptone Dextrose) medium, consisting of 20 g/L peptone, 10 g/L yeast extract, and 20 g/L glucose, pH 6.3.

Cultivation of yeast *Saccharomyces cerevisiae* M437

The *Saccharomyces cerevisiae* M437 strain was selected from a live culture collection for use in the experiments. This strain was stored in a laboratory refrigerator at 4°C in test tubes containing slanted agar (Medium 1). For inoculum preparation, yeast cells were washed from the agar surface to obtain a suspension with a concentration of 10^5-10^6 cells/mL. The resulting inoculum, constituting 5% of the medium volume, was added to 100 mL of pre-sterilized liquid YPD medium (Medium 2). The liquid medium was prepared by mixing and dissolving the appropriate components in distilled water, followed by sterilization in an autoclave at 121°C for 15 minutes. Cultivation of the inoculum was carried out in 250 mL Erlenmeyer flasks containing 100 mL of liquid YPD medium at 30°C and 250 rpm for 48 hours until an optical density at 600 nm (OD_{600}) of 2.5 was reached.

Intracellular biosynthesis of selenium nanoparticles

Obtaining yeast biomass. After 48 hours of cultivation, *Saccharomyces cerevisiae* M437 biomass was harvested by centrifugation (4000 rpm, 20 min). To remove soluble medium components and extracellular metabolites, the cells were washed three times with sterile distilled water. The supernatant was discarded, and sterile distilled water was added to the cell pellet. The cells were resuspended and centrifuged again (4000 rpm, 20 min). This process was repeated three times.

Preparation of sodium selenite as a precursor for selenium nanoparticles. A 1 M sodium selenite (Na_2SeO_3) solution was prepared by dissolving 17.2948 g of Na_2SeO_3 salt in 100 mL of distilled water. After complete dissolution, the solution was sterilized via cold filtration using a sterile syringe filter with a 0.22 μm pore size. The 1 M sodium selenite solution was stored in a sterile glass tube.

Biosynthesis procedure. The washed yeast cells were resuspended in 100 mL of sterile distilled water in a 250 mL flask, and the sodium selenite solution was added to achieve a final concentration of 1 mM. Intracellular SeNP biosynthesis was carried out under the following conditions: 30°C, 250 rpm using an ES-20/60 Biosan SIA orbital shaker-incubator (Latvia). For the first control, a flask with washed yeast in sterile distilled water without sodium selenite was used. For the second control, a flask with a 1 mM sodium selenite solution was used. Observations were conducted over seven days, during which the cell color changed from milky white to pink and then red, indicating nanoparticle formation.

Characteristics of biosynthesized selenium nanoparticles

Light microscopy. For microscopy of *Saccharomyces cerevisiae* M437, a "crushed drop" preparation was made. Samples were collected after seven days of intracellular SeNPs biosynthesis. Under aseptic conditions, 2 mL of cell suspension was collected, and a few drops were placed on a microscope slide and stained with methylene blue. A coverslip was placed on top, and excess moisture was removed with filter paper. A drop of glycerin was applied to the coverslip, and microscopy was performed using an XS-3330 LED MICROmed light microscope (China) with an immersion objective (total magnification: ×1000).

UV-Visible spectroscopy. On day seven, the SeNPs biosynthesis process was terminated. Yeast cells were separated by centrifugation (5000 rpm, 40 min). The supernatant was analyzed using a UV-Vis spectrophotometer (Thermo Spectronic UV300, Spectronic Unicam, England). Four milliliters of the supernatant were transferred in a quartz cuvette, and the absorption spectrum was measured in the wavelength range of 200-800 nm with a resolution of 2 nm (Hashem et al., 2023).

The hydrodynamic diameter determination. The hydrodynamic diameter of biosynthesized SeNPs was measured using a Zetasizer Nano ZS (Malvern, UK), based on dynamic light scattering (DLS). Zeta potential and polydispersity index (PDI) were also determined. All measurements were performed at a constant temperature of 25°C in a neutral medium (pH = 7.0). Each analysis was repeated three times to ensure the reliability of the results (Nwoko et al., 2021).

Results and discussion

Selection of sodium selenite concentration

One of the key parameters influencing the efficiency of selenium nanoparticle biosynthesis is the concentration of the precursor – sodium selenite (Na_2SeO_3). Based on an extensive review of current scientific literature on microbial SeNP biosynthesis, a concentration of 1 mM Na_2SeO_3 is widely regarded as optimal for many microorganisms (Table 3).

This concentration balances high selenite reduction efficiency with minimal toxicity to cells. For instance, using *Acinetobacter* sp. SW30 biomass, amorphous SeNPs with antioxidant and antimicrobial properties were synthesized at 1.0 mM sodium selenite. However, at concentrations above 2 mM, crystalline nanorods with antitumor activity were produced but exhibited high cytotoxicity (Wadhwani et al., 2017). Another study describing intracellular SeNP biosynthesis using the culture medium of *Saccharomyces cerevisiae* reported that lower concentrations of selenite salts produced smaller SeNPs with higher antioxidant activity. Nevertheless, the overall process efficiency was reduced due to low yield, limited productivity, and high polydispersity (Faramarzi et al., 2020). Additionally, Shoeibi and Mashreghi (2017) investigated SeNP biosynthesis using *Enterococcus faecalis* at sodium selenite concentrations ranging from 0.19 mM to 2.97 mM. Higher precursor concentrations resulted in the formation of fewer nanoparticles.

Table 3

Sodium selenite concentrations for selenium nanoparticle biosynthesis

Microorganism	Culture medium	SeNPs biosynthesis conditions	Reference
Bacillus subtilis AL43	LB broth	pH 7,2, 30°C, 150 rpm, 24 h, 1 mM Na_2SeO_3 at the beginning of the cultivation process	Abdel-Moneim et al., 2022
Streptomyces sp E3	NB	32°C, 180 rpm, 72 h, 1 mM Na_2SeO_3, biomass	El-deeb et al., 2023
Vibrio natriegens ATCC14048	LB broth	30°C, 12 h, 1 mM Na_2SeO_3 at the beginning of the cultivation process	Fernández-Llamosas et al., 2017
Paenibacillus terreus	TSB broth	37°C, 150 rpm, 24 h, 1 mM Na_2SeO_3 at the beginning of the cultivation process	Nile et al., 2023
Saccharomyces cerevisiae BY4741	YNB, added with amino acids	30°C, 150 rpm, 48 h, 1 mM Na_2SeO_3 at the beginning of the cultivation process	Pereira et al., 2018
Streptomyces sp. M10A65	ISP2 medium	28°C, 120 rpm, 24-48 h, 1 mM Na_2SeO_3, biomass	Ramya et al., 2020
Nematospora coryli	YPG broth	28°C, 130 rpm, 48 h, 1 mM Na_2SeO_3, biomass	Rasouli, 2019
Lysinibacillus macroides DS15	LB broth	35°C, 180 rpm, 36 h, 1 mM Na_2SeO_3 at the beginning of the cultivation process	Zhang et al., 2019

Note: LB, Luria-Bertani; YPG, Yeast extract, peptone, dextrose; TSB, Tryptone-soy; YNB, Yeast nitrogen base; ISP2, International Streptomyces Project-2 medium, containing yeast extract, malt extract, and dextrose.

Based on this evidence, a sodium selenite concentration of 1 mM was selected for selenium nanoparticle biosynthesis using *Saccharomyces cerevisiae* M437. Although yeast holds significant promise for SeNPs biosynthesis, the number of studies in this area remains limited (Nie et al., 2023).

Intracellular biosynthesis of selenium nanoparticles

After adding sodium selenite to *Saccharomyces cerevisiae* M437 cells, a color change from milky white to light pink was observed on the second day. Over the seven-day observation period, the color intensified, reaching a distinct red by the seventh day (Figure 1).

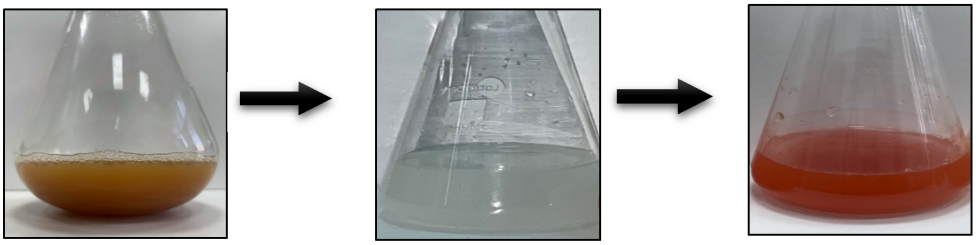

a **b** **c**

Figure 1. Stages of intracellular biosynthesis of selenium nanoparticles by *Saccharomyces cerevisiae* M437: a – native yeast grown on YPD medium; b – washed yeast biomass; c – yeast on day 7 of nanoparticle biosynthesis

The color change from milky to red indicates intracellular SeNP formation, resulting from the biological reduction of selenite oxyanions (SeO_3^{2-}) to elemental selenium (Se^0), one of whose allotropic forms exhibits a characteristic red color. Intracellular yeast metabolites facilitate this process (Tan et al., 2018). Similar results have been reported in studies where SeNP biosynthesis was accompanied by characteristic color changes. For instance, the formation of biogenic SeNPs using the supernatant of *Anabaena variabilis* NCCU-441 was confirmed by a color change from sky blue to orange-red (Afzal et al., 2021). SeNPs biosynthesis using *Lactobacillus paracasei* HM1 (El-Saadony et al., 2021) and *Bacillus subtilis* (Chandramohan et al., 2018) resulted in culture medium color changes from yellow to dark red within 48 hours. Likewise, using *Saccharomyces cerevisiae* culture fluid, SeNP formation was indicated by a color change from pale yellow to dark orange within four days (Faramarzi et al., 2020).

On days 5–7, biosynthesized intracellular SeNPs began to release in the solution. It was indicated by the pale red color of the supernatant after centrifugation. Literature analysis confirmed this observation. Pereira et al. demonstrated that SeNPs were synthesized intracellularly by *Saccharomyces cerevisiae* BY4741 within 48 hours and were subsequently released into the extracellular medium by 96 hours without compromising cell integrity (Pereira et al., 2018). Further analysis showed that intracellular SeNPs were concentrated near or protruded from the cell membrane, and extracellular SeNPs possessed well-defined organic shells. The presence of extracellular nanoparticles suggests a vesicular transport mechanism, where yeast cells expel excess selenium via vesicle-like structures (Wu et al., 2021). This intracellular biosynthesis and subsequent extracellular release is advantageous, as it simplifies nanoparticle isolation and purification compared to solely intracellular biosynthesis, which requires cell disruption methods such as ultrasonication, enzymatic cell wall degradation, mechanical disruption with glass or metal beads, or chemical lysis using bases and anionic detergents (Sajnóg et al., 2023). Studies on using *Yarrowia lipolytica* also showed that SeNPs are synthesized intracellularly, are associated with cell membranes, and may be localized in various cellular compartments, indicating the presence of multiple nucleation sites for selenite reduction and intracellular nanoparticle formation in *Yarrowia lipolytica* cells (Lashani et al., 2024).

The light microscopy was performed on day 7 to confirm SeNP formation and localization. Analysis revealed that, compared to native yeast cells with homogeneous cytoplasm, samples with synthesized SeNPs exhibited scattered or clustered inclusions within and outside the cells, potentially indicating SeNPs and their localization (Figure 2). Future studies are planned to employ scanning electron microscopy (SEM) to determine the detailed morphology of the synthesized nanoparticles and their interactions with cellular organelles. SEM enables rapid acquisition of high-resolution 3D images of nanoparticle surfaces with minimal sample preparation. In addition, transmission electron microscopy (TEM) will be used to provide ultra-high-resolution imaging for analyzing the internal structure of the formed nanoparticles (Kumar, 2021).

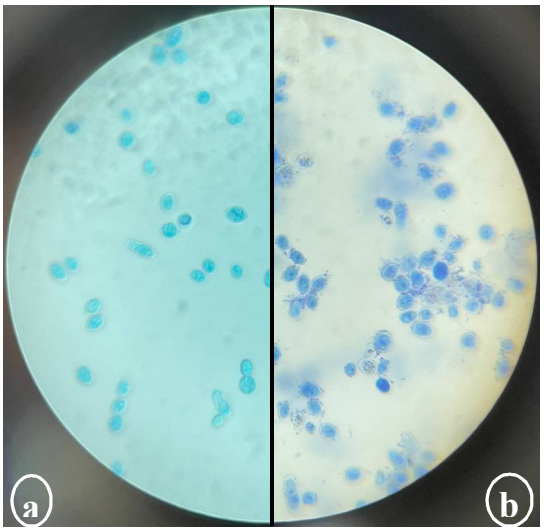

Figure 2. Cells of *Saccharomyces cerevisiae* M437:
a – native yeast cells;
b – yeast cells with biosynthesized selenium nanoparticles; magnification ×1000

UV-Visible spectroscopy

UV-vis spectroscopy is a common method to confirm SeNP formation by detecting their characteristic red color absorbance at specific wavelengths, attributed to surface plasmon resonance (SPR) excitation – an effect that arises when conduction electrons in a thin metallic layer are excited by incident light (Fath-Alla et al., 2024). During the SeNPs biosynthesis process, we visually observed a color change not only in the yeast cells but also in the reaction mixture itself, suggesting the release of SeNPs into the extracellular medium. UV-Vis spectroscopy analysis revealed distinct absorption peaks within the 200–800 nm wavelength range, with two maxima at 207 and 252 nm (Figure 3).

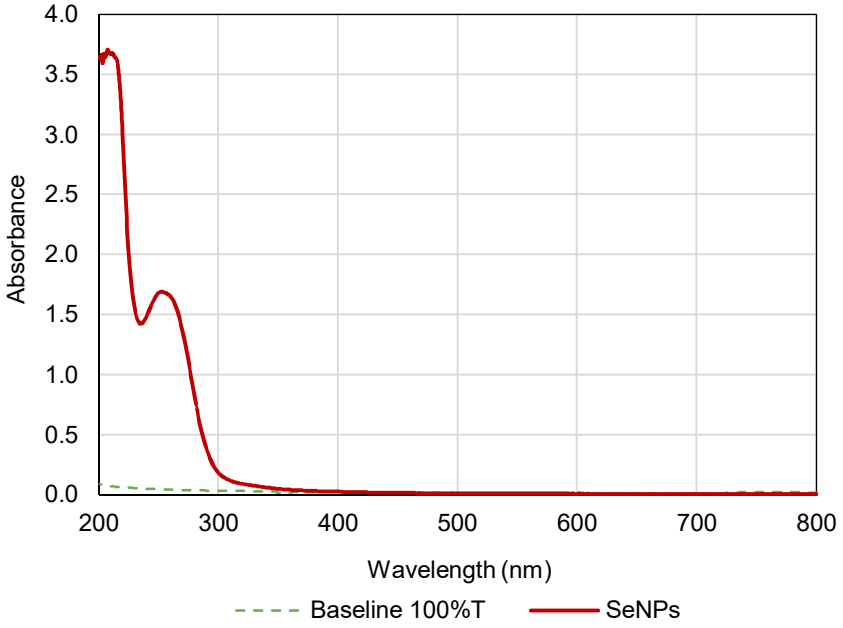

Figure 3. UV-Vis spectrum of biosynthesized selenium nanoparticles using *Saccharomyces cerevisiae* M437

The results (Figure 3) are consistent with earlier findings on SeNP biosynthesis using the supernatant of *Aspergillus terreus*, where absorbance measurements in the 200–800 nm range showed two major peaks at 218 and 284 nm. The first absorbance peak may correspond to interband and fundamental electronic transitions, such as transitions from lower energy levels to the conduction or upper bands, while the second peak is likely associated with coherent oscillation of free electrons across the nanoparticle surface known as SPR (Saied et al., 2023). Similarly, biosynthesized SeNPs obtained using a cell-free aqueous extract of *Monascus purpureus* ATCC16436 showed a maximum absorption peak at 593 nm after 30 minutes of biosynthesis, also measured in the 200–800 nm range (El-Sayed et al., 2020). Comparable results were obtained for SeNPs biosynthesis using the probiotic strain *Bacillus subtilis* BSN313, where UV-Vis spectra after 24 hours of biosynthesis showed a transition point at 362 nm and a prominent absorption peak at 650 nm (Ullah et al., 2021). Biosynthesis of SeNPs using *Lactobacillus paracasei* HM1 also followed similar trends, with an absorption maximum of 300 nm within the extended 200-1000 nm range (El-Saadony et al., 2021).

Characterization of biosynthesized selenium nanoparticles

The sizes of the selenium nanoparticles were determined using a nanosizer. Our analysis showed that the majority of nanoparticles had a size of 225.6 nm, while only 2% were significantly smaller – 42.18 nm. Consequently, the average hydrodynamic diameter was 179.3 nm (Figure 4).

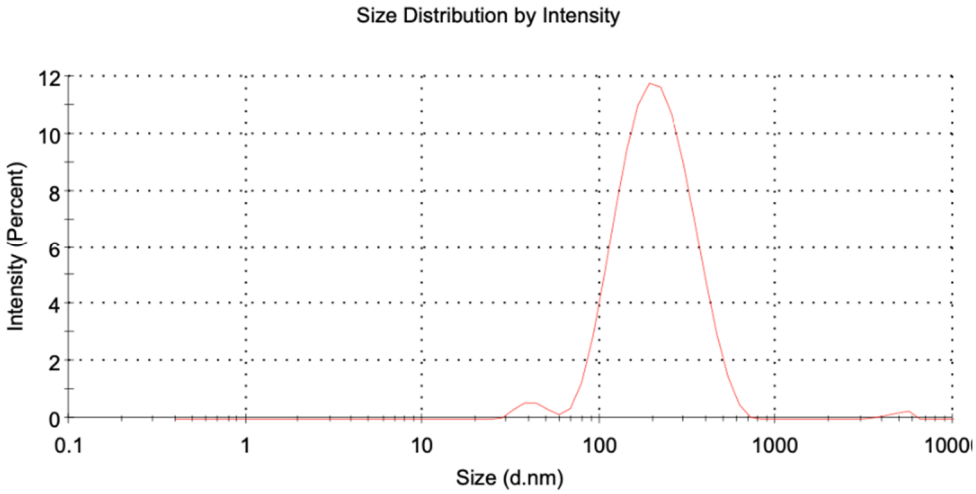

Figure 4. Sizes of biosynthesized selenium nanoparticles

This value considerably exceeds the typical dimensions obtained by electron microscopy techniques such as transmission (TEM) or scanning (SEM) electron microscopy, where nanoparticles are often in the tens of nanometers, depending on biosynthesis conditions. This discrepancy arises from the dynamic light scattering (DLS) method employed by the nanosizer, which measures not only the crystalline core of the nanoparticles but also the surrounding organic coating composed of biomolecules (e.g., proteins, lipids, polysaccharides). This organic coating influences the hydrodynamic radius of nanoparticles in solution, increasing their apparent size. Therefore, the larger nanoparticle sizes obtained through DLS, compared to those measured by electron microscopy, should be considered a positive indicator, as the presence of the organic shell is key to colloidal stability, bioavailability, and biological activity of SeNPs (Hashem et al., 2023). This has been corroborated by multiple studies. For instance, Fath-Alla et al. (2024) reported that the sizes of spherical SeNPs synthesized using *Saccharomyces cerevisiae* ranged from 34 to 125 nm as measured by TEM, whereas the average size determined by nanosizer was 173.9 nm (Table 4).

Overall, SeNP sizes vary widely depending on the biosynthesis method and conditions (Table 4). For example, during SeNP biosynthesis using Saccharomyces cerevisiae, nanoparticle sizes ranged from 75 to 709 nm (Faramarzi et al., 2020). SeNPs biosynthesized by Bacillus subtilis exhibited an average diameter of 530 nm (Ullah et al., 2021). Much smaller nanoparticles were obtained using Lactobacillus acidophilus, 34.13 nm (Alam et al., 2020) and Monascus purpureus, 46.58 nm (El-Sayed et al., 2020).

The zeta potential of the biosynthesized SeNPs, which was -16.2 mV (Figure 5), indicating satisfactory stability and dispersion of the nanoparticles in suspension.

Table 4

Sizes of selenium nanoparticles biosynthesized using microorganisms

Microorganism	Average Size, nm (Z-average)	Reference
Candida pseudojiufengensis	14	Ali et al., 2024
Saccharomyces cerevisiae	173.9	Fath-Alla et al., 2024
Bacillus subtilis BSN313	530	Ullah et al., 2021
Penicillium corylophilum	72	Salem et al.,2021
Penicillium verhagenii	91.2	Nassar et al., 2023
Aspergillus Flavus	49.72	Mohammed et al., 2024
Eurotium cristatum	231.7	Li et al., 2024
Trichoderma sp.	211.4	Arunthirumeni et al., 2022
Fusarium semitectum	92.33 ± 48.5	Abbas and Abou Baker, 2020
Yarrowia lipolytica ATCC 18942	110	Lashani et al., 2024
Saccharomyces cerevisiae M437	179.3	Own research

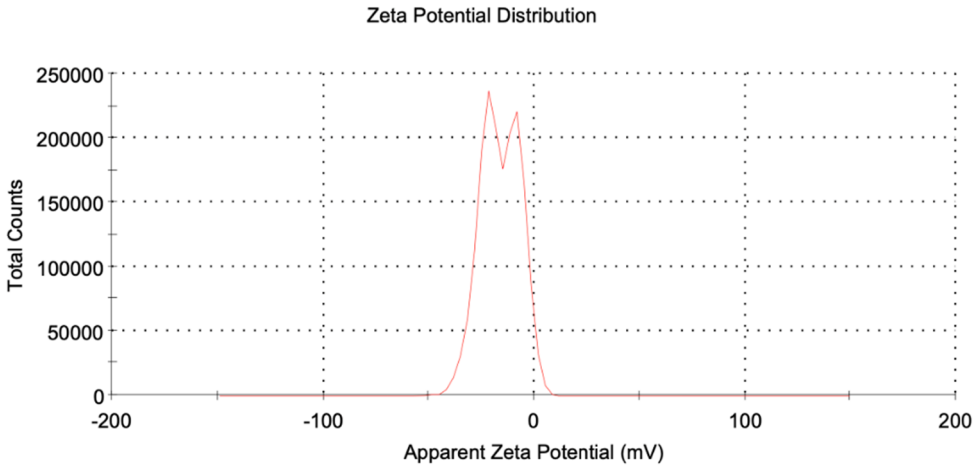

Figure 5. Zeta potential of biosynthesized selenium nanoparticles

Zeta potential is a key parameter for evaluating colloidal stability, with values varying across studies. The zeta potential of SeNPs biosynthesized by Saccharomyces cerevisiae ranged from -7.06 to -10.3 mV (Faramarzi et al., 2020), whereas SeNPs produced using Bacillus subtilis exhibited a more negative value of -26.9 mV (Ullah et al., 2021). In contrast, SeNPs biosynthesized by Lactobacillus acidophilus showed a positive zeta potential of +37.86 mV (Alam et al., 2020), while those obtained using *Monascus purpureus* had a zeta potential of –24.01 mV (El-Sayed et al., 2020).

The polydispersity index (PDI) of the SeNPs solution was 0.229, indicating high polydispersity, a low tendency toward agglomeration, and a relatively narrow range of nanoparticle sizes. PDI reflects nanoparticle size homogeneity and distribution variance. For SeNPs biosynthesized using *Saccharomyces cerevisiae*, the PDI values ranged from 0.189 to

0.989 (Faramarzi et al., 2020), for those biosynthesized with *Bacillus subtilis*, the PDI was 0.282 (Ullah et al., 2021). The PDI of SeNPs obtained using *Lactobacillus acidophilus* was 0.285 (Alam et al., 2020), and using *Monascus purpureus*, it was 0.205 (El-Sayed et al., 2020). The higher the polydispersity index (PDI), the less uniform the nanoparticle size distribution in the solution. Conversely, a lower PDI value indicates a more uniform nanoparticle size distribution and a reduced tendency for agglomeration in the sample (Skóra et al., 2021).

Zeta potential and PDI values from various studies are summarized in Table 5.

Table 5

Zeta potential and polydispersity index of selenium nanoparticles biosynthesized using microorganisms

Microorganism	Zeta potential, mV	PDI	Reference
Lactobacillus acidophilus	+37.86	0.285	Alam et al., 2020
Candida pseudojiufengensis	+34	0.15	Ali et al., 2024
Eurotium cristatum	-15.5	0.277	Li et al., 2025
Saccharomyces cerevisiae	-22.4	0.503	Fath-Alla et al., 2024
Monascus purpureus	-24.01	0.205	El-Sayed et al., 2020
Bacillus subtilis BSN313	-26.9	0.282	Ullah et al., 2021
Penicillium verhagenii	-32	-	Nassar et al., 2023
Trichoderma sp.	-	0.287	Arunthirumeni et al., 2022
Yarrowia lipolytica ATCC 18942	-34.51	1	Lashani et al., 2024
Saccharomyces cerevisiae M437	-16.2	0.229	Own research

Mechanisms of intracellular selenium nanoparticles biosynthesis

The intracellular biosynthesis of SeNPs biosynthesis is a complex process based on microbial mechanisms that reduce selenite to elemental selenium, resulting in nanoparticle formation. Key enzymes involved in selenite reduction include sulfite reductase and thioredoxin reductase, which utilize electron donors such as NADPH or NADH to catalyze the reduction reaction (Wang et al., 2018). In *Bacillus mycoides*, thiol compounds like glutathione and N-acetyl-L-cysteine participate in selenite reduction. Other metabolites, such as 4-hydroxybenzoate and indole-3-acetic acid, are produced by *Bacillus mycoides* in response to stress and contribute to SeNPs biosynthesis (Baggio et al., 2021). In *Stenotrophomonas maltophilia*, a homolog of alcohol dehydrogenase is involved in the biosynthesis of SeNPs (Lampis et al., 2017). In *Pichia pastoris*, selenite reduction is mediated by NADH-dependent cytochrome b5 reductase (Elahian et al., 2017).

Thus, various biomolecules are involved in the intracellular biosynthesis of selenium nanoparticles. The localization of SeNPs also varies. In most cases, they are initially formed intracellularly and may later be released into the extracellular medium. For example, the biosynthesis of SeNPs using *Stenotrophomonas maltophilia* involves intracellular formation followed by their release into the extracellular medium (Lampis et al., 2017). When *Rhodococcus aetherivorans* was used for SeNP biosynthesis, the resulting nanoparticles were surrounded by an organic shell that enhanced their stability and prevented aggregation (Presentato et al., 2018). Additionally, in *Shewanella oneidensis*, modulation of the

extracellular electron transfer (EET) pathway has been demonstrated through genetic alteration of the CymA gene, which encodes a key component of the electron transport chain. Such modifications influence the localization, composition, and size of the synthesized nanoparticles (Tian et al., 2017).

In summary, intracellular biosynthesis of selenium nanoparticles is a complex and multifactorial process dependent on the specific enzymatic systems of microorganisms. Understanding these mechanisms is crucial for the further development of biotechnological approaches for the synthesis of SeNPs with tunable properties for medical, environmental, and industrial applications.

Conclusions

Selenium nanoparticles exhibit considerable potential for applications in the food industry. Their pronounced antimicrobial properties enable effective suppression of a wide range of foodborne pathogens, making them particularly promising for use in active food packaging systems aimed at extending product shelf life. Among the various approaches to SeNP synthesis, biosynthesis using microorganisms such as bacteria, fungi, or yeast is regarded as one of the most efficient methods. Yeast of the genus *Saccharomyces* is of particular interest due to its ease of cultivation, safety profile, and lack of strict biosafety requirements. In this study, *Saccharomyces cerevisiae* M437 was identified as a promising candidate for the intracellular biosynthesis of selenium nanoparticles.

The study confirmed the ability of strain M437 to synthesize SeNPs intracellularly. Light microscopy revealed the presence of inclusions both inside and outside the yeast cells, indicating nanoparticle formation followed by extracellular release. The release of SeNPs into the culture medium was observed between days 5 and 7 of cultivation, facilitating subsequent recovery and purification. UV-Vis spectroscopy analysis revealed a distinct absorption peak at 252 nm, characteristic of SeNPs and likely associated with surface plasmon resonance. DLS analysis indicated a mean hydrodynamic diameter of 179.3 nm, encompassing both the nanoparticle core and the surrounding organic capping layer. This organic shell plays a key role in maintaining colloidal stability, enhancing bioavailability, and contributing to the biological activity of SeNPs. A measured zeta potential of –16.2 mV suggests the stability of the nanoparticles in suspension. A polydispersity index of 0.229 reflects a high degree of uniformity in the nanoparticle suspension.

Despite the promising properties of *Saccharomyces cerevisiae* in SeNP biosynthesis, research in this area remains limited. Nevertheless, the results obtained in this study demonstrate that *Saccharomyces cerevisiae* M437 is capable of producing biogenic SeNPs with characteristics suitable for future applications in food-related technologies.

References

Abbas H., Abou Baker D. (2020), Biological evaluation of selenium nanoparticles biosynthesized by *Fusarium semitectum* as antimicrobial and anticancer agents, *Egyptian Journal of Chemistry*, 63(4), pp. 1119-1133. https://doi.org/10.21608/ejchem.2019.15618.1945

Abdel-Moneim A.M.E., El-Saadony M.T., Shehata A.M., Saad A.M., Aldhumri S.A., Ouda S.M., Mesalam N.M. (2022), Antioxidant and antimicrobial activities of *Spirulina platensis* extracts and biogenic selenium nanoparticles against selected pathogenic

bacteria and fungi, *Saudi Journal of Biological Sciences*, 29(2), pp. 1197-1209. https://doi.org/10.1016/j.sjbs.2021.09.046

Afzal B., Yasin D., Naaz H., Sami N., Zaki A., Rizvi M.A., Kumar R., Srivastava P., Fatma T. (2021), Biomedical potential of *Anabaena variabilis* NCCU-441 based selenium nanoparticles and their comparison with commercial nanoparticles, *Scientific Reports*, 11(1), 13507. https://doi.org/10.1038/s41598-021-91738-7

Alam H., Khatoon N., Khan M.A., Husain S.A., Saravanan M., Sardar M. (2020), Synthesis of selenium nanoparticles using probiotic bacteria *Lactobacillus acidophilus* and their enhanced antimicrobial activity against resistant bacteria, *Journal of Cluster Science*, 31, pp. 1003-1011. https://doi.org/10.1007/s10876-019-01705-6

Ali B.A., Allam R.M., Hasanin M.S., Hassabo A.A. (2024), Biosynthesis of selenium nanoparticles as a potential therapeutic agent in breast cancer: G2/M arrest and apoptosis induction, *Toxicology Reports*, 13, 101792. https://doi.org/10.1016/j.toxrep.2024.101792

Ao B., Du Q., Liu D., Shi,X., Tu J., Xia X. (2023), A review on synthesis and antibacterial potential of bio-selenium nanoparticles in the food industry, *Frontiers in Microbiology*, 14, 1229838. https://doi.org/10.3389/fmicb.2023.1229838

Arunthirumeni M., Veerammal V., Shivakumar M.S. (2022), Biocontrol efficacy of mycosynthesized selenium nanoparticle using *Trichoderma* sp. on insect pest *Spodoptera litura*, *Journal of Cluster Science*, 33(4), pp. 1645-1653. https://doi.org/10.1007/s10876-021-02095-4

Baggio G., Groves R.A., Chignola R., Piacenza E., Presentato A., Lewis I.A., Lampis S., Vallini G., Turner R.J. (2021), Untargeted metabolomics investigation on selenite reduction to elemental selenium by *Bacillus mycoides* SeITE01, *Frontiers in Microbiology*, 12, 711000. https://doi.org/10.3389/fmicb.2021.711000

Bafghi M.H., Zarrinfar H., Darroudi M., Zargar M., Nazari R. (2022), Green synthesis of selenium nanoparticles and evaluate their effect on the expression of ERG3, ERG11 and FKS1 antifungal resistance genes in Candida albicans and Candida glabrata, *Letters in Applied Microbiology*, 74(5), pp. 809-819. https://doi.org/10.1111/lam.13667

Chandramohan S., Sundar K., Muthukumaran A. (2018), Monodispersed spherical shaped selenium nanoparticles (SeNPs) synthesized by *Bacillus subtilis* and its toxicity evaluation in zebrafish embryos, *Materials Research Express*, 5(2), 025020. https://doi.org/10.1088/2053-1591/aaabeb

Dutta N., Ray S. (2024), An overview on bioinspired selenium nanoparticles synthesis using various natural sources with its mechanism of action, *Journal of Agriculture and Educafion Research*, 2(3), pp. 1-6.

El-deeb B.A., Asem E., Mohammed K. (2023), Biosynthesis and optimization of selenium nanoparticles using *Streptomyces* sp., *Sohag Journal of Sciences*, 8(1), pp. 1-6. https://doi.org/10.21608/sjsci.2022.164668.1034

El-Saadony M.T., Saad A.M., Taha T.F., Najjar A.A., Zabermawi N.M., Nader M.M., AbuQamar S.F., El-Tarabily K.A., Salama A. (2021), Selenium nanoparticles from *Lactobacillus paracasei* HM1 capable of antagonizing animal pathogenic fungi as a new source from human breast milk, *Saudi Journal of Biological Sciences*, 28(12), pp. 6782-6794. https://doi.org/10.1016/j.sjbs.2021.07.059

El-Sayed E.S.R., Abdelhakim H.K., Ahmed A.S. (2020), Solid-state fermentation for enhanced production of selenium nanoparticles by gamma-irradiated *Monascus purpureus* and their biological evaluation and photocatalytic activities, *Bioprocess and Biosystems Engineering*, 43, pp. 797-809. https://doi.org/10.1007/s00449-019-02275-7

Elahian F., Reiisi S., Shahidi A., Mirzaei S.A. (2017), High-throughput bioaccumulation, biotransformation, and production of silver and selenium nanoparticles using genetically

engineered *Pichia pastoris*, *Nanomedicine: Nanotechnology*, *Biology and Medicine*, 13(3), pp. 853-861. https://doi.org/10.1016/j.nano.2016.10.009

Faramarzi S., Anzabi Y., Jafarizadeh-Malmiri H. (2020), Nanobiotechnology approach in intracellular selenium nanoparticle synthesis using *Saccharomyces cerevisiae* – fabrication and characterization, *Archives of Microbiology*, 202(5), pp. 1203-1209. https://doi.org/10.1007/s00203-020-01831-0

Fath-Alla A.A., Khalil N.M., Mohamed A.S., El-Ghany A., Mohamed N. (2024), Antiradical and anti-inflammatory activity of *Saccharomyces cerevisiae*-mediated selenium nanoparticles, *Egyptian Journal of Botany*, 64(2), pp. 773-787. https://doi.org/10.21608/ejbo.2024.267306.2692

Fernández-Llamosas H., Castro L., Blázquez M.L., Díaz E., Carmona M. (2017), Speeding up bioproduction of selenium nanoparticles by using *Vibrio natriegens* as microbial factory, *Scientific Reports*, 7(1), 16046. https://doi.org/10.1038/s41598-017-16252-1

Ghazi S., Diab A.M., Khalafalla M.M., Mohamed R.A. (2021), Synergistic effects of selenium and zinc oxide nanoparticles on growth performance, hemato-biochemical profile, immune and oxidative stress responses, and intestinal morphometry of Nile tilapia (*Oreochromis niloticus*), *Biological Trace Element Research*, 200, pp. 364–374. https://doi.org/10.1007/s12011-021-02631-3

Goud K.G., Veldurthi N.K., Vithal M., Reddy G. (2016), Characterization and evaluation of biological and photocatalytic activities of selenium nanoparticles synthesized using yeast fermented broth, *Journal of Materials NanoScience*, 3(2), pp. 33-40. https://pubs.thesciencein.org/journal/index.php/jmns/article/view/203

Grasso G., Zane D., Dragone R. (2020), Microbial nanotechnology: challenges and prospects for green biocatalytic synthesis of nanoscale materials for sensoristic and biomedical applications, *Nanomaterials (Basel)*, 10, 11. https://doi.org/10.3390/nano10010011

Gregirchak N., Sinyavskaya D., Khonkiv M., Stabnikov V. (2023), Lactic acid bacteria for the synthesis of metals nanoparticles, *Ukrainian Food Journal*, 12(4), pp. 599-626. https://doi.org/10.24263/2304-974X-2023-12-4-8

Hamza F., Vaidya A., Apte M., Kumar A.R., Zinjarde S. (2017), Selenium nanoparticle-enriched biomass of *Yarrowia lipolytica* enhances growth and survival of *Artemia salina*, *Enzyme and Microbial Technology*, 106, pp. 48-54. https://doi.org/10.1016/j.enzmictec.2017.07.002

Hariharan H., Al-Harbi N., Karuppiah P., Rajaram S. (2012), Microbial synthesis of selenium nanocomposite using *Saccharomyces cerevisiae* and its antimicrobial activity against pathogens causing nosocomial infection, *Chalcogenide Letters*, 9(12), pp. 509-515.

Hashem A.H., El-Sayyad G.S., Al-Askar A.A., Marey S.A., AbdElgawad H., Abd-Elsalam K.A., Saied E. (2023), Watermelon rind mediated biosynthesis of bimetallic selenium-silver nanoparticles: characterization, antimicrobial and anticancer activities, *Plants*, 12(18), 3288. https://doi.org/10.3390/plants12183288

Hu D., Yu S., Yu D., Liu N., Tang Y., Fan Y., Wang C., Wu A. (2019), Biogenic *Trichoderma harzianum*-derived selenium nanoparticles with control functionalities originating from diverse recognition metabolites against phytopathogens and mycotoxins, *Food Control*, 106, 106748. https://doi.org/10.1016/j.foodcont.2019.106748

Huang T., Holden J.A., Reynolds E.C., Heath D.E., O'Brien-Simpson N.M., O'Connor A.J. (2020), Multifunctional antimicrobial polypeptide-selenium nanoparticles combat drug-resistant bacteria, *ACS Applied Materials & Interfaces*, 12(50), pp. 55696-55709. https://doi.org/10.1021/acsami.0c17550

Hussein H.G., El-Sayed E.S.R., Younis N.A., Hamdy A.E.H.A., Easa S.M. (2022), Harnessing endophytic fungi for biosynthesis of selenium nanoparticles and exploring their bioactivities, *AMB Express*, 12(1), 68. https://doi.org/10.1186/s13568-022-01408-8

Ibrahim M.S., El-gendy G.M., Ahmed A.I., Elharoun E.R., Hassaan M.S. (2021), Nanoselenium versus bulk selenium as a dietary supplement: Effects on growth, feed efficiency, intestinal histology, haemato-biochemical and oxidative stress biomarkers in Nile tilapia (*Oreochromis niloticus* Linnaeus, 1758) fingerlings, *Aquaculture Research*, 52(11), pp. 5642-5655. https://doi.org/10.1111/are.15439

Jahanbakhshi A., Pourmozaffar S., Adeshina I., Mahmoudi R., Erfanifar E., Ajdari, A. (2021), Selenium nanoparticle and selenomethionine as feed additives: Effects on growth performance, hepatic enzymes' activity, mucosal immune parameters, liver histology, and appetite-related gene transcript in goldfish (*Carassius auratus*), *Fish Physiology and Biochemistry*, 47, pp. 639-652. https://doi.org/10.1007/s10695-021-00937-6

Jamróz E., Kopel P., Juszczak L., Kawecka A., Bytesnikova Z., Milosavljevic V., Makarewicz M. (2019a), Development of furcellaran-gelatin films with Se-AgNPs as an active packaging system for extension of mini kiwi shelf life, *Food Packaging and Shelf Life*, 21, 100339. https://doi.org/10.1016/j.fpsl.2019.100339

Jamróz E., Kulawik P., Kopel P., Balková R., Hynek D., Bytesnikova Z., Gagic M., Milosavljevic V., Adam V. (2019b), Intelligent and active composite films based on furcellaran: Structural characterization, antioxidant and antimicrobial activities, *Food Packaging and Shelf Life*, 22, 100405. https://doi.org/10.1016/j.fpsl.2019.100405

Kieliszek M., Bierla K., Jiménez-Lamana J., Kot A.M., Alcántara-Durán J., Piwowarek K., Błażejak S., Szpunar J. (2020), Metabolic response of the yeast *Candida utilis* during enrichment in selenium, *International Journal of Molecular Sciences*, 21(15), 5287. https://doi.org/10.3390/ijms21155287

Kumar R. (2021), Microscopy, working and types, *Asian Journal of Pharmacy and Technology*, 11(3), pp. 245-248. https://doi.org/10.52711/2231-5713.2021.00040

Lampis S., Zonaro E., Bertolini C., Cecconi D., Monti F., Micaroni M., Turner R.J., Butler C.S., Vallini G. (2017), Selenite biotransformation and detoxification by *Stenotrophomonas maltophilia* SeITE02: Novel clues on the route to bacterial biogenesis of selenium nanoparticles, *Journal of Hazardous Materials*, 324, pp. 3-14. https://doi.org/10.1016/j.jhazmat.2016.02.035

Lashani E., Moghimi H., Turner R.J., Amoozegar M.A. (2024), Characterization and biological activity of selenium nanoparticles biosynthesized by *Yarrowia lipolytica*, *Microbial Biotechnology*, 17(10), e70013. https://doi.org/10.1111/1751-7915.70013

Li N., Yang Y., Qi J., Li J., Cheng Y., Li Z., Yue T., Yuan Y. (2025), Selenium nanoparticles biosynthesized by *Eurotium cristatum* with antimicrobial activity, *Food Science and Human Wellness*, 14(7), 9250158. https://doi.org/10.26599/FSHW.2024.9250158

Lian S., Diko C.S., Yan Y., Li Z., Zhang H., Ma Q., Qu Y. (2019), Characterization of biogenic selenium nanoparticles derived from cell-free extracts of a novel yeast *Magnusiomyces ingens*, *3 Biotech*, 9, 221. https://doi.org/10.1007/s13205-019-1748-y

Malyugina S., Skalickova S., Skladanka J., Slama P., Horky P. (2021), Biogenic selenium nanoparticles in animal nutrition: a review, *Agriculture*, 11(12), 1244. https://doi.org/10.3390/agriculture11121244

Mohammed E.J., Abdelaziz A.E., Mekky A.E., Mahmoud N.N., Sharaf M., Al-Habibi M.M., Khairy N.M., Al-Askar A.A., Youssef F.S., Gaber M.A., Saied E., AbdElgayed G., Metwally S.A., Shoun A.A. (2024), Biomedical promise of *Aspergillus flavus*-biosynthesized selenium nanoparticles: A green synthesis approach to antiviral, anticancer, anti-biofilm, and antibacterial applications, *Pharmaceuticals*, 17(7), 915. https://doi.org/10.3390/ph17070915

Nabi F., Arain M.A., Hassan F., Umar M., Rajput N., Alagawany M., Syed S.F., Soomro J., Somroo F., Liu J. (2020), Nutraceutical role of selenium nanoparticles in poultry nutrition: A review, *World's Poultry Science Journal*, 76(3), pp. 459-471. https://doi.org/10.1080/00439339.2020.1789535

Nassar A.R.A., Eid A.M., Atta H.M., El Naghy W.S., Fouda A. (2023), Exploring the antimicrobial, antioxidant, anticancer, biocompatibility, and larvicidal activities of selenium nanoparticles fabricated by endophytic fungal strain *Penicillium verhagenii*. *Scientific Reports*, 13(1), 9054. https://doi.org/10.1038/s41598-023-35360-9

Ndwandwe B.K., Malinga S.P., Kayitesi E., Dlamini B.C. (2021), Advances in green synthesis of selenium nanoparticles and their application in food packaging, *International Journal of Food Science and Technology*, 56(6), pp. 2640-2650. https://doi.org/10.1111/ijfs.14916

Nie X., Yang X., He J., Liu P., Shi H., Wang T., Zhang D. (2023), Bioconversion of inorganic selenium to less toxic selenium forms by microbes: A review, *Frontiers in Bioengineering and Biotechnology*, 11, 1167123. https://doi.org/10.3389/fbioe.2023.1167123

Nile S.H., Thombre D., Shelar A., Gosavi K., Sangshetti J., Zhang W., Sieniawska E., Patil R., Kai G. (2023), Antifungal properties of biogenic selenium nanoparticles functionalized with nystatin for the inhibition of *Candida albicans* biofilm formation, *Molecules*, 28(4), 1836. https://doi.org/10.3390/molecules28041836

Nwoko K.C., Liang X., Perez M.A., Krupp E., Gadd G.M., Feldmann J. (2021), Characterisation of selenium and tellurium nanoparticles produced by *Aureobasidium pullulans* using a multi-method approach, *Journal of Chromatography A*, 1642, 462022. https://doi.org/10.1016/j.chroma.2021.462022

Pereira A.G., Gerolis L.G.L., Gonçalves L.S., Pedrosa T.A., Neves M.J. (2018), Selenized *Saccharomyces cerevisiae* cells are a green dispenser of nanoparticles, *Biomedical Physics & Engineering Express*, 4(3), 035028. https://doi.org/10.1088/2057-1976/aab524

Presentato A., Piacenza E., Anikovskiy M., Cappelletti M., Zannoni D., Turner R.J. (2018), Biosynthesis of selenium-nanoparticles and-nanorods as a product of selenite bioconversion by the aerobic bacterium *Rhodococcus aetherivorans* BCP1, *New Biotechnology*, 41, pp. 1-8. https://doi.org/10.1016/j.nbt.2017.11.002

Ramya S., Shanmugasundaram T., Balagurunathan R. (2020), Actinobacterial enzyme mediated synthesis of selenium nanoparticles for antibacterial, mosquito larvicidal and anthelminthic applications, *Particulate Science and Technology*, 38(1), pp. 63-72. https://doi.org/10.1080/02726351.2018.1508098

Rasouli M. (2019), Biosynthesis of selenium nanoparticles using yeast *Nematospora coryli* and examination of their anti-candida and anti-oxidant activities, *IET Nanobiotechnology*, 13(2), pp. 214-218. https://doi.org/10.1049/iet-nbt.2018.5187

Saied E., Mekky A.E., Al-Askar A.A., Hagag A.F., El-bana, A.A., Ashraf M., Walid A., Nour T., Fawzi M.M., Arishi A.A., Hashem A.H. (2023), *Aspergillus terreus*-mediated selenium nanoparticles and their antimicrobial and photocatalytic activities, *Crystals*, 13(3), 450. https://doi.org/10.3390/cryst13030450

Sajnóg A., Bierła K., Szpunar J., Jiménez-Lamana J. (2023), Critical evaluation of sample preparation for SP-ICP-MS determination of selenium nanoparticles in microorganisms – focus on yeast, *Journal of Analytical Atomic Spectrometry*, 38(11), pp. 2448-2457. https://doi.org/10.1039/D3JA00181D

Salem S.S., Fouda M.M., Fouda A., Awad M.A., Al-Olayan E.M., Allam A.A., Shaheen T.I. (2021), Antibacterial, cytotoxicity and larvicidal activity of green synthesized selenium nanoparticles using *Penicillium corylophilum*, *Journal of Cluster Science*, 32, pp. 351-361. https://doi.org/10.1007/s10876-020-01794-8

Shoeibi S., Mashreghi M. (2017), Biosynthesis of selenium nanoparticles using *Enterococcus faecalis* and evaluation of their antibacterial activities, *Journal of Trace Elements in Medicine and Biology*, 39, pp. 135-139. https://doi.org/10.1016/j.jtemb.2016.09.003

Skóra B., Krajewska U., Nowak A., Dziedzic A., Barylyak A., Kus-Liśkiewicz M. (2021), Noncytotoxic silver nanoparticles as a new antimicrobial strategy, *Scientific Reports*, 11(1), 13451. https://doi.org/10.1038/s41598-021-92812-w

Song X., Qiao L., Yan S., Chen Y., Dou X., Xu C. (2021), Preparation, characterization, and in vivo evaluation of anti-inflammatory activities of selenium nanoparticles synthesized by *Kluyveromyces lactis* GG799, *Food & Function*, 12(14), pp. 6403-6415. https://doi.org/10.1039/D1FO01019K

Stabnikova O., Khonkiv M., Kovshar I., Stabnikov V. (2023), Biosynthesis of selenium nanoparticles by lactic acid bacteria and areas of their possible applications, *World Journal of Microbiology and Biotechnology*, 39, 230. https://doi.org/10.1007/s11274-023-03673-6

Tan L.C., Nancharaiah Y.V., van Hullebusch E.D., Lens P.N. (2018), Selenium: Environmental significance, pollution, and biological treatment technologies, *Anaerobic treatment of mine wastewater for the removal of selenate and its co-contaminants*, pp. 9-71. https://doi.org/10.1201/9780429448676-2

Tian L.J., Li W.W., Zhu T.T., Chen J.J., Wang W.K., An P.F., Zhang L., Dong J.C., Guan Y., Liu D.F., Zhou N.Q., Liu G., Tian Y.C., Yu H.Q. (2017), Directed biofabrication of nanoparticles through regulating extracellular electron transfer, *Journal of the American Chemical Society*, 139(35), pp. 12149-12152. https://doi.org/10.1021/jacs.7b07460

Ullah A., Yin X., Wang F., Xu B., Mirani Z.A., Xu B., Chan M.W.H., Ali A., Usman M., Ali N., Naveed M. (2021), Biosynthesis of selenium nanoparticles (*via Bacillus subtilis* BSN313), and their isolation, characterization, and bioactivities, *Molecules*, 26(18), 5559. https://doi.org/10.3390/molecules26185559

Vera P., Canellas E., Nerín C. (2018), New antioxidant multilayer packaging with nanoselenium to enhance the shelf-life of market food products, *Nanomaterials*, 8(10), 837. https://doi.org/10.3390/nano8100837

Vinu D., Govindaraju K., Vasantharaja R., Amreen Nisa S., Kannan M., Vijai Anand K. (2021), Biogenic zinc oxide, copper oxide and selenium nanoparticles: preparation, characterization and their anti-bacterial activity against *Vibrio parahaemolyticus*, *Journal of Nanostructure in Chemistry*, 11, pp. 271-286. https://doi.org/10.1007/s40097-020-00365-7

Wadhwani S.A., Gorain M., Banerjee P., Shedbalkar U.U., Singh R., Kundu G. C., Chopade B.A. (2017), Green synthesis of selenium nanoparticles using *Acinetobacter* sp. SW30: Optimization, characterization and its anticancer activity in breast cancer cells, *International Journal of Nanomedicine*, 12, pp. 6841-6855. https://doi.org/10.2147/IJN.S139212

Wang Y., Shu X., Zhou Q., Fan T., Wang T., Chen X., Li M., Ma Y., Ni J., Hou J., Zhao W., Li R., Huang S., Wu L. (2018), Selenite reduction and the biogenesis of selenium nanoparticles by *Alcaligenes faecalis* Se03 isolated from the gut of *Monochamus alternatus* (Coleoptera: Cerambycidae), *International Journal of Molecular Sciences*, 19(9), 2799. https://doi.org/10.3390/ijms19092799

Wu Z., Ren Y., Liang Y., Huang L., Yang Y., Zafar A., Hasan M., Yang F., Shu X. (2021), Synthesis, characterization, immune regulation, and antioxidative assessment of yeast-derived selenium nanoparticles in cyclophosphamide-induced rats, *ACS Omega*, 6(38), pp. 24585-24594. https://doi.org/10.1021/acsomega.1c03205

Zhang H., Li Z., Dai C., Wang P., Fan S., Yu B., Qu Y. (2021), Antibacterial properties and mechanism of selenium nanoparticles synthesized by *Providencia* sp. DCX, *Environmental Research*, 194, 110630. https://doi.org/10.1016/j.envres.2020.110630

Zhang J., Wang Y., Shao Z., Li J., Zan S., Zhou S., Yang R. (2019), Two selenium tolerant *Lysinibacillus* sp. strains are capable of reducing selenite to elemental Se efficiently

under aerobic conditions. *Journal of Environmental Sciences*, 77, pp. 238-249. https://doi.org/10.1016/j.jes.2018.08.002

Zhang L., Li D., Gao P. (2012), Expulsion of selenium/protein nanoparticles through vesicle-like structures by *Saccharomyces cerevisiae* under microaerophilic environment, *World Journal of Microbiology and Biotechnology*, 28, pp. 3381-3386. https://doi.org/10.1007/s11274-012-1150-y

Zhang T., Qi M., Wu Q., Xiang P., Tang D., Li Q. (2023), Recent research progress on the synthesis and biological effects of selenium nanoparticles, *Frontiers in Nutrition*, 10, 1183487. https://doi.org/10.3389/fnut.2023.1183487

Zhang T., Yao C., Hu Z., Li D., Tang R. (2022). Protective effect of selenium on the oxidative damage of kidney cells induced by sodium nitrite in grass carp (*Ctenopharyngodon idellus*), *Biological Trace Element Research*, 200, pp. 3876–3884. https://doi.org/10.1007/s12011-021-02982-x

Cite:

UFJ Style

Skrotska O., Protsenko M., Zholobko M., Marynin M. (2025), Biosynthesis and characterization of selenium nanoparticles by Saccharomyces cerevisiae M437, *Ukrainian Journal of Food Science*, 13(1), pp. 91–110, https://doi.org/10.24263/2310-1008-2025-13-1-10

APA Style

Skrotska, O., Protsenko, M., Zholobko, M., & Marynin, M. (2025). Biosynthesis and characterization of selenium nanoparticles by Saccharomyces cerevisiae M437. *Ukrainian Journal of Food Science, 13*(1), 91–110. https://doi.org/10.24263/2310-1008-2025-13-1-10

Instructions for Authors

Dear colleagues!

The Editorial Board of scientific periodical «**Ukrainian Journal of Food Science**» invites you to publish of your scientific research.

A manuscript should describe the research work that has not been published before and is not under consideration for publication anywhere else. Submission of the manuscript implies that its publication has been approved by all co-authors as well as by the responsible authorities at the institute where the work has been carried out.

It is mandatory to include a covering letter to the editor which includes short information about the subject of the research, its novelty and significance; state that all the authors agree to submit this paper to Ukrainian Journal of Food Science; that it is the original work of the authors.

Manuscript requirements

Authors must prepare the manuscript according to the instructions for authors. Editors reserve the right to adjust the style to certain standards of uniformity.

Title page, references, tables and figures should be included in the manuscript body.

Language – English

Manuscripts should be submitted in as a Word document.

Use 1.0 spacing and 2 cm margins.

Use a normal font 14-point Times New Roman for text, tables, and captions for figures.

Provide tables and figures in the text of the manuscript.

Consult a recent issue of the journal for a style check.

Number all pages consecutively.

Abbreviations should be defined on first appearance in text and used consistently thereafter. No abbreviation should be used in title and section headings.

Please submit math equations as editable text and not as images (It is recommended to use MathType or Microsoft Equation Editor software).

Minimal size of the research article (without Abstract and References) is 10 pages; for the review article minimal size is 25 pages (without Abstract and References).

Manuscript should include:

Title (should be concise and informative). Avoid abbreviations in it.

Authors' information: the name(s) of the author(s); the affiliation(s) of the author(s), city, country. One author has been designated as the corresponding author with e-mail address. If available, the 16-digit ORCID of the author(s).

Declaration of interest

Author contributions

Abstract. The **abstract** should contain the following mandatory parts:

Introduction provides an aim for the study (2-3 lines).

Materials and methods briefly describe the materials and methods used in the study (3-5 lines).

Results and discussion describe the main findings (23-26 lines).

Conclusion provides the main conclusions (2-3 lines).

The abstract should not contain any undefined abbreviations or references to the article.

Keywords. Immediately after the abstract provide 4 to 6 keywords.

Text of manuscript
References

Manuscripts should be divided into the following sections:

- **Introduction**
- **Materials and methods**
- **Results and Discussion**
- **Conclusions**
- **References**

Introduction. Provide background information without an extensive literature review, and clearly state the aim of the present research. Identify knowledge gaps and justify the relevance of the topic. The length should not exceed 1.5 pages.

Materials and methods. Provide sufficient detail to enable an independent researcher to replicate the study. For methods that are already published, cite the original references and provide only a brief summary. Full descriptions are required only for new techniques. Clearly describe any modifications made to existing methods.

Results and discussion. Results should be presented clearly and concisely, using tables and/or figures where appropriate. The significance of the findings should be discussed, including comparisons with existing literature.

Conclusions. The main conclusions should be drawn from results and be presented in a short Conclusions section.

Acknowledgments(if necessary). Acknowledgments of individuals, grants, or funding sources should be placed in a separate section. List the names of all persons who contributed to the research. Funding organizations should be named in full.

Divide your article into sections and into subsections if necessary. Any subsection should have a brief heading.

References

Please, check references carefully.

The list of references should include works that are cited in the text and that have been published or accepted for publication.

All references mentioned in the reference list are cited in the text, and vice versa.

Cite references in the text by name and year in parentheses. Some examples:

(Drobot, 2008); (Qi and Zhou, 2012); (Bolarinwa et al., 2019; Rabie et al., 2020; Sengev et al., 2013).

Reference list should be alphabetized by the last names of the first author of each work: for one author, by name of author, then chronologically; for two authors, by name of author,

then name of coauthor, then chronologically; for more than two authors, by name of first author, then chronologically.

If available, please include full DOI links in your reference list (e.g. “https://doi.org/abc”).

Reference style

Journal article

Please follow this style and order: author's surname, initial(s), year of publication (in brackets), paper title, *journal title (in italic)*, volume number (issue), first and last page numbers, e.g.:

Ivanov V., Shevchenko O., Marynin A., Stabnikov V., Gubenia O., Stabnikova O., Shevchenko A., Gavva O., Saliuk A. (2021), Trends and expected benefits of the breaking edge food technologies in 2021–2030, *Ukrainian Food Journal*, 10(1), pp. 7–36, https://doi.org/10.24263/2304-974X-2021-10-1-3

The names of all authors should be provided. Journal names should not be abbreviated.

Book

Deegan C. (2000), *Financial Accounting Theory*, McGraw-Hill Book Company, Sydney.

Book chapter in an edited book

Kochubei-Lytvynenko O., Bilyk O., Bondarenko Y., Stabnikov V. (2022), Whey proteins in bakery products, In: O. Paredes-López, O. Shevchenko, V. Stabnikov, V. Ivanov (Eds.), *Bioenhancement and Fortification of Foods for a Healthy Diet*, pp. 67-88, CRC Press, Boca Raton, https://doi.org/10.1201/9781003225287-5

Online document

Mendeley, J.A., Thomson, M., Coyne, R.P. (2017), *How and When to Reference*, Available at: https://www.howandwhentoreference.com

Conference paper

Arych M. (2018), Insurance's impact on food safety and food security, *Resource and Energy Saving Technologies of Production and Packing of Food Products as the Main Fundamentals of Their Competitiveness: Proceedings of the 7th International Specialized Scientific and Practical Conference, September 13, 2018,* NUFT, Kyiv, pp. 52–57.

Figures

All figures should be made in graphic editor using a font Arial.

The font size on the figures and the text of the article should be the same.

Black and white graphic with no shading should be used.

The figure elements (lines, grid, and text) should be presented in black (not gray) colour.

Figure parts should be denoted by lowercase letters (a, b, etc.).

All figures are to be numbered using Arabic numerals.

Figures should be cited in text in consecutive numerical order.

Place figure after its first mentioned in the text.

Figure captions begin with the term Figure in bold type, followed by the figure number, also in bold type.

Each figure should have a caption describing what the figure depicts in bold type.

Supply all figures and EXCEL format files with graphs additionally as separate files.

Photos are not advisable to be used.

If you include figures that have already been published elsewhere, you must obtain permission from the copyright owner(s).

Tables

Number tables consecutively in accordance with their appearance in the text.

Place footnotes to tables below the table body and indicate them with superscript lowercase letters.

Place table after its first mentioned in the text.

Ensure that the data presented in tables do not duplicate results described elsewhere in the article.

Suggesting / excluding reviewers

Authors are welcome to suggest reviewers and/or request the exclusion of certain individuals when they submit their manuscripts.

When suggesting reviewers, authors should make sure they are totally independent and not connected to the work in any way. When suggesting reviewers, the Corresponding Author must provide an institutional email address for each suggested reviewer. Please note that the Journal may not use the suggestions, but suggestions are appreciated and may help facilitate the peer review process.

Submission

Email for all submissions and other inquiries:

ukrfoodscience@meta.ua

Ukrainian Journal of Food Science публікує оригінальні наукові статті, короткі повідомлення, оглядові статті, новини та огляди літератури.

Тематика публікацій в **Ukrainian Journal of Food Science:**

Харчова інженерія
Харчова хімія
Мікробіологія
Властивості харчових продуктів
Якість та безпека харчових продуктів
Нанотехнології
Процеси та обладнання
Економіка і управління
Автоматизація процесів
Упаковка для харчових продуктів
Здоров'я

Періодичність журналу 2 номери на рік (червень, грудень).

Результати досліджень, представлені в журналі, повинні бути новими, мати зв'язок з харчовою наукою і представляти інтерес для міжнародного наукового співтовариства.

Ukrainian Journal of Food Science індексується наукометричними базами**:**

EBSCO (2013)
Google Scholar (2013)
Index Copernicus (2014)
Directory of Open Access scholarly Resources (ROAD) (2014)
CAS Source Index (CASSI) (2016)
FSTA (Food Science and Technology Abstracts) (2018)

Ukrainian Journal of Food Science включено у перелік наукових фахових видань України з технічних наук, в якому можуть публікуватися результати дисертаційних робіт на здобуття наукових ступенів доктора і кандидата наук (Наказ Міністерства освіти і науки України № 793 від 04.07.2014)

Рецензія рукопису статті. Наукові статті, представлені для публікації в «**Ukrainian Journal of Food Science**» проходять «подвійне сліпе рецензування» (рецензент не знає, чию статтю рецензує, і, відповідно, автор не знає рецензента) двома вченими, призначеними редакційною колегією: один є членом редколегії, інший – незалежний учений.

Авторське право. Автори статей гарантують, що робота не є порушенням будь-яких існуючих авторських прав, і відшкодовують видавцю порушення даної гарантії. Опубліковані матеріали є правовою власністю видавця «Ukrainian Journal of Food Science», якщо не узгоджено інше.

Політика академічної етики. Редакція «**Ukrainian Journal of Food Science**» користується правилами академічної етики, викладеними в праці Miguel Roig (2003, 2006) "Avoiding plagiarism, self-plagiarism, and other questionable writing practices. A guide to ethical writing". Редакція пропонує авторам, рецензентам і читачам дотримуватися вимог, викладених у цьому посібнику, щоб уникнути помилок в оформленні наукових праць.

Редакційна колегія

Шановні колеги!

Редакційна колегія наукового періодичного видання
«**Ukrainian Journal of Food Science**»
запрошує Вас до публікації результатів наукових досліджень.

Вимоги до оформлення статей

Мова статей – англійська.

Мінімальний обсяг статті – **10 сторінок** формату А4 (без врахування анотацій і списку літератури)**.**

Для всіх елементів статті шрифт – **Times New Roman**, кегль – **14**, інтервал – 1.

Всі поля сторінки – по 2 см.

Структура статті:

1. **Назва статті.**
2. Автори статті (ім'я та прізвище повністю, приклад: Денис Озерянко).
3. *Установа, в якій виконана робота.*
4. Анотація. **Обов'язкова** структура анотації:
   - Вступ (2–3 рядки).
   - Матеріали та методи (до 5 рядків)
   - Результати та обговорення (пів сторінки).
   - Висновки (2–3 рядки).
5. Ключові слова (3–5 слів, але не словосполучень).

Пункти 2–6 виконати англійською і українською мовами.

6. Основний текст статті. Має включати такі обов'язкові розділи:
   - Вступ
   - Матеріали та методи
   - Результати та обговорення
   - Висновки
   - Література.

За необхідності можна додавати інші розділи та розбивати їх на підрозділи.

7. Авторська довідка (Прізвище, ім'я та по батькові, вчений ступінь та звання, місце роботи, електронна адреса або телефон).
8. Контактні дані автора, до якого за необхідності буде звертатись редакція журналу.

Рисунки виконуються якісно. Скановані рисунки не приймаються. Розмір тексту на рисунках повинен бути **співрозмірним** (!) тексту статті. **Фотографії можна використовувати лише за їх значної наукової цінності.**

Фон графіків, діаграм – лише білий. Колір елементів рисунку (лінії, сітка, текст) – чорний (не сірий).

Рисунки та графіки EXCEL з графіками додатково подаються в окремих файлах.

Скорочені назви фізичних величин в тексті та на графіках позначаються латинськими літерами відповідно до системи СІ.

У списку літератури повинні переважати англомовні статті та монографії, які опубліковані після 2010 року.

Оформлення цитат у тексті статті:

Кількість авторів статті	Приклад цитування у тексті
1 автор	(Arych, 2019)
2 і більше авторів	(Bazopol et al., 2021)

Приклад тексту із цитуванням: It is known (Bazopol et al., 2006; Kuievda, 2020), the product yield depends on temperature, but, there are some exceptions (Arych, 2019).

У цитуваннях необхідно вказувати одне джерело, звідки взято інформацію.
Список літератури сортується за алфавітом, літературні джерела не нумеруються.

Правила оформлення списку літератури

В **Ukrainian Journal of Food Science** взято за основу загальноприйняте спрощене оформлення списку літератури згідно стандарту Garvard. Всі елементи посилання розділяються **лише комами**.

1. Посилання на статтю:

Автори А.А. (рік видання), Назва статті, *Назва журналу (курсивом)*, Том (номер), сторінки, DOI.

Ініціали пишуться після прізвища.

Всі елементи посилання розділяються комами.

1. Приклад:
   Ivanov V., Shevchenko O., Marynin A., Stabnikov V., Gubenia O., Stabnikova O., Shevchenko A., Gavva O., Saliuk A. (2021), Trends and expected benefits of the breaking edge food technologies in 2021–2030, *Ukrainian Food Journal*, 10(1), pp. 7–36, https://doi.org/10.24263/2304-974X-2021-10-1-3

2. Посилання на книгу:

Автори (рік), *Назва книги (курсивом)*, Видавництво, Місто.

Ініціали пишуться після прізвища.

Всі елементи посилання розділяються комами.

Приклад:

2. Wen-Ching Yang (2003), *Handbook of fluidization and fluid-particle systems*, Marcel Dekker, New York.

Посилання на електронний ресурс:

Виконується аналогічно посиланню на книгу або статтю. Після оформлення даних про публікацію пишуться слова **Available at:** та вказується електронна адреса.

Приклади:

(2013), *Svitovi naukovometrychni bazy*, Available at: http://www.nas.gov.ua/publications/q_a /Pages/scopus.aspx

Cheung T. (2011), *World's 50 most delicious drinks*, Available at: http://travel.cnn.com/explorations/drink/worlds–50-most-delicious-drinks–883542

Список літератури оформлюється лише латиницею. Елементи списку українською та російською мовою потрібно транслітерувати. Для транслітерації з українською мови використовується паспортний стандарт.

Зручний сайт для транслітерації з української мови: http://translit.kh.ua/#lat/passport

Детальні інструкції для авторів розміщені на сайті:

http://ukrfoodscience.nuft.edu.ua

Стаття надсилається за електронною адресою:

ukrfoodscience@meta.ua

Наукове видання

Ukrainian Journal of Food Science

Volume 13, Issue 1
2025

Том 13, № 1
2025

Адреса редакції:

Національний університет
харчових технологій
Вул. Володимирська, 68
Київ
01601
Україна

E-mail:

Ukrfoodscience@meta.ua

Підп. до друку 30.06.2025 р. Формат 70x100/16.
Обл.-вид. арк. 2.35. Ум. друк. арк. 2.96.
Гарнітура Times New Roman. Друк офсетний.
Наклад 100 прим. Вид. № 25н/25.

НУХТ 01601 Київ–33, вул. Володимирська, 68

Свідоцтво про державну реєстрацію
друкованого засобу масової інформації
КВ 19324–9124Р
видане 23 липня 2012 року.